THE EFFECT OF A POROUS COLLAGEN-GLYCOSAMINOGLYCAN MATRIX ON HEALING OF THE INJURED RAT SPINAL CORD

by

Mark H. Spilker

B.S. Mechanical Engineering
University of Utah, 1994

Submitted to the Department of Mechanical Engineering
in Partial Fulfillment of the Requirements for the
Degree of

Master of Science in Mechanical Engineering

at the
Massachusetts Institute of Technology
February 1997

Signature of Author_____
Department of Mechanical Engineering
January 8, 1997

Certified by_____
Professor Ioannis V. Yannas
Professor of Mechanical Engineering
Thesis Supervisor

Accepted by_____
Professor Ain A. Sonin
Professor of Mechanical Engineering
Chairman, Department Committee

THE EFFECT OF A POROUS COLLAGEN-GLYCOSAMINOGLYCAN MATRIX ON HEALING OF THE INJURED RAT SPINAL CORD

by

Mark H. Spilker

Submitted to the Department of Mechanical Engineering
on January 8, 1997, in Partial Fulfillment of the
Requirements for the Degree of Master of Science in
Mechanical Engineering

ABSTRACT

Following injury to the adult mammalian spinal cord, central nervous system (CNS) axons do not spontaneously regenerate over significant distances. Recent attempts to facilitate the regrowth of spinal cord axons have shown that following implantation of graft tissue or prosthetic devices, severed CNS axons are capable of regrowing over significant distances.

The overall goal of our work is the development of a resorbable collagen-based tubular implant to promote the regeneration of injured spinal cord axons. Previous research in this laboratory has shown that a resorbable device, consisting of a collagen tube containing a highly porous collagen-glycosaminoglycan (collagen-GAG) matrix, was capable of inducing regeneration of peripheral nerves across a gap of 15 mm. In the current study, similar collagen-based devices were implanted into 5-mm gap injuries in the spinal cords of adult rats.

A 5-mm gap was created in the spinal cord of adult Sprague-Dawley rats by performing complete transections at T7 and T9 and removing the intervening spinal cord tissue. This gap either remained unbridged or was bridged with a tubular implant of the type described below. Resorbable collagen-GAG devices consisted of two components: a non-porous collagen tube containing a specific collagen-GAG matrix, of known chemical composition and pore structure. Four experimental implant groups were included in this study: Group I - no tube implant; Group II - empty collagen tube; Group III - collagen tube containing collagen-GAG matrix of pore diameter 95 μm; and Group IV - collagen tube containing collagen-GAG matrix of pore diameter 5 μm.

At 30 days, the gaps of group I animals were filled with fibrous scar tissue. In animals receiving tubular implants (Groups II, III, and IV), a cable of reparative tissue was found within the tube bridging the gap. Collagen tube implants were also found to modify the organization of the glial scar at the injury site. Numerous myelinated axons had regrown into the tissue within the gap in all groups.

These results demonstrate that collagen-based implants are capable of supporting the regrowth of axons and facilitating other positive regenerative changes following spinal cord injury.

Thesis Supervisor: Ioannis V. Yannas
Title: Professor of Mechanical Engineering

ACKNOWLEDGMENTS

First and above all I would like to thank God for making all things possible. For blessing me so richly with opportunities and the strength to overcome obstacles. I remain in awe of the complexity and elegance of God's creation of human life. I consider it my honor to try to gain an understanding.

My thanks to Professor Yannas for his careful direction, guidance, and advice. I am grateful for the place I hold in his laboratory and for his providing me with the opportunity to do research at a place like MIT. I hope I have made progress in my attempts to become a scientist with his help. I thank Professor Spector for his enthusiasm, energy, and motivation. I have learned so much from both of you. I thank Dr. Kostyk for teaching me about neuroscience and antibody staining. Sometimes the lab at West Roxbury almost seemed like home away from home.

Dr. Hsu, I think we have seen more rats than either of us really wanted to! But, you were always willing to squeeze in that one extra day of surgeries. Thanks.

I thank Sandra Taylor, Evelyn Flynn, Neil Jenkins, and Amy Yu for their technical help with various parts of the project.

As always, I remember my parents who continue to motivate and encourage me. I thank my whole family for reminding where I come from and what things are really important.

I can't forget the "Tissue Engineering Gang" including Lila, Libby, Bernie, Sunil, Howie, Diane, Jon, Donna, Satayan (wow this list gets long). I'm glad I have such a great group of people to work with and to hang out with.

Maybe last on the list are the boys at the house including Eddy, Jeff, Pete, Mark, etc. You guys have made my stay in Boston enjoyable.

I guess I still have some room on the page, so I'd like to thank the striped bass of Cape Cod and Nantuckett for providing hours of challenging angling!

TABLE OF CONTENTS

LIST OF TABLES

LIST OF FIGURES

CHAPTER 1: INTRODUCTION

1.1 Statement of the Problem

Severe injury to the adult mammalian spinal cord results in a loss of both sensory and motor function below the injury site. Nerve fibers (axons) of the spinal cord which are severed by injury exhibit only abortive regrowth and do not restore a connection with the original target. The result is a permanent loss of function. An estimated 15,000 people per year suffer spinal cord injury[15,40]. An estimated one million people currently live with deficits caused by a spinal cord injury, and 500,000 people are currently designated as paraplegic or quadriplegic[15].

Current clinical treatments for spinal cord injury are successful in minimizing the severity of the injury by suppressing the inflammatory response and immune reaction at the injury site. However, these therapies are not effective in facilitating the repair of nerve fibers which were injured by the initial injury. Current research in the field of spinal cord injury is attempting to solve the problem of facilitating the regrowth or regeneration of injured nerve fibers, with the ultimate goal of the return of function.

1.2 Normal Nervous System

Communication between the various parts of the body is carried out by the transmission of electrical impulses by specialized cells of the nervous system called neurons. Neurons are capable of receiving and sending signals. The neuron cell body (which contains the cell nucleus) is responsible for the metabolic requirements of the cell and for receiving signals from a variety of sources. These signals are processed and relayed via a long cell process of the neuron called an axon (see figure 1.1 on the following page).

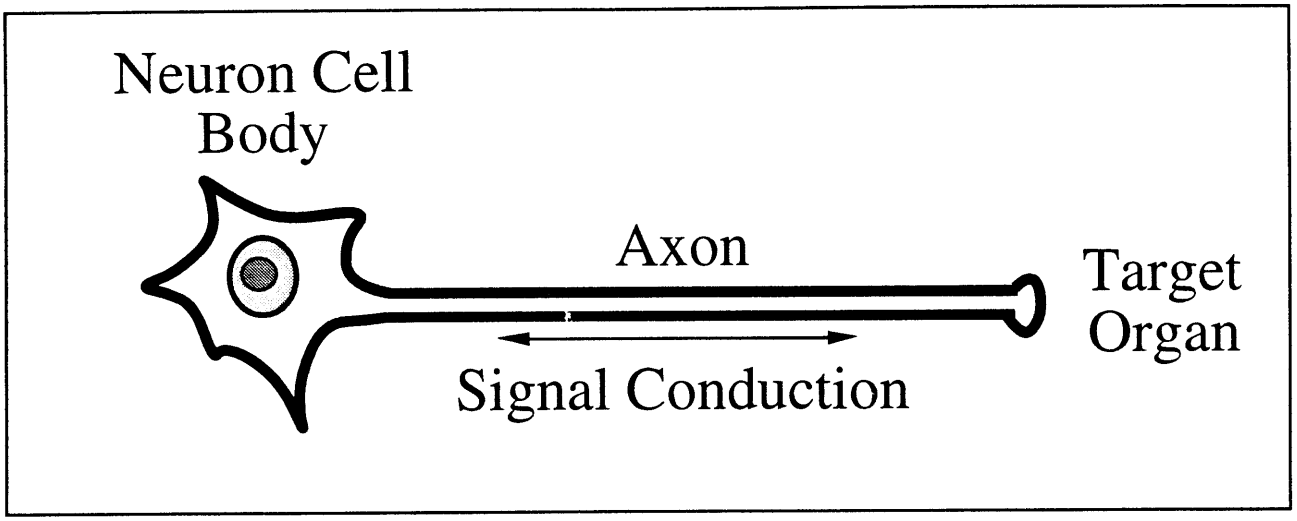

Figure 1.1. Neuron cell body and signal conduction along the axon.

Axons are often surrounded by a sheath of a lipoprotein called myelin which provides electrical insulation increasing the speed of conduction of impulses. Myelin consists of tightly wrapped layers of plasma membrane belonging to a myelinating cell. Myelinating cells of the peripheral nervous system are called Schwann cells, and myelinating cells of the central nervous system are called oligodendrocytes.

The nervous system consists of two general divisions: the peripheral nervous system (PNS) and the central nervous system (CNS). The peripheral nervous system consists of bundles of axons which carry impulses to and from the extremities of the body. These bundles of axons make up peripheral nerves. The central nervous system consists of the neuron cell bodies and the axons responsible for communication between neuron cell bodies. The central nervous system is contained within the brain and the spinal cord. This project is primarily concerned with injury to the central nervous system, particularly the spinal cord.

Figure 1.2 on the following page schematically depicts communication between the brain and a skeletal muscle endpoint. A signal originates in a motor neuron within the brain and is carried along an axon into the spinal cord where it forms a synapse with a second neuron. The neuron within the spinal cord relays the signal along its axon within a peripheral nerve. The signal terminates at a muscle endplate. The muscle is signaled to contract or relax.

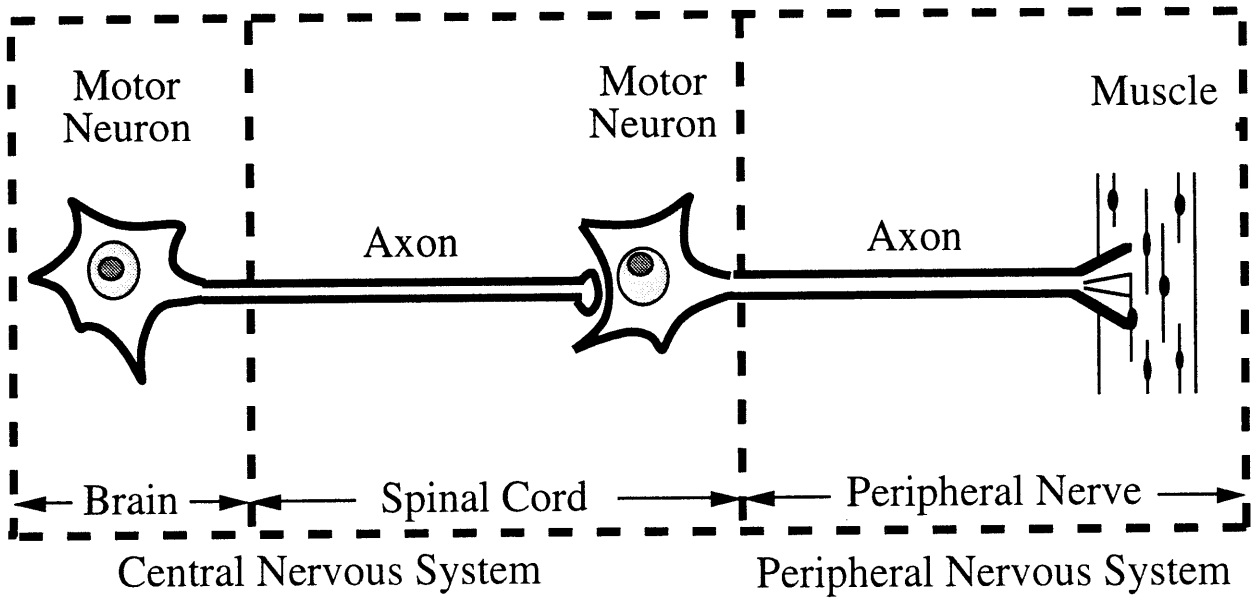

Figure 1.2. Normal nervous system communication.

The spinal cord contains four general cell types: neurons, oligodendrocytes, astrocytes, and microglia. As discussed previously, neurons are the cells responsible for receiving, processing, and sending signals. Oligodendrocytes are responsible for producing and maintaining the myelin sheath of axons of the spinal cord. They are also seen in close association with unmyelinated axons. Astrocytes basically fill the spaces between neurons and their processes. Astrocytes provide physical support for the cellular elements of the nervous system and may also play a role in nutrition and metabolic activities of neurons. Microglia are equivalent to the resident macrophages of other tissue types. When stimulated by injury or infection, they express phagocytic activity.

Grossly, the spinal cord lies within the vertebral column descending from the brain for approximately one half meter in the adult human[5]. The vertebrae and ligaments provide mechanical support and protection for the spinal cord. Additional protection is provided by the meninges, which are the three layers of tissue which surround the spinal cord. The outermost layer, or dura mater, consists of connective tissue and performs a mechanical and structural function. The inner layers, the pia and the arachnoid, perform functions of maintaining the cerebrospinal fluid which bathes the brain and the spinal cord. Two rows of nerve roots intermittently emerge on either side

of the spinal cord. These spinal nerves branch to form peripheral nerves which distribute motor and sensory function to all parts of the body.

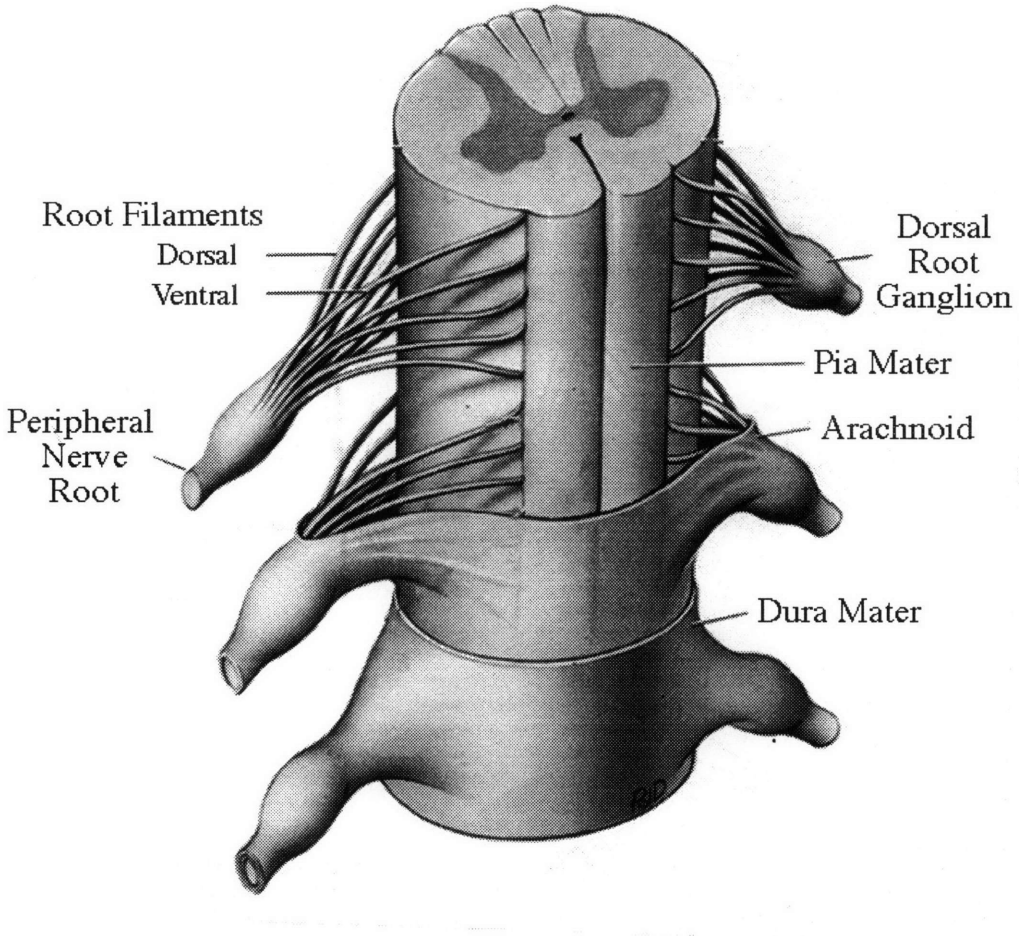

Figure 1.3. Spinal cord and peripheral nerve roots (adapted from Heimer 1995[35]).

1.3 Injury to the Nervous System

A mechanical injury to the nervous system disrupts intact axons and prevents the transfer of signals, hence the loss of function below the injury site. When an axon has been transected, the portion of the axon no longer attached to the cell body (distal to the lesion) becomes necrotic, and is phagocytosed by macrophages. The myelin sheath which surrounded that axon also degrades and is removed by macrophages. This process is known as Wallerian degeneration. Many

neurons die when their axons are transected, however a significant population of neurons survive and are capable of regenerating an axon.

Peripheral Nervous System

Axons of the PNS show significant ability to spontaneously regenerate following injury. Provided that the injury is small enough, peripheral nerve axons regrow and establish functional connection. When an axon is severed, the neuron cell body undergoes changes in preparation for a regenerative response. The cell body begins to produce nucleic acids structural proteins which provide the building material for the regrowing axon. The tip of the axon at the site of transection may branch into a number of sprouts, each with an enlarged tip called a growth cone. These growth cones advance through the lesion site and may eventually form a function connection with the original target.

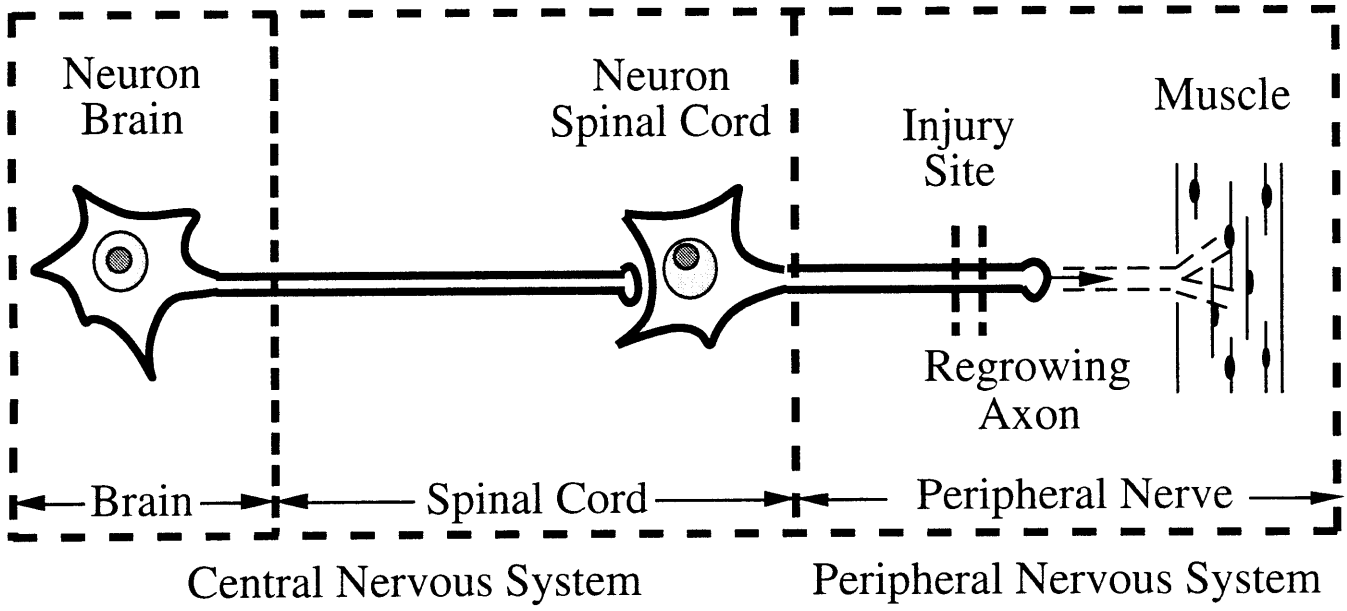

Figure 1.4. Injury and regeneration of the peripheral nervous system.

Central Nervous System

In contrast to axons of the PNS, axons of the CNS show very little capacity to spontaneously regenerate. An initial sprouting of axons growth cones is usually abortive. Under normal conditions, severed axons of the CNS do not regrow and function is never restored.

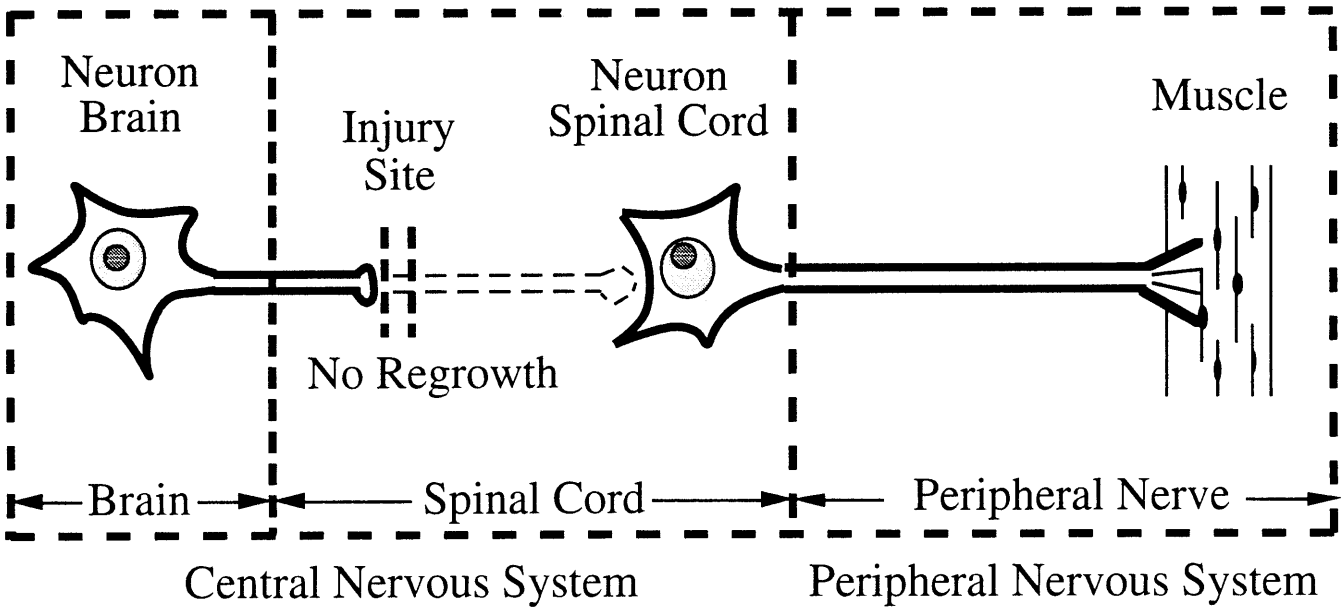

Figure 1.5. Injury to the central nervous system.

Cajal historically documented the aborttive regrowth of CNS axons in 1928[13]. He hypothesized that the lack of regeneration was not due to an intrinsic inability of CNS axons to regrow, but that the environment a the site of CNS injury was not permissive for the regrowth of axons. More recent studies have identified elements present at the site of CNS injury which act as barriers to axons regeneration.

1.4 Barriers to CNS Regeneration

Two factors have been hypothesized to inhibit the regrowth of spinal cord axons: 1) the formation of a dense fibrous scar within the wound site and 2) the formation of a continuous glial scar encapsulating the injured spinal cord stumps[9,13,32,46,65,79].

Immediately following injury, the site of a wound is filled with blood. Macrophages from blood sources begin to phagocytose debris and necrotic tissue. The wound soon becomes infiltrated with fibroblasts invading from the non-neural tissue surrounding the spinal cord. These cells form a connective tissue matrix which increases in density forming a fibrous scar between the cut ends of the spinal cord. Numerous investigators have discovered that axons of the spinal cord fail to regrow into or across the fibrous scar[13,24,42,79]. Fibrous scarring following spinal cord injury is discussed in more detail in sections 3.1.4 and 4.1.3

Astrocytes become active in response to injury and extend their cytoplasmic processes into regions of damage. The end result is the formation of a distinct partition between intact CNS tissue and wounded tissue. This partition, known as the glial scar, is composed of a densely packed network of reactive astrocyte processes. Two characteristics of the glial scar are implicated as being responsible for blocking the regeneration of axons. It has been demonstrated *in vitro* that reactive astrocytes characteristic of those in the glial scar do not provide a preferred environment for axon elongation. The hypertrophy of astrocyte processes forms a dense network of processes which axons do not preferentially cross[7,31,39,51,79]. Astrocytes of the glial scar have been shown to be responsible for forming a continuous layer of basement membrane (also known as the glial limitans) encapsulating intact spinal cord tissue and blocking the progress of advancing axons[29,43]. The glial scar as an impediment to regeneration is also discussed in section 4.1.4.

1.5 Requirements for Successful Regeneration of the Spinal Cord

The endpoint of successful regeneration of the spinal cord is the return of function to areas denervated by the injury. Function can be classified as either sensory or motor. The return of both sensory and motor function is necessary. A return of function following injury to the spinal cord would require the completion of three processes: 1) the sprouting and elongation of injured axons from the wound site; 2) the regrowth of these axons eventually reaching their original endpoints; and 3) the formation of functional connections (synapses). It is the work of the researcher to find ways to facilitate these processes and to measure our success with applicable quantitative metrics.

The state of the art for treatment of spinal cord injury has not yet obtained complete recovery, and success is usually measured in terms of the individual processes leading up to functional recovery. The sprouting and regrowth of axons can be measured by histological methods with which axons are identified. Neuroanatomical tracing methods can be used to identify the path of regrowing axons determining whether these axons have regrown to their original endpoints. Functional connections can be measured by observing the locomotion of the animal and focusing on cues which correspond to reinervation of certain muscle groups or sensory regions. Electrophysiological techniques test the ability of axons or nerves to carry an impulse to the target.

1.6 Progress Toward Spinal Cord Regeneration

Historically, Cajal confirmed that axons do not successfully regenerate following injury to the spinal cord[13]. Cajal showed that spinal axons initially sprout and mount a regenerative response, however any regrowth is abortive and digresses within two weeks. The research of Windle and colleagues confirmed the observations of Cajal. Windle hypothesized that neurons of the CNS were capable of regeneration, but the growth of axons was blocked by the presence of glial and fibrous scar at the wound site[24,79]. As early as 1957, the use of a tube implant to encourage the regeneration of spinal cord tissue was studied. A group lead by Campbell found that axons were capable of regrowing within a nylon/millipore tube within the site of spinal cord injury in the cat[6,14]. However, functional recovery was not confirmed by any investigators.

Kao initially bridged spinal cord injuries of dogs with autologous grafts of sciatic nerve and demonstrated the regrowth of axons into the grafts[43]. More recently, David and Aguayo conclusively confirmed that axons of the CNS were able to regrow through segments of peripheral nerve grafted into a gap lesion in the adult rat spinal cord[26]. Various other techniques have since been used to encourage the regrowth of spinal cord axons. In 1986, Reier and colleagues transplanted fetal spinal cord tissue into a spinal cord lesion in adult rats[66]. The transplanted tissue became integrated with the host cord and supported the regrowth of axons, however, no functional

reconnection of axons was documented. Other investigators also observed similar results following the transplantation of fetal tissue[38,68].

An alternative approach was taken by Schwab and his colleagues who identified specific compounds in the spinal cord itself which inhibited the regrowth of axons[69]. When the inhibitors were neutralized using antibodies, axons were able to regrow over substantial distances[10].

The capacity of synthetic biomaterials to encourage axon regrowth following spinal cord injury has been studied. In 1989, Houle and Johnson found that axons from peripheral sources were able to regrow when strips of nitrocellulose treated with nerve growth factor were inserted into the spinal cord[37]. Khan and colleagues discovered that carbon filaments provided an aligned substrate which supported the regrowth of axons when implanted into spinal cord lesions[45]. Natural biomaterials, such as collagen have, also been evaluated for their ability to support the regrowth of axons. DeLaTorre, Gelderd, and Marchand have studied the implantation of collagen gels into spinal cord wounds[27,30,58].

As mentioned previously, tubes have been used to bridge spinal cord lesions as early as 1957[6,14]. More recently, Xu et. al. used blind-ended acrylonitrile/vinylchloride copolymer (PAN/PVC) tubes as a vehicle for the delivery cultured cells into site of spinal cord injury[81]. CNS axons were able to regrow into the tubes. Montgomery found that injured spinal cord axons were able to regrow into polycarbonate tubes[63]. Fuctional recovery was not observed in any case.

Until recently, experimental treatments of complete spinal cord injury in adult mammals had not resulted in a return of function. However, Cheng and colleagues recently observed that, following treatment, experimental rats whose spinal cords had been completely transected were able to bear weight with their hindlimbs[22]. The return of function was seen only in rats which had received multiple nerve grafts across the transection site held in place by fibrin glue containing acidic fibroblast growth factor. This result is encouraging, since it demonstrates that axons which regrow across spinal cord lesions are ultimately capable of restoring function

1.7 Previous Research in This Laboratory

A family of bioresorbable matrices composed of a collagen-glycosaminoglycan (collagen-GAG) copolymer has been demonstrated to promote regenerative changes following injury to several tissue types. Collagen-GAG matrix has been shown to induce the regeneration of a physiologic dermis in the guinea pig[84-87, 89] and human[12,34,71]. Collagen-GAG matrix has also been demonstrated to facilitate regeneration of a function meniscus in the dog following 80 percent transection[74].

Collagen-GAG matrix has also been shown to enhance the inherent regenerative capacity of tissue of the peripheral nervous system. Axons were able to regrow across a 15-mm gap in the rat sciatic nerve when the gap was bridged with a silicone tube containing collagen-GAG matrix[88]. Axons did not regrow across the gap within empty tubes. The robustness of the regenerative response was later found to depend on the chemical composition and pore structure of the matrix[18-20, 53]. In these studies, the collagen-GAG matrix was contained within a non-degradable silicone tube implanted into the lesion site. Recent research suggests that the silicone tube may be replaced by a completely resorbable collagen tube with an equivalent regenerative response[17,40]. These resorbable devices, consisting of collagen tubes and collagen-GAG matrix, show promise for the repair of damaged peripheral nerves in human patients.

The success of tubular implants containing collagen-GAG matrix in promoting the regrowth of peripheral nerve axons suggests that a similar device may be capable of promoting the regrowth of axons in the spinal cord.

1.8 Project Goal

The overall objective of this project is to develop a completely resorbable implant device which promotes the regeneration of axons following spinal cord injury. The specific goal of the work presented in this thesis was to examine the early healing response following injury to the rat spinal cord and the effects of tubular implants on this healing process.

This study consisted of three parts, each discussed separately in chapters 2, 3, and 4. In chapter 2, collagen-GAG matrix was prepared and its pore structure characterized. In chapter 3, an animal model of spinal cord injury was established. In chapter 4, this animal model was used to test the effects of various implant devices on spinal cord healing. The implant devices consisted of collagen tubes which either remained empty or were filled with collagen-GAG matrix with a specific pore structure.

CHAPTER 2: PREPARATION AND CHARACTERIZATION OF COLLAGEN-GLYCOSAMINOGLYCAN MATRIX

2.1 Introduction

2.1.1 Previous Applications of Collagen-Glycosaminoglycan Matrix

As previously discussed in section 1.7, a family of porous collagen-glycosaminoglycan matrix (CG matrix) implants has been shown to favorably alter the wound healing process following injury to several tissue types. CG matrix is capable of facilitating partial regeneration of the injured dermis in the guinea pig[84-87, 89] and human[12,34,71]. Regeneration of the knee meniscus of the greyhound was achieved following 80 percent transection and implantation of CG matrix[74]. A functional rat sciatic nerve was found to regrow across a 15-mm gap in the presence of a CG matrix implant[88].

In the animal models for the study of dermal and peripheral nerve regeneration, studies were performed in which CG matrices of different pore structure were compared *in vivo*[18,19,25]. For each tissue type, a CG matrix with specific pore structure yielded the most effective regeneration. Therefore, one important factor which determines the effectiveness of CG matrix implants in a specific injured tissue is its pore structure

One goal of the work described in this chapter was to determine the manufacturing parameters required to produce collagen-GAG matrix implants for use in the spinal cord. Particularly, two types of pore structure are of interest: 1) axially aligned pores of small diameter (approximately 5 μm), and 2) axially aligned pores of large diameter (approximately 100 μm).

2.1.2 Theory of Freeze-Drying Fabrication of CG Matrix

Collagen-glycosaminoglycan matrix implants are manufactured in this laboratory by a freeze-drying process comprising multiple steps: 1) a copolymer of type I collagen and chondroitin 6-sulfate is formed as a suspension in dilute (0.05M) acetic acid; 2) the suspension is frozen, forming ice dendrites; 3) the ice dendrites are removed by freeze-drying leaving a porous network

of collagen-GAG copolymer and void spaces in place of the sublimed ice; 4) dehydrothermal treating the collagen-GAG network to form covalent crosslinks between polymer chains.

CG matrix implants for a particular application (dermis, nerve, meniscus) require a geometric shape to match the form of the tissue being studied. Since skin is thin and flat, CG matrix implants for replacement of injured dermis are fabricated in sheets 2-mm thick. In the rat, the sciatic nerve takes the form of a long cylinder 1.5 mm in diameter. Implants for nerve are fabricated as hollow cylinder-shaped segments 1.5 mm in diameter. The thoracic spinal cord of the adult rat is cylindrical having a diameter of 3.0 mm. CG matrix implants for the spinal cord need to be cylindrical and 3.0 mm in diameter, twice the diameter of sciatic nerve implants.

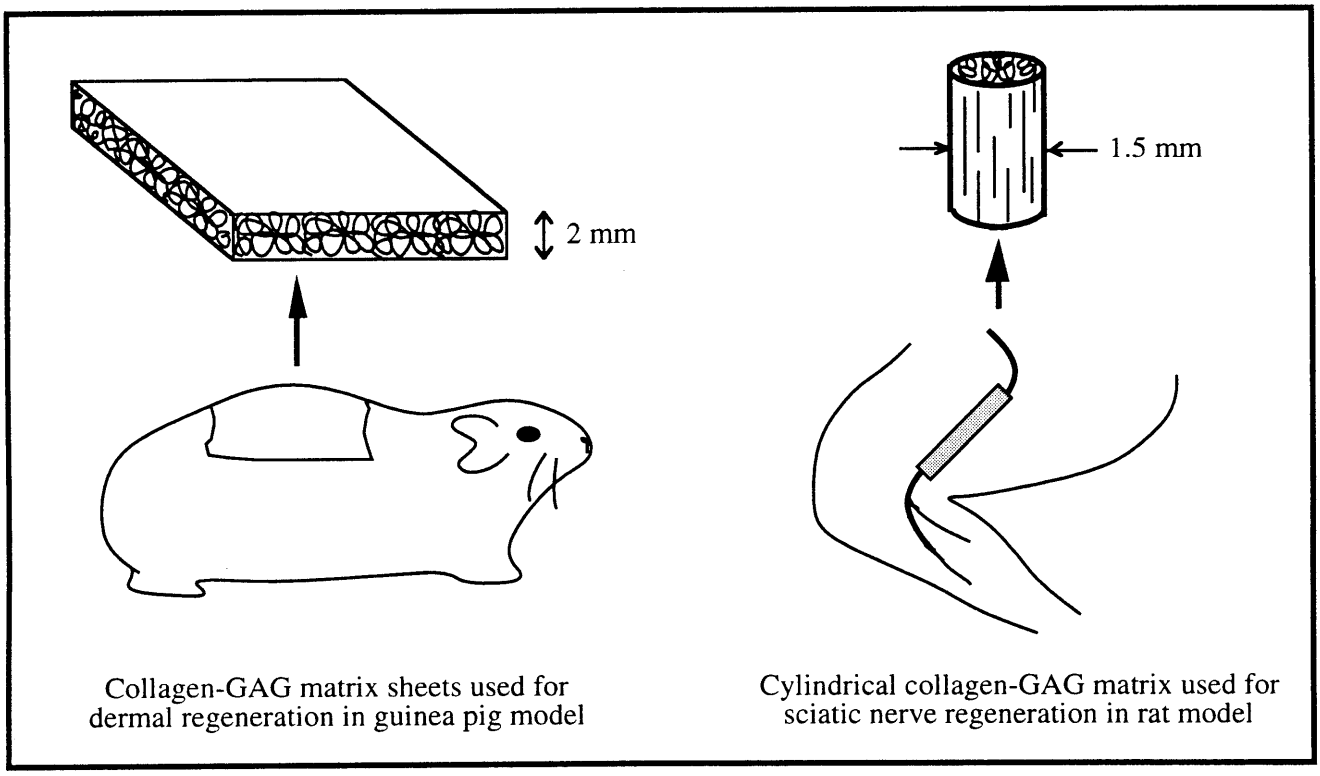

Figure 2.1. Collagen-GAG matrix implants for skin and peripheral nerve

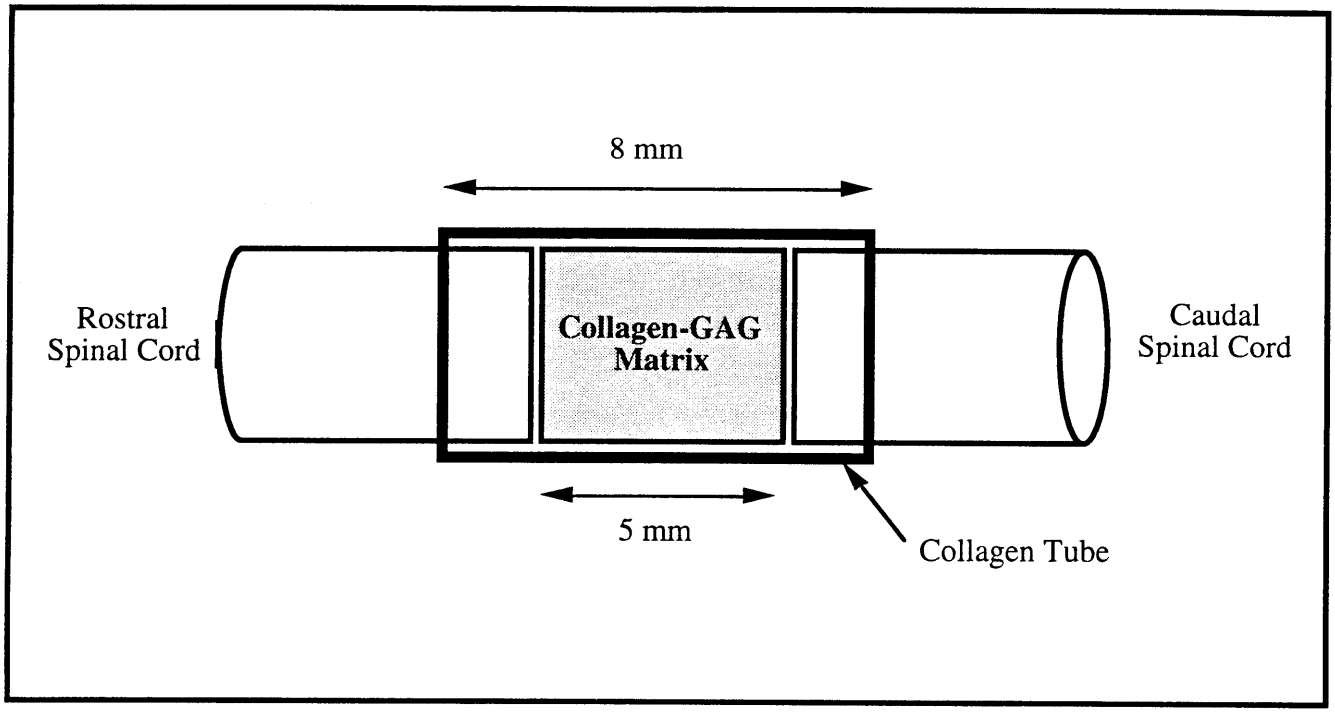

Figure 2.2. Schematic of collagen-GAG implant in the injured spinal cord.

Flat sheets are produced by pouring collagen-GAG suspension into an aluminum tray. The temperature is lowered, and the shallow pool freezes. The frozen sheet is freeze-dried to form a thin flat sheet of CG matrix. Cylindrical specimens are formed by lowering a tube filled with collagen-GAG suspension into a low-temperature bath. The freezing front travels axially within the tube forming ice dendrites elongated parallel to the axis of the tube. During freeze-drying, the ice dendrites are removed by sublimation to create pores which are also aligned axially.

The relationship between manufacturing parameters and pore structure has been previously established for flat sheets of CG matrix[21]. The freeze-drying of CG matrix cylinders 1.5 mm in diameter has also been studied in detail[52]. Most recently, Louie studied the manufacture of CG matrix cylinders 3.8 mm in diameter[54]. The size and orientation of pores in the CG matrix is determined by the size and orientation of the ice dendrites which form during the freezing process. In general, lower freezing temperatures produce smaller pores, and higher temperatures produce larger pores. The work of Loree[52] demonstrated that in cylindrical CG matrix, not only can pore size be controlled by freezing temperature, but the pores can be aligned along the cylinder axis by

lowering the tube of collagen-GAG suspension into a cooling bath at different velocities. The degree of pore alignment depends on the coupling of freezing temperature and lowering velocity.

In all previous studies of pore structure of CG matrix[21,41,52,54], the CG matrix was prepared using collagen provided by the United States Department of Agriculture (USDA, Philadelphia, PA). Specifically, USDA collagen is insoluble type I collagen extracted and refined from bovine hide. For the experiments discussed in this chapter, CG matrix was produced using insoluble type I bovine achilles tendon collagen provided by Integra LifeSciences Corporation (Plainsboro, NJ). There may exist subtle differences between CG matrix produced using USDA bovine hide collagen and CG matrix produced using Integra bovine tendon collagen. A primary goal of the work presented in this chapter is to manufacture CG matrix using Integra tendon collagen and to compare its pore structure with the previously studied pore structure of CG matrix produced using USDA hide collagen.

2.1.3 Objectives of Work in this Chapter

The goal of work presented in this chapter was to establish general relationships between manufacturing parameters and pore structure of CG matrix. This work differed from similar previous studies in two respects: the collagen source for these experiments was Integra bovine tendon rather than USDA bovine hide, and the geometry of spinal cord implants is a 3.0-mm diameter cylinder (1.5-mm and 3.8-mm diameter CG matrices were previously studied).

Two types of CG matrix are desirable for study as spinal cord implants: CG matrix with axially aligned pores of small diameter (approximately 5 μm), and CG matrix with axially aligned pores of large diameter (approximately 100 μm). The second goal of this research was to determine the manufacturing parameters required to produce these particular matrices.

2.2 Materials and Methods

2.2.1 Preparation of Collagen-glycosaminoglycan Matrix

The process for preparing collagen-GAG spinal cord implants is derived from previously established protocols for implants for peripheral nerve[52]. The process involves four basic steps: 1) forming a suspension of collagen-chondroitin 6-sulfate copolymer in dilute (0.05M) acetic acid; 2) freezing the collagen-GAG suspension by lowering into a bath of low-temperature coolant; 3) freeze-drying the solid suspension to form a highly porous network of collagen-GAG fibers; 4) dehydrating the porous collagen-GAG at elevated temperature and under vacuum to form covalent crosslinks between polymer chains. Detailed protocols for each of these procedures is included in appendix A.

The collagen component of collagen-GAG matrix is insoluble type I collagen derived from bovine achilles tendon (Integra LifeSciences Corp., Plainsborough, NJ). Chondroitin 6-sulfate is available as a white crystalline powder (product C-4383, Sigma Chemical, St. Louis, MO). To prepare collagen-GAG suspension, 13.69 g of Integra collagen was weighed and pulled into small pieces using forceps. The collagen pieces were added to 600 ml of 0.05 M acetic acid maintained at 4°C in an overhead blender (Granco overhead blender, Granco Co., Kansas City, MO, Brinkman cooler model RC-3T, Brinkman Co., Westbury, NY). This mixture was blended at 2000 rpm while cooled at 4°C for 90 minutes. 0.32 g of chondroitin 6-sulfate was weighed and dissolved in 120 ml of 0.05 M acetic acid. The chondroitin 6-sulfate solution was added to the 600 ml of blended collagen over 15 minutes using a peristaltic pump (Manostat cassette pump, Manostat, New York, NY). Blending was continued during the addition of the chondroitin 6-sulfate solution. The mixture of collagen and chondroitin 6-sulfate was blended at 4°C for an additional 90 minutes at 2000 rpm. During blending, a coprecipitate of collagen and chondroitin 6-sulfate was formed which remains in suspension in the dilute acetic acid. The blended suspension was degassed for 15 minutes in a 6 liter vacuum flask.

Using a 3-ml syringe (Becton Dickenson & Co., Rutherford NJ) degassed collagen-GAG suspension was injected into the open end of a 10 cm length of silicone tubing (ID, 5/32 inch, OD,

7/32 inch, Cole Parmer, Niles IL) in preparation for freezing. An insulating sleeve of PVC (ID, 6 mm, OD, 9 mm, Cole Parmer, Niles IL) was slipped over the length of the tube. After filling with CG suspension, the ends of the silicone tube were clamped. A diagram of the clamped silicone tube (containing collagen-GAG suspension), PVC sleeve, and surface of cooling bath is shown in Figure 2.3. The PVC sleeve, silicone tube, and CG suspension inside were lowered axially into a bath containing a silicone-based coolant (Syltherm XLT Heat Transfer Liquid, Dow Corning Corp., Midland MI). The coolant bath was maintained at any desired temperature between -10°C and -80°C.

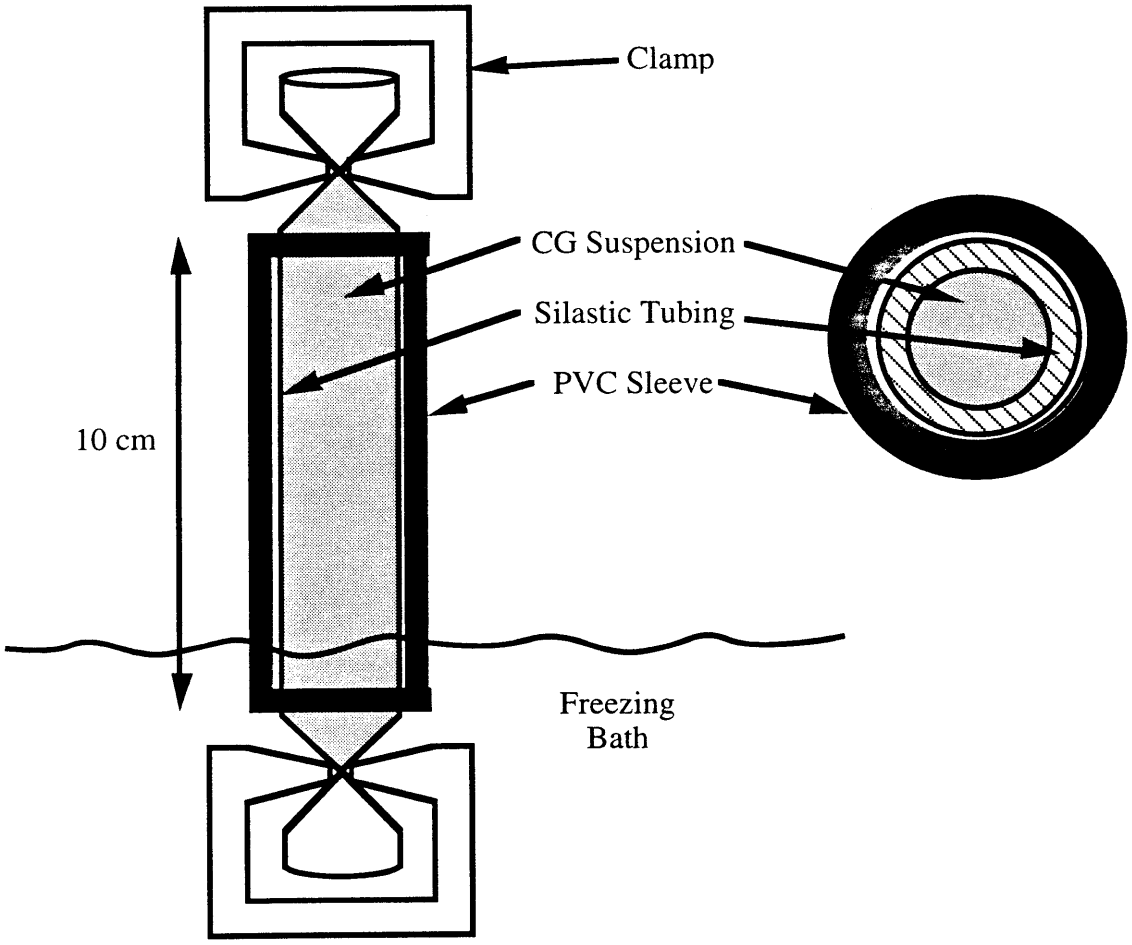

Figure 2.3. Collagen-GAG suspension contained within silicone tube and PVC sleeve

The velocity at which the tubing and collagen-GAG suspension were lowered into the coolant bath was controlled within the range between $2x10^{-5}$ m/s and $10x10^{-5}$ m/s. One end of the silicone tube was connected to a vertically hanging cord which was attached to a 1/30 RPM timing motor (Cramer model 117P, Conrac Co., Old Saybrook, CT). By changing the size of the gear on the motor (Berg model GG33S14-12, GGS14-30, GGS14-64, Winfred M. Berg Inc., East Rockaway, NY), the velocity at which the suspension was lowered could be controlled. A schematic diagram of the complete freezing bath and lowering apparatus[52] is shown in Figure 2.4. Once the suspension had completely lowered into the bath and was submerged, it remained in the bath for approximately 30-60 minutes to ensure complete solidification.

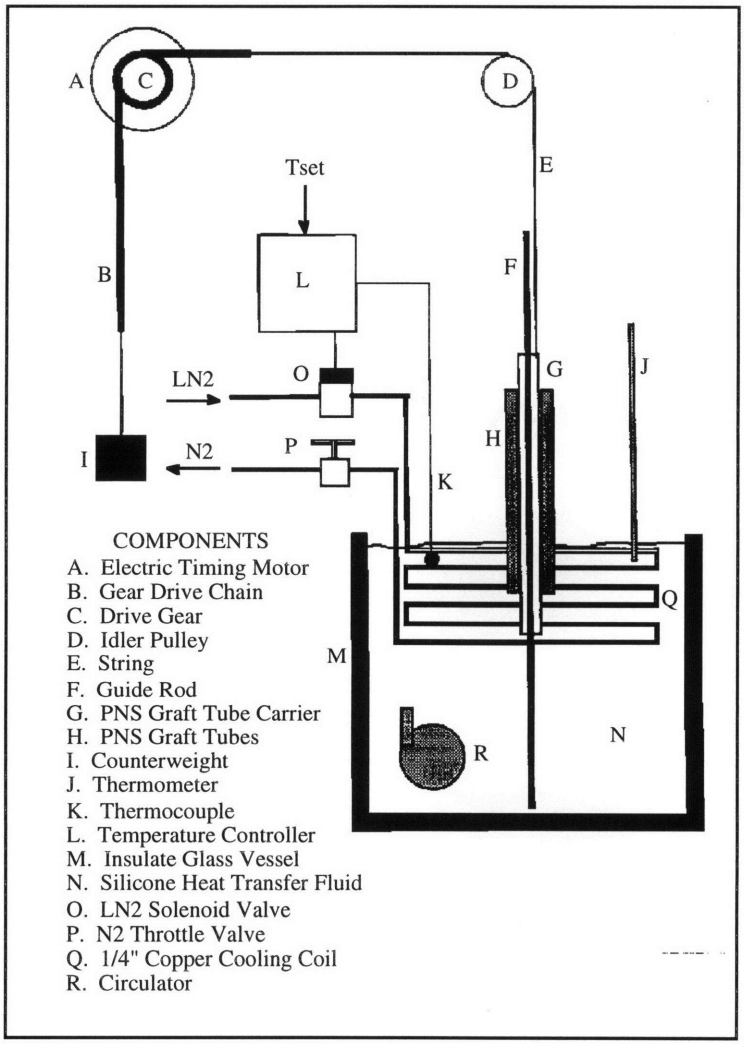

Figure 2.4. Schematic diagram of Loree 2000 freezing apparatus (adapted from Loree[52]).

In this experiment, two parameters were varied independently: 1) the temperature of the cooling bath, and 2) the velocity at which the collagen-GAG suspension was lowered into the cooling bath. Three cooling bath temperatures were used: -10°C, -45°C , and -80°C. At each temperature, three lowering velocities were used: $2x10^{-5}$ m/s, $5x10^{-5}$ m/s, and $10x10^{-5}$ m/s. This gives a total of nine groups matching each temperature with one of three lowering velocities.

As the suspension was lowering into the cooling bath, the VirTis freeze-drying apparatus (VirTis Genesis, VirTis, Gardiner, NY) and one aluminum tray were cooled and allowed to equilibrate to -30°C. The pre-cooled aluminum tray served as a cold surface on which the following procedure was performed. While frozen solid, the 10-cm length of silicone tube and CG suspension was cut using a razor blade into 2.5-cm segments. The segments at each end of the tube (nearest the clamps) were discarded, and the segments in the middle of the tube were retained for freeze-drying.

The segments of frozen CG suspension were placed horizontally on the pre-cooled aluminum tray, and the tray was placed in the FTS freeze-dryer chamber. The freeze-dryer was again allowed to equilibrate to -30°C. A vacuum of 100 mtorr was pulled in the chamber which was maintained at -30°C. Under vacuum of 100 mtorr, the temperature of the chamber was raised to 0°C and held for 24 hours. At this low pressure and elevated temperature, the ice crystals within the CG suspension were sublimed, leaving a porous network of collagen-GAG copolymer. Following complete sublimation, the temperature of the chamber was raised to 22°C and held for an additional 45 to 90 minutes to equilibrate to room temperature. The vacuum was released, and the dry CG matrix segments were removed.

The freeze-dried CG matrix was ready for dehydrothermal (DHT) treatment. Each segment of matrix was placed in an open-ended packet made of aluminum foil. These packets were placed in a vacuum oven (Fisher Isotemp vacuum oven, Fisher Scientific, Medford, MA). A vacuum of 30 mmHg was pulled, and the temperature was raised to 105°C for 24 hours. As the packets were removed from the oven, the open end was sealed. The sealed packets containing CG matrix were stored in a desiccating chamber. DHT treatment served two purposes: 1) to effectively sterilize the

CG matrix implants, and 2) to form covalent crosslinks between collagen-GAG copolymer chains[82].

2.2.2 Characterization of Pore Structure of Collagen-Glycosaminoglycan Matrix

Previously, the relationship between manufacturing parameters and pore structure of axially frozen CG matrix segments has been examined[52,54]. The particular manufacturing parameters of interest are: 1)cooling bath temperature, and 2) the velocity at which CG suspension was lowered into the cooling bath. Pore structure has been characterized and described by numerous features, among them average pore diameter and pore channel orientation. In this experiment, average pore diameter was measured quantitatively, and pore channel orientation was assessed qualitatively.

Microscopic examination of CG matrix samples was performed using an environmental scanning electron microscope (ESEM, Electroscan, Waltham, MA). The collagen-GAG matrix samples do not conduct charge well. In order to view CG matrix samples in the SEM, they would need to be sputter coated with a conducting material such as gold. Viewing with ESEM has the advantage over conventional SEM since the samples do not need to be coated. Coating with gold could alter the fine porous structure of the matrix.

In preparation for ESEM viewing, samples of CG matrix were cut transversely with a razor blade into 3-mm thick wafers and mounted onto SEM stubs with two-sided conductive tape. Segments of matrix were also cut longitudinally to observe pore channel orientation. ESEM micrographs were developed on thermal paper (Mitsubishi, Japan) and on instant photographic film (Polaroid Corporation, Cambridge, MA). Each image contained its own scale bar, allowing for later calibration of pore size measurements. These images were used as follows to examine pore structure.

Thermal prints of each ESEM micrograph were converted to TIFF format computer files using a laser scanner (UMAX model UC1260, UMAX Data Systems Inc., Industrial Park, Hsinchu, Taiwan, Republic of China). The TIFF images were imported into a computer

stereology package (NIH Image, available via internet FTP from zippy.nimh.gov or on disk from NTIS, 5285 Port Royal Road, Springfield, VA 22161 part no. PB 93-504868). The size scale of each image was defined using the ESEM scale bar and the measured on-screen distance in pixels. Each image had a slightly different size conversion due to the changing magnification of the ESEM.

Following calibration, individual pores present in the image were outlined using the computer mouse. The NIH image software contains an automated process which measures the area of each circled pore as well as the length of the perimeter of each pore. The software also numbers and counts each pore. Since the pores are not exactly circular in shape, a true circular diameter cannot be measured. The following equation defines an equivalent or hydraulic diameter of each pore:

$$D_h = \frac{4 \cdot A_{pore}}{P_{pore}}$$

where D_h is the equivalent hydraulic diameter of the pore in μm, A_{pore} is the measured area of the pore in μm^2, and P_{pore} is the measured perimeter of the pore in μm. The hydraulic diameter is defined as the diameter of an exact circle having the same cross sectional area as the pore in question. Thus yielding an equivalent diameter for a non-circular shape. Figure 2.5a on the following page shows an ESEM micrograph of the porous structure of CG matrix. Figure 2.5b shows the same image following analysis with NIH Image software. A number of individual pores are shown selected and analyzed.

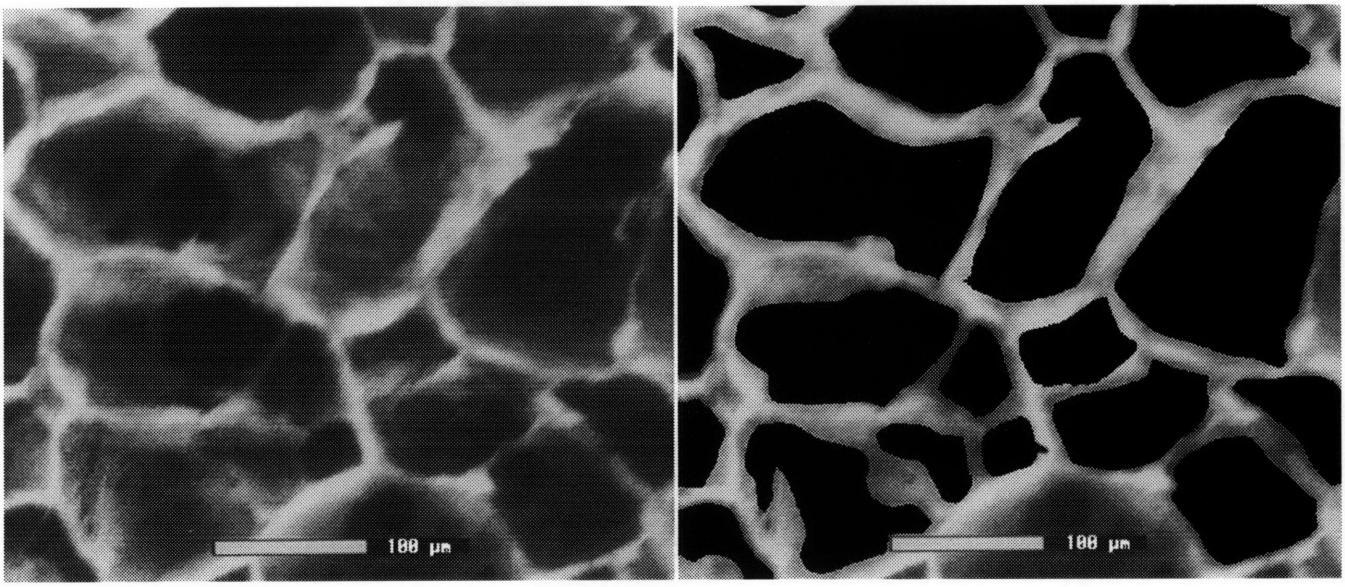

Figure 2.5a. ESEM image of CG matrix before analysis.

Figure 2.5b. Image with analyzed pores.

ESEM micrographs of longitudinally cut CG matrix specimens were evaluated qualitatively for alignment of pore channels. Pore channel orientation was categorized as 1) axial aligned, 2) radial aligned, or 3) no apparent orientation.

2.3 Results

2.3.1 Average Pore Diameter

The quantitative results for pore diameter measurement are shown in Table 2.1 on the following page. The grid contains the nine combinations of cooling bath temperature and lowering velocity. For each combination of freezing temperature and lowering velocity, three ESEM images were analyzed and the pore size measured. Each result is presented as the mean +/- standard deviation based on three samples.

Lowering Velocity (m/s)	Cooling Bath Temperature (Celsius) -80°C	-45°C	-10°C
$10x10^{-5}$ m/s	5.48 +/- 1.1 μm	9.96 +/- 0.64 μm	152 +/- 26.6 μm
$5x10^{-5}$ m/s	12.3 +/- 2.6 μm	10.5 +/- 3.3 μm	88.7 +/- 4.4 μm
$2x10^{-5}$ m/s	41.3 +/- 4.8 μm	41.3 +/- 3.4 μm	93.1 +/- 7.2 μm

Table 2.1. Measured pore size for combinations of cooling bath temperature and lowering velocity

These results show that cylindrical CG matrices with pore diameters ranging between 5.48 μm and 152 μm can be produced by the axial freezing process. The smallest average pores (5.48 μm diameter) resulted from a freezing bath temperature of -80°C and a lowering velocity of $10x10^{-5}$ m/s. The largest average pores (152 μm) resulted from a freezing bath temperature of -10°C and a lowering velocity of $10x10^{-5}$ m/s. In general, higher temperatures yielded larger pores, and lower temperatures yielded smaller pores.

Below are shown sample SEM micrographs from CG matrix with relatively large and relatively small pores. The sample in Figure 2.6a was produced with a cooling bath temperature of -10°C and a lowering velocity of $10x10^{-5}$ m/s. The sample in Figure 2.6b was produced with a cooling bath temperature of -80°C and a lowering velocity of $10x10^{-5}$ m/s. Note that the two images have different magnification.

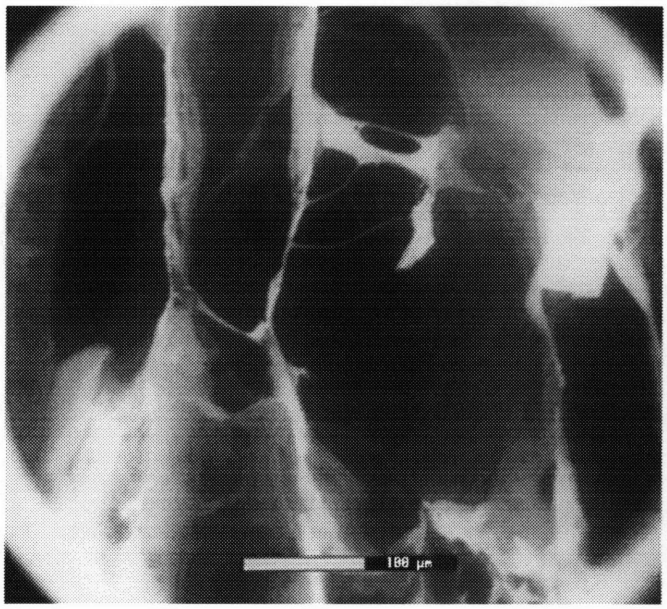

Figure 2.6a. ESEM image of CG matrix with large pores.

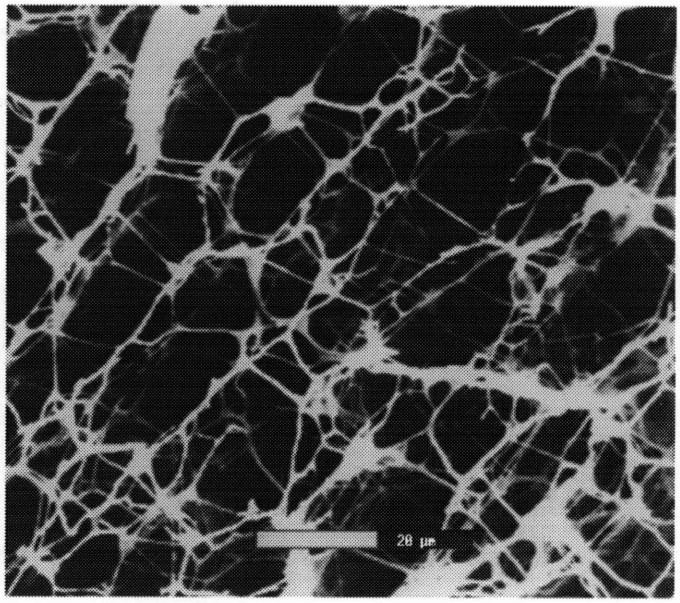

Figure 2.6b. ESEM image of CG Matrix with small pores.

2.3.2 Pore Channel Orientation

For the pore diameter analysis presented in the previous section, cylindrical CG matrix samples were viewed with ESEM in a direction along the long axis of the cylinder. To assess pore channel orientation, CG matrix samples were viewed with the ESEM longitudinally (i.e., cut in a direction perpendicular to the long axis of the cylinder). For each group of CG matrix samples produced with a particular combination of cooling bath temperature and lowering velocity, pore channel orientation was qualitatively categorized as 1) axially aligned, 2) radially aligned, or 3) no noticeable orientation. Table 2.2 on the following page summarizes pore orientation observations for the nine combinations of cooling bath temperature and lowering velocity.

Lowering Velocity (m/s)	Cooling Bath Temperature (Celsius) -80°C	-45°C	-10°C
$10x10^{-5}$ m/s	Axially Aligned	No Noticeable Orientation	No Noticeable Orientation
$5x10^{-5}$ m/s	Axially Aligned	Axially Aligned	Slight Radial Orientation
$2x10^{-5}$ m/s	Axially Aligned	Axially Aligned	Axially Aligned

Table 2.2. Pore orientation for different combinations of cooling bath temperature and lowering velocity

Table 2.2 illustrates the fact that cylindrical CG matrix can be produced with pores aligned parallel to the long axis of the cylinder. In most cases, the pores themselves were not elongated in a direction parallel to the long axis of the cylinder, but columns of pores form distinct channels which were aligned parallel to the long axis of the cylinder. An example of pore channels with random orientation is shown in Figure 2.7a below, and pore channels with axial alignment were shown in Figure 2.7b.

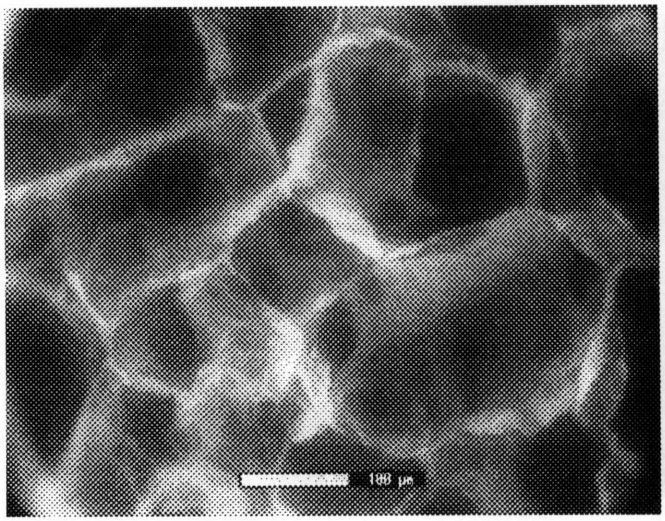

Figure 2.7a. ESEM image of CG matrix with random pore channel orientation.

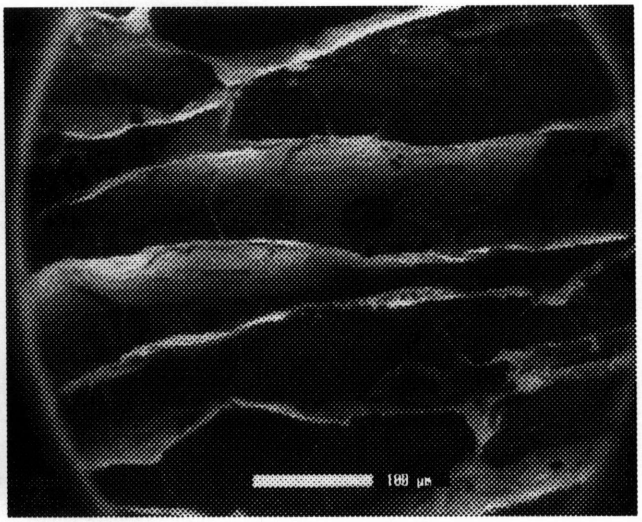

Figure 2.7b. ESEM image of CG Matrix with axially aligned pore channels.

2.4 Discussion

2.4.1 Effect of Cooling Bath Temperature on Pore Size and Pore Channel Orientation

The chart in Figure 2.8 on the following page illustrates the effect of cooling bath temperature on average pore size. In general, the larger pore sizes were produced using higher cooling bath temperatures. Smaller pore sizes result from lower temperatures.

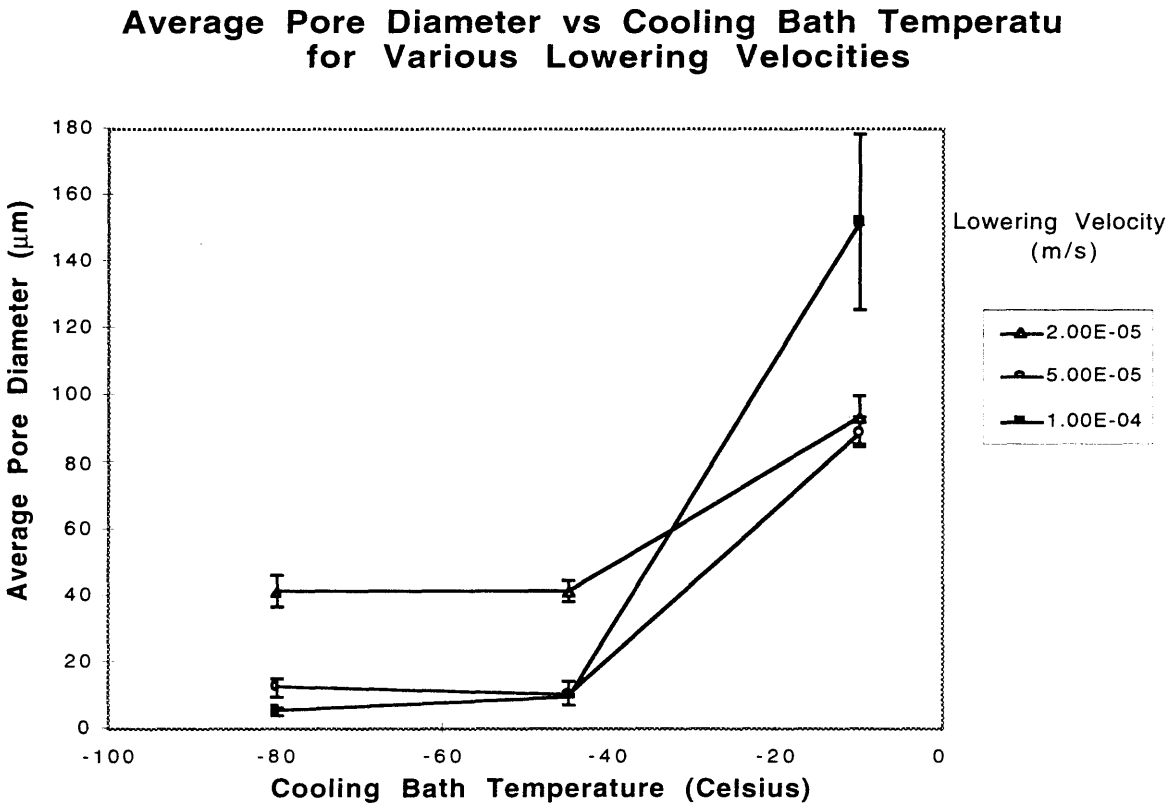

Figure 2.8. Chart illustrating the relationship between average pore diameter and cooling bath temperature for three lowering velocities.

The effect of cooling bath temperature on average pore size becomes more apparent at higher cooling bath temperatures. There was very little change in pore size with a change in cooling bath temperature from-80°C and -45°C (pore diameter changes from 19.7 µm to 20.6 µm averaged based on three levels of lowering velocity). However, there was a larger change in pore size cooling bath temperature was changed from -45°C to -10°C (pore diameter changes from 20.6 µm to 111.3 µm averaged across three lowering velocities).

With reference to Table 2.2, pore channel orientation tends to change from axially aligned to slightly radially aligned or no noticeable orientation with increasing cooling bath temperature. However, with the lowering velocity of $2x10^{-5}$ m/s, pore channels were axially aligned regardless of cooling bath temperature.

2.4.2 Effect of Lowering Velocity on Pore Size and Pore Channel Orientation

The chart in Figure 2.9 below illustrates the effect of lowering velocity on average pore size. The general trend was a decrease in pore diameter as the lowering velocity was changed from $2x10^{-5}$ m/s to $5x10^{-5}$ m/s (pore size decreases from 55.8 μm to 37.2 μm averaged across three cooling bath temperatures). However, as lowering velocity was changed from $5x10^{-5}$ m/s and $10x10^{-5}$ m/s there were mixed results; pore size increases when the cooling bath temperature was -10°C and decreases when the cooling bath temperature was -45°C or -80°C.

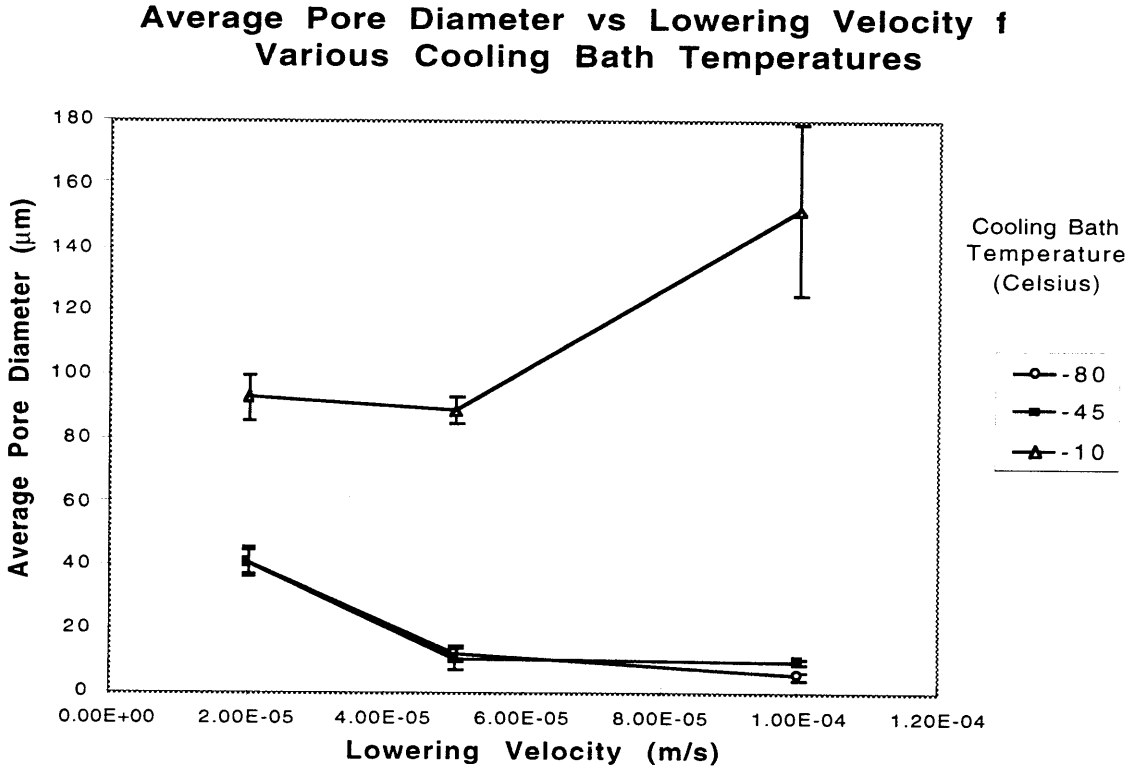

Figure 2.9. Chart illustrating the relationship between average pore diameter and lowering velocity for three cooling bath temperatures.

Referring to Table 2.2, increasing the lowering velocity tends to change pore channel orientation from axially aligned to slightly radially aligned or no noticeable orientation. However, with a cooling bath temperature of -80°C, pore channels were axially aligned with all lowering velocities ($2x10^{-5}$ m/s, $5x10^{-5}$ m/s, and $10x10^{-5}$ m/s).

2.4.3 Comparison to Previous Results

The relationship between manufacturing parameters and resulting pore structure of cylindrical CG matrix has been previously studied in this lab by Loree and Louie[52,54]. The conditions for the present study and those for previous studies differed in two respects. First, the source for collagen in previous experiments was USDA bovine hide, while the present study used Integra bovine tendon collagen. Second, the diameter of Loree's CG matrix was 1.5 mm, and the diameter of Louie's matrix was 3.8 mm. The diameter of CG matrix in this experiment was 3.0 mm. Loree and Louie separately established that for cylindrical CG matrix, there are two general links between manufacturing parameters and pore structure. Lower cooling bath temperatures result in small pores while higher temperatures result in larger pores. And, only certain combinations of cooling bath temperature and lowering velocity result in axially aligned pore channels. Despite the differences in source collagen and cylinder diameter, the results of this experiment agree with the findings of Loree and Louie.

Both Loree and Louie also found that certain combinations of cooling bath temperature and lowering velocity resulted in CG matrix with radially aligned pores. In this experiment, only one combination of temperature and velocity (-10°C and $5x10^{-5}$ m/s) resulted in pores with only a slight radial orientation.

2.5 Conclusions

Cylindrical specimens of CG matrix 3.0 mm in diameter were produced with pore size ranging between approximately 5 and 100 μm. With specific combinations of cooling bath temperature and lowering velocity, pore channels were aligned axially, aligned radially, or without noticeable orientation. To summarize the effects of cooling bath temperature on pore size and pore channel orientation: 1) an increase in cooling bath temperature tended to produce CG matrix with larger pores, and 2) pore channel orientation tended to be less axially aligned as cooling bath temperature was increased. To summarize the effects of lowering velocity on pore size and pore

channel orientation: 1) an increase in lowering velocity had mixed effects on average pore size depending on the cooling bath temperature, and 2) with respect to pore channel orientation, higher lowering velocities tended to form pore channels which were less axially aligned.

CG matrices of two specific pore geometries are desirable for use as spinal cord implants. CG matrix with small pores (average 5.48 μm diameter) and axially aligned pore channels was produced with a cooling bath temperature of -80°C and a lowering velocity of $10x10^{-5}$ m/s. CG matrix with large pores (average 93.1 μm in diameter) and axially aligned pore channels was produced with a cooling bath temperature of -10°C and a lowering velocity of $2x10^{-5}$ m/s.

CHAPTER 3: COMPARISON OF ANIMAL MODELS OF SPINAL CORD INJURY

3.1 Introduction

The overall goal of this project was to study the effect of collagen-based tubular implants on spinal cord healing. The specific focus of this chapter was the establishment of an animal model of spinal cord injury in which the effects of tubular implants can be evaluated.

3.1.1 Animal Models of Spinal Cord Injury

Numerous animal models have been used for the study of healing following spinal cord injury. The most common experimental animal is the rat, and this chapter will be focused on rat models. The most simple method of injuring the spinal cord is to impose damage to the spinal cord tissue by use of various mechanical devices. A number of methods have been used to cause damage. A blunt impact, which is referred to as contusion, is usually applied by dropping a weighted piston directly onto the spinal cord. This injury model has been characterized and used by several investigators[8,73,76,80]. An injury may also be created by crushing the spinal cord tissue using forceps. This injury type is referred to as compression and has been studied by other groups[33,61,75]. It is important to note that after contusion and compression injuries, although the spinal cord has been damaged, a geometrically continuous cord of necrotic tissue remains intact in the lesion site. A schematic of contusion and compression injuries is shown in figure 3.1 on the following page.

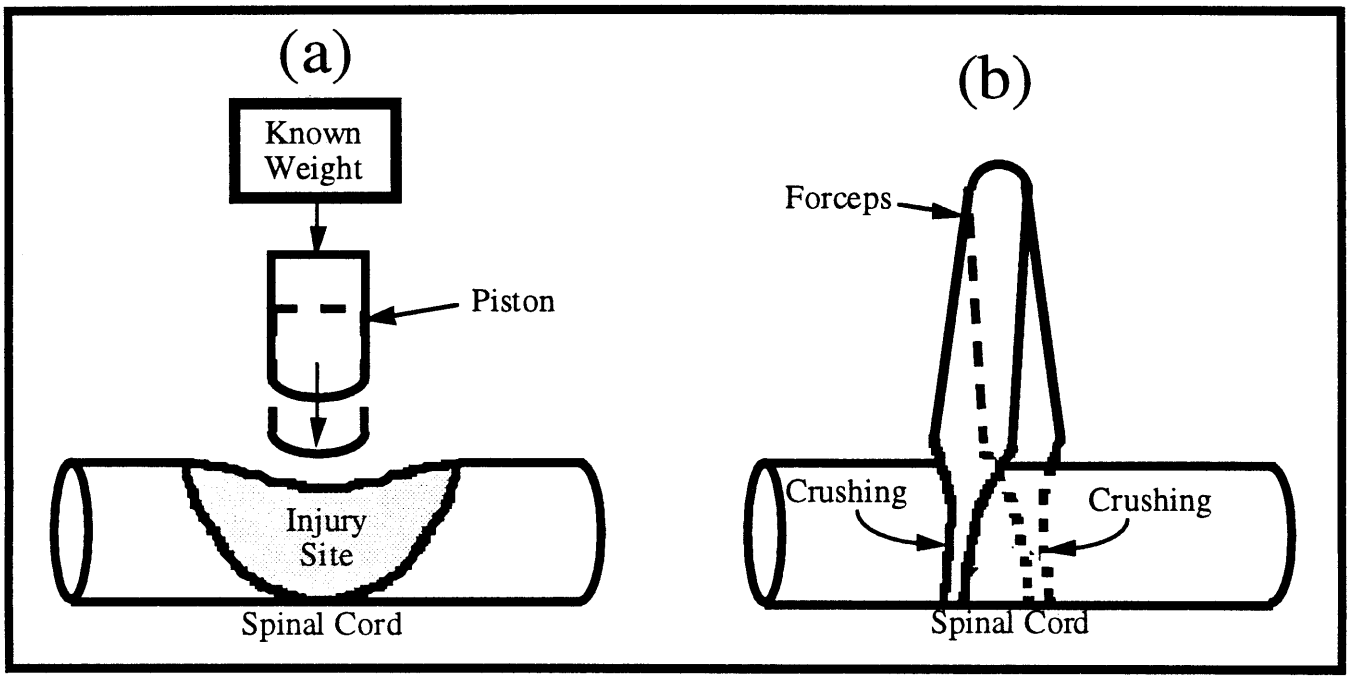

Figure 3.1. (a) Contusion and (b) compression spinal cord injury models.

Other methods of injuring the spinal cord involve directly severing the spinal cord tissue using a surgical blade. A surgical lesion may disrupt part of the spinal cord (partial transection or hemisection) or the entire spinal cord (complete transection). A hemisection model in which half of the spinal cord is cut has been used by many groups[10,36,63,68]. A complete transection model has been used by other investigators[29,45,59]. Another alternative surgical model of spinal cord injury is the complete transection of the cord with the subsequent removal of a length of spinal cord tissue. This type of injury is often referred to as a gap injury, since a segment of tissue has been completely removed. This model has been used in other laboratories[28,30,57,67,81]. Figure 3.2 on the following page shows schematics of (a) hemisection, (b) complete transection, and (c) gap surgical lesions. For reference, the diameter of the rat spinal cord (approximately 3 mm) is shown.

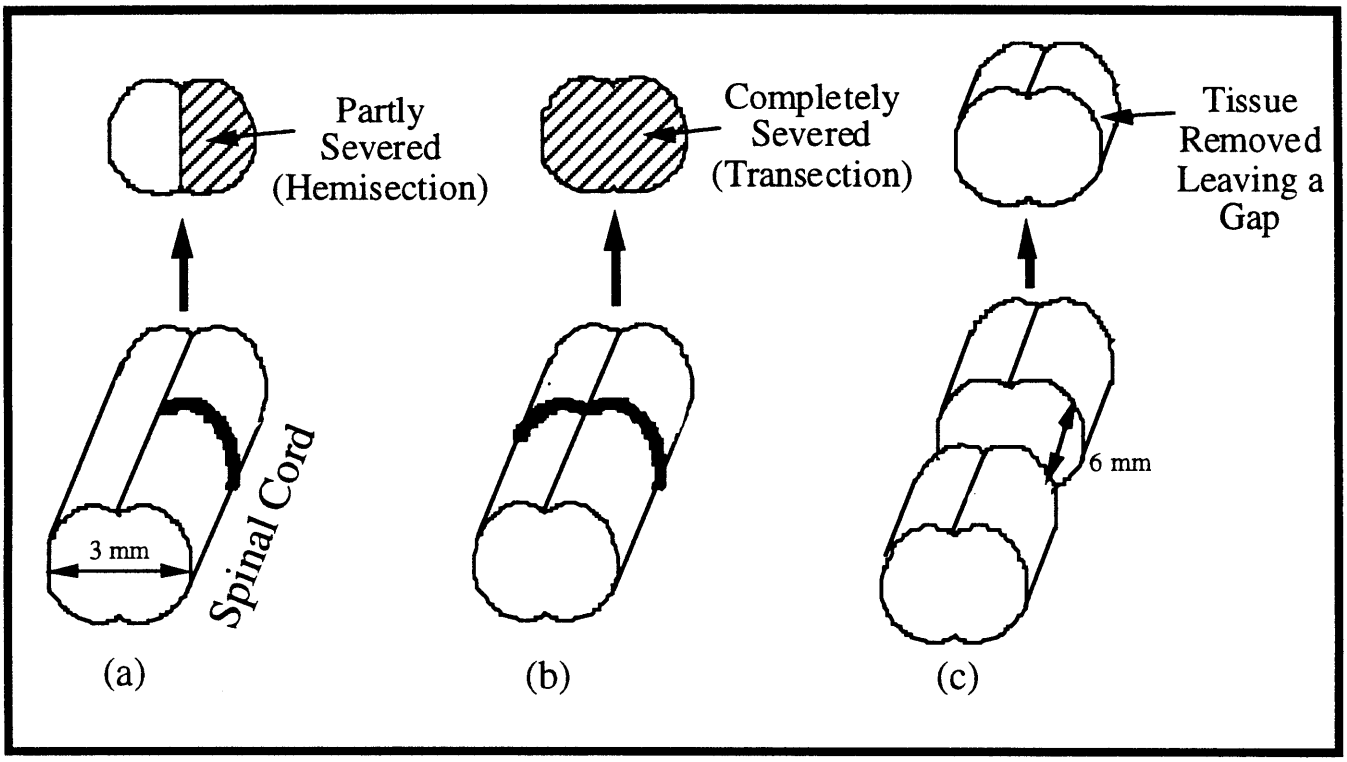

Figure 3.2. (a) Hemisection, (b) complete transection, and (c) gap lesions.

One goal of the research presented in this chapter was to compare different surgical models of spinal cord injury, specifically the hemisection, complete transection, and gap, from the viewpoint of the desired study of the effect of tubular implants on healing.

3.1.2 Device Implantation

Contusion and compression models closely simulate spinal cord injuries seen in human patients. However, since the tissue is crushed and not severed, injured spinal cord tissue remains at the injury site. The presence of injured tissue hinders the possible insertion of a graft or a device into the wound. For this reason, contusion or compression injury types were ruled out as possible models in which a tubular implant could be studied.

Surgical lesions (hemisection, complete transection, and gap) are more conducive to the use of implants since a space is created into which a device can be implanted. Hemisection and complete transection lesions create a narrow opening into which a thin disc-shaped implant can be

inserted (figure 3.3a and 3.3b). Gap injuries create a larger cavity into which a tubular implant can be inserted (figure 3.3c). Approximate dimensions are given for scale.

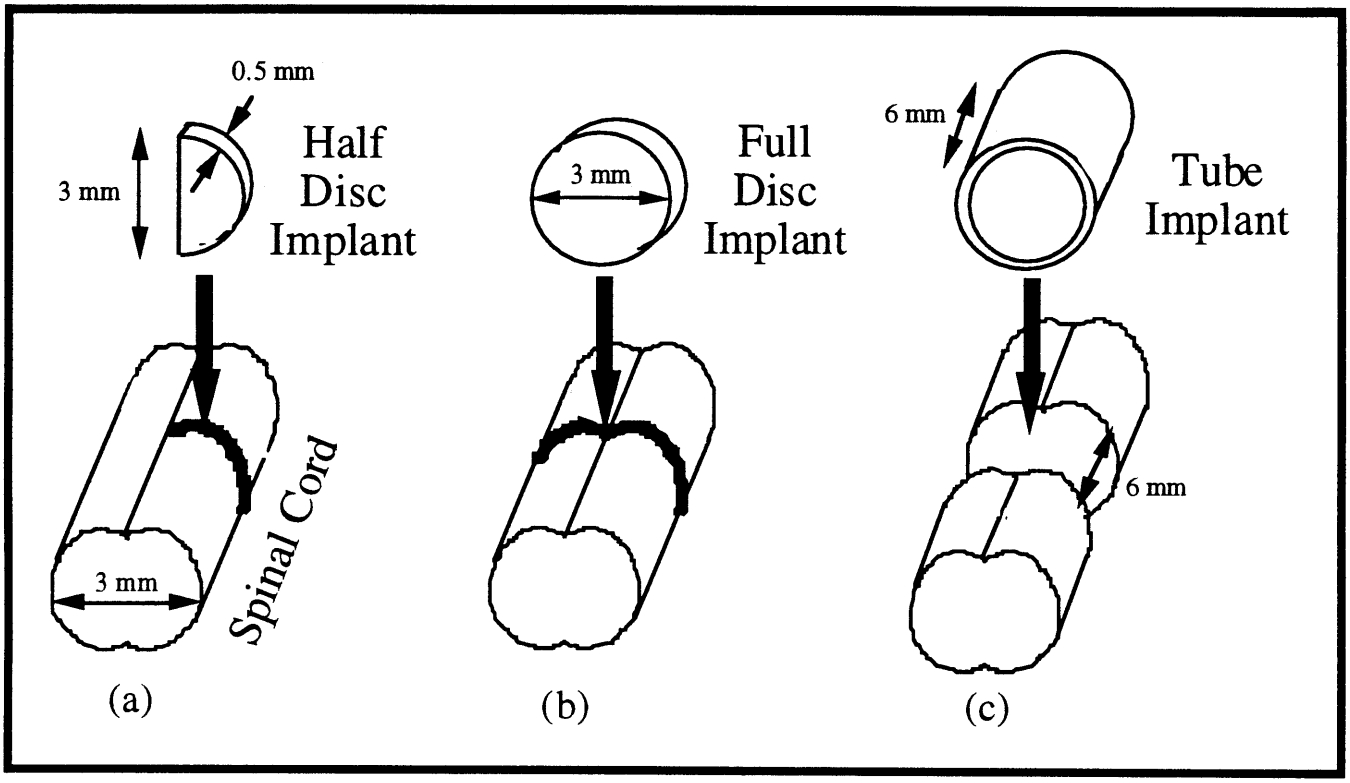

Figure 3.3. Implants for (a) hemisection, (b) complete transection, and (c) gap lesions.

A surgical lesion must be reproduced from one animal to the next. If a hemisection is performed, it is important that 50 percent of the tissue is severed consistently. If a complete transection is performed, it is important that the entire spinal cord is cut, since any tissue that remains intact in the wound site may be later mistaken as regenerated tissue. One purpose of the work presented in this chapter was to determine if spinal cord lesions can be reproducibly created and if it is feasible to deliver an implant device into such lesions.

3.1.3 Effects of Spinal Cord Injury on Animal Survival

Trauma to the mammalian spinal cord causes short and long-term physiological deficits. Animals temporarily lose reflex bladder function and lose voluntary motor function below the

lesion site. The initial trauma as well as the resulting deficits often result in death. Different lesion types may inflict more or less trauma and result in a higher or lower post-operative mortality rate. In choosing a surgical lesion, one important factor is the resulting animal death rate. For a useful lesion, an acceptable number of animals, of order of 50 percent, must survive to the end of a study period of at least 30 days.

3.1.4 Isolation of Spinal Cord Wounds from Adjacent Non-Neuronal Tissue

The invasion of dense fibrous scar tissue into spinal cord wounds has been shown to be an impediment to favorable healing and a barrier to the regrowth of axons[33,46,48,59]. Previous investigators have placed synthetic membranes over the dorsal aspect of the wound site as barriers to fibrous scar migrating into the wound from injured muscle tissue[36,48,68,81]. These synthetic membranes are effective in restricting invasion of scar tissue, but they are not resorbable and therefore would remain permanently in the wound site. A thin, non-porous, biodegradable collagen-GAG (CG) membrane, produced in this laboratory and referred to below as a CG dorsal barrier, was used to prevent invasion of scar from the wounded muscle tissue immediately adjacent to the injured cord.

3.1.5 Objectives of Work in this Chapter

To summarize, the general goal of the work described in this chapter was to compare different lesion types with the purpose of establishing an animal model for the study of spinal cord. Hemisection, complete transection, and gap lesions were studied with or without the addition of a CG dorsal barrier. The following parameters for a satisfactory animal model were assessed in this study: 1) satisfactory animal survival and maintenance; 2) animal-to-animal reproducibility of the lesion; and 3) feasibility of implantation of test devices.

3.2 Materials and Methods

3.2.1 Experimental Groups

The specific aims of the research discussed in this chapter are two fold. First, three surgical injuries to the rat spinal cord were compared (hemisection, complete transection, and gap). Second, the effectiveness of a non-porous CG dorsal barrier in reducing the ingrowth of fibrous scar tissue was studied. With this purpose, a total of 25 experimental animals were grouped as shown in Table 3.1. Animals were allowed to survive for 5 weeks.

Surgical Lesion	CG Dorsal Barrier	
	A. No	B. Yes
I. Hemi-section	Group IA n=4	Group IB n=4
II. Complete Transection	Group IIA n=6	Group IIB n=5
III. 6-mm Gap	Group IIIA n=3	Group IIIB n=3

Table 3.1. Experimental Groups

3.2.2 Preparation of CG Dorsal Barrier

The CG dorsal barrier was manufactured from the collagen-GAG suspension described in the previous chapter (section 2.2.1). A detailed protocol for preparation of the suspension is located in appendix A. The suspension was degassed for 15 minutes in a 6-liter vacuum flask attached to a vacuum pump at 30 mm Hg. The degassed suspension was poured into a shallow

plastic weigh boat, (Catalog #12577-027, VWR Scientific, Boston, MA) taking care not to create bubbles as the suspension was poured. To produce a collagen membrane 0.005" thick, 3.5 ml of collagen-GAG suspension was poured for every square centimeter of weigh boat area. The collagen-GAG suspension contained in the weigh boat was placed in the laminar flow hood (Sterigard Hood, Model #VBM-400, The Baker Company Inc., Sanford, ME) to evaporate at room temperature in the absence of airborne particles. Following evaporation and drying, the shallow pool of suspension was transformed to a thin, non-porous membrane. Drying was complete in 72 hours. In preparation for dehydrothermal (DHT) treatment, the CG dorsal barrier was placed in packets made from aluminum foil. Each packet was placed in a vacuum oven (Fisher Isotemp vacuum oven, Fisher Scientific, Medford, MA) for 24 hours at a vacuum of 30 mm Hg and a temperature of 105°C. DHT treatment effectively sterilizes the collagen-GAG film, and produces covalent crosslinks between polymer chains[82]. Care must be taken to expose the film to temperature of 105°C only after the moisture content of the film has been previously reduced below 10 weight-percent in order to prevent melting of the collagen triple helix to gelation at this temperature level[83].

Sterile rectangles of CG dorsal barrier 12 mm x 8 mm were prepared for surgery in a laminar flow hood (Relialab, Tenney Engineering Inc., Union, NJ) using sterile gloves, gown, mask, and instruments. A detailed protocol for sterile CG dorsal barrier preparation is located in appendix A. Rectangular segments of dry membrane 12 mm x 8 mm were cut using sterilized scissors and forceps. Each segment was immersed briefly in sterile 100 percent ethanol followed by two rinses in sterile phosphate buffered saline (PBS mix packets, Sigma, St. Louis, MO). Segments of collagen-GAG membrane were placed in sterile glass vials containing sterile PBS. Bottles were maintained sterile until surgery by storage in sealed sterile bags (Sterile Sampling Bags, Fisher Scientific, Pittsburgh, PA).

3.2.3 Surgical Procedure and Post-operative Care

The animals used in this experiment were adult female Sprague-Dawley rats weighing 250-350 grams (Taconic, Germantown, NY). Rats were anesthetized by intraperitoneal injection of sodium pentobarbital (Nembutal solution, 50 mg/ml, Abbot Laboratories, North Chicago, IL) with a dosage of 45 mg per kilogram of animal body weight. In some animals an additional injection of 0.05 cc Nembutal solution was necessary to obtain sufficient anesthesia. While unconscious, each animal's back was shaved and cleaned with Betadine disinfectant scrub (Redi Products, Prichard, WV). The animal was positioned lying prone on a flat operating board with all four limbs gently constrained in an extended position by use of rubber bands. The thoracic region of the spine was slightly elevated by placing a gauze pad under the chest of the animal.

Surgical procedures were performed under aseptic conditions in room 101 of the West Roxbury Veterans Administration Medical Center animal facility, West Roxbury, MA. A longitudinal incision, 2 inches long was made through the skin along the animal's back beginning between the shoulder blades and terminating just below the rib-cage. The underlying musculature was incised and retracted laterally exposing the dorsal aspect of the bones of the spinal column. The thoracic 7-9 segments of the spine were identified by measuring the distance away from the interscapular fat pad and by counting the number of vertebral segments away from the termination of the rib-cage at thoracic 13. The dorsal half of each vertebral segment (thoracic 7, 8, and 9) was removed using bone rongeurs and fine surgical scissors. This process, known as a laminectomy, exposes the spinal cord ensheathed in the dura mater. Minor bleeding was controlled using Gelfoam (The Upjohn Co., Kalamazoo, MI), and excessive bleeding was stopped using a bipolar cautery (ValleyLab Inc., Boulder, CO). Local anesthesia was provided as necessary by dripping 1 percent Lidocaine (Abbot Laboratories, North Chicago, IL) into the wound.

The dura mater of segments thoracic 7-9 was incised at the midline using a number 11 blade. Groups of rats were given one of three different surgical lesions as follows (see section 3.1.1 of this thesis for a schematic diagram of each lesion). Hemisection lesions were created at thoracic 7 by plunging a number 11 blade vertically into the center of the cord and pulling it

laterally away from the center severing half of the spinal cord. Complete transections were produced by running the blade transversely through the entire spinal cord while maintaining contact between the tip of the blade and the underlying spinal bones. A 6-mm gap was created by completely severing the spinal cord at levels of approximately thoracic 7 and 9 and removing enough intervening tissue to create a 6-mm gap. The cavity was filled with Gelfoam (The Upjohn Co., Kalamazoo, MI).

Depending on the experimental group to which each animal belonged, the lesion either remained uncovered or was covered dorsally with a CG dorsal barrier described in the preceding section. The membrane was placed over the spinal cord in a blanket-like fashion covering the entire wound bed as shown in Figure 3.4 below.

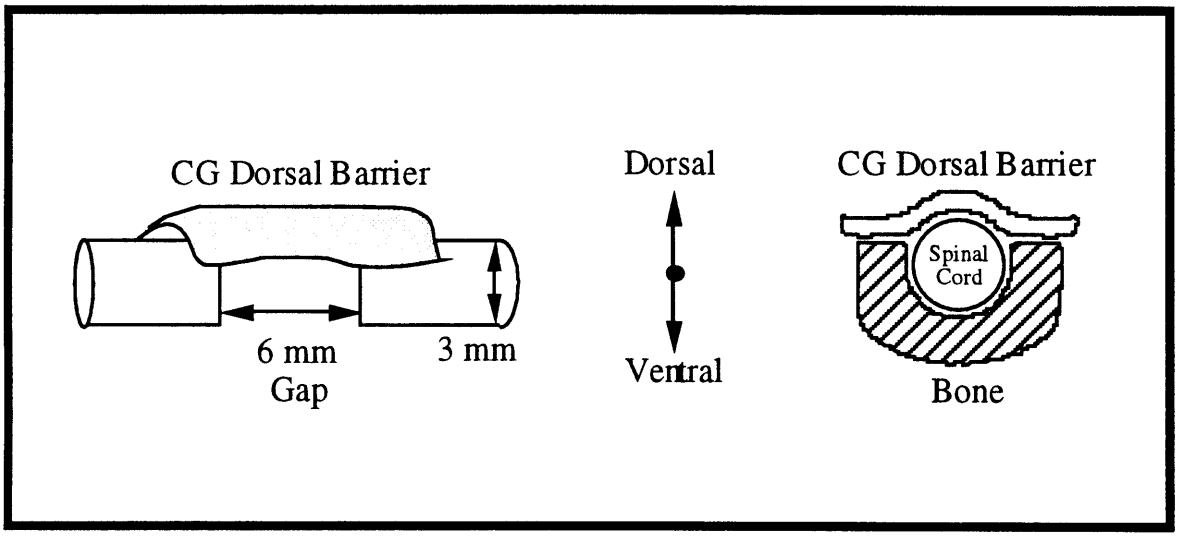

Figure 3.4. Schematic of CG dorsal barrier covering a 6-mm gap lesion.

The function of the barrier was to isolate the wound site from invasion by scar tissue originating from muscle tissue, adjacent to the injured cord, which was damaged during the surgical procedure. Muscle and skin were then closed in layers using 4-0 vicryl sutures (Johnson & Johnson, Sommerville, NJ) and wound clips.

Animals were housed and cared for post-operatively in room 6 of the West Roxbury Veterans Administration Hospital animal facility. Unconscious rats were placed on a mild heating pad for about 6 hours until alert and able to move about the cage. Following injury to the spinal

cord, animals lost function of their lower limbs but maintained adequate mobility, grooming, and access to food and water by use of the forelimbs. Animals also temporarily lost reflex bladder function. For this reason, bladders were voided manually twice daily until reflex function returned, usually within 2 weeks.

Rats were routinely inspected 4-5 times daily for the first week and twice daily thereafter for signs of urine scalding and pressure sores. When needed, the skin and fur was washed with water and Betadine and gently dried. Daily subcutaneous injections of 5 ml lactated Ringer's solution were given for the first two days to compensate for fluids lost during surgery. Antibiotics were not administered in this study. Any rats showing continuously poor physical condition were euthanized by carbon dioxide inhalation.

3.2.4 Animal Sacrifice

At 5 weeks post-operative, rats were deeply anesthetized by intraperitoneal injection of sodium pentobarbital (Nembutal solution, 50 mg/ml, Abbott Laboratories, North Chicago, IL) with a dosage of 55 mg per kg of animal body weight. Each rat was positioned with chest exposed lying on its back in a rectangular Pyrex dish. The forelimbs were gently constrained in an extended position with surgical tape. The skin and abdominal cavity just below the ribcage were opened using dissecting scissors. The ribs were cut, and the chest was opened along the sternum using heavy scissors, exposing the heart. An 18 gauge needle connected to I.V. tubing was inserted into the left ventricle without entering the right ventricle or exiting the heart chamber. 200 ml of cold heparinized saline (20 units heparin per ml of PBS) was perfused through the left ventricle with the reservoir of perfusate elevated at a height of 1 meter above the animal. Heparinized saline was prepared by injecting 20,000 units of heparin (Abbot Laboratories, North Chicago, IL) into a 1 liter I.V. bag of phosphate buffered saline (PBS). Just as the perfusate began to flow, the right atrium of the heart was punctured using dissecting scissors allowing body fluids to exit. The saline solution was immediately followed by 150 ml of Yannof's fixative. (Detailed Protocols can be found in appendix A).

Following perfusion, the original skin incision was located. The skin and musculature were reopened using a scalpel. In order to expose a 2-cm segment of the spinal cord, the dorsal aspect of four additional vertebrae were removed. The exact location of the original spinal cord lesion was identified. A 15-mm segment of the spinal cord was removed with the lesion site at the center of the segment. The removed tissue was further fixed in Yannof's fixative for an additional 24 hours at 4°C followed by 10 percent neutral buffered formalin for 24 hours in preparation for embedding and histological processing.

3.2.5 Histological Processing

Each spinal cord tissue segment was removed from fixative and rinsed thoroughly in PBS. The tissue was dehydrated by soaking in a series of graded ethanol solutions and prepared for embedding in paraffin by soaking in two rinses of xylenes (Mallinckrodt Chemical, Paris, KY). The tissue was infiltrated for 30 minutes in two baths of liquid paraffin (Paraplast+, Oxford Labware, St. Louis, MO) maintained between 57 and 60°C. The tissue was then oriented for longitudinal sectioning in a paraffin block and solidified by placing in the refrigerator at 4°C for 24 hours. Detailed protocols for paraffin embedding are located in appendix A.

Longitudinal sections were cut at 10-15 μm on a microtome (model 1512, Leitz-Wetzlar, Easton, MA) and floated on water maintained at 46°C in a heated water bath (Lo Boy, Lab-Line Instruments, Inc., Melrose Park, IL). Tissue sections were captured on glass microscope slides (Gold Seal Rite-on, Gold Seal Products, Highland Park, IL) and placed in a dehydrating oven (Harvest Maid, Alternative Pioneering Systems Inc., Chaska, MN) at 45°C for 24 hours to ensure adhesion of the tissue to the glass slides. Slides were pre-treated with poly-L-lysine solution (catalog #P8920, Sigma Diagnostics, St. Louis, MO) to enhance tissue adhesion. Sections were cleared in xylenes and rehydrated through graded ethanol solutions and stained with hematoxylin and eosin (H&E) or Masson's trichrome. Following staining, slides were dehydrated through graded ethanol, cleared with xylenes and coverslipped with Permount (Fisher Scientific, Fair Lawn, NJ). Detailed protocols for histological staining can be found in appendix A.

3.2.6 Data Collection

Post-operative animal survival rate was measured as the fraction of animals in any particular group which survived the entire predetermined 5-week study period. The number of days required to regain reflex bladder function was also recorded. An animal was considered to have regained bladder function when the bladder was found empty before manual voiding for one or more consecutive days.

Examination of histological tissue sections was performed on a light microscope (Optiphot, Nikon, Tokyo, Japan), and photomicrographs were generated on 35-mm film with the aid of a photographic attachment (Microflex AFX-IIA, Nikon, Tokyo, Japan). For each animal, a number of longitudinal sections were examined to determine the extent of the lesion. This data was expressed as the percent of the spinal cord cross section area that was severed (% lesion area) averaged over several histological sections for each animal.

Tissue sections stained with Masson's trichrome were used to assess collagenous scar tissue formed at the wound site. Tissue from each animal was qualitatively scored on a scale from 0 to 5 based on the amount of fibrous scar tissue found within the lesion. A score of 0 corresponds to minimal scarring, and a score of 5 corresponds to severe scarring. Numerical scores were used to make qualitative comparisons among groups.

During the surgical procedure, sample implant devices were tested in order to determine if it is possible to insert a device into each lesion type. After each lesion was created, the surgeon attempted to insert an implant of the appropriate shape (see section 3.1.2) into the lesion. These implants were immediately removed and discarded. The purpose of this was not to test the long-term effects of implantable devices, but only to determine if each lesion type lends itself to the insertion of an implant device.

3.3 Results

3.3.1 Animal Survival and Bladder Function

Of the 25 animals included in this experiment 13 survived the entire 5-week study period, which gives an overall survival rate of 52 percent. Table 3.2, below, shows the survival rate of animals divided by experimental group.

Surgical Lesion	CG Dorsal Barrier	
	A. No	B. Yes
I. Hemi-section	50%	75%
II. Complete Transection	50%	40%
III. 6-mm Gap	33%	67%

Table 3.2. Survival Rate by Experimental Group

Animals which survived the surgical procedure regained bladder function between 1 and 20 days post-operative. Over all animals, the average time required was 8.4 days. Table 3.3 below shows the number of days before return of bladder reflex for animals in each experimental group.

Surgical Lesion	CG Dorsal Barrier	
	A. No	B. Yes
I. Hemi-section	1.0 days	2.7 days
II. Complete Transection	8.7 days	16.0 days
III. 6-mm Gap	20.0 days	10.5 days

Table 3.3. Number of Days Before Return of Reflex Bladder Function

3.3.2 Gross Observations

Upon removal of spinal cord tissue at 5 weeks post-operative, the lesion was grossly identifiable by the presence of fibrous scar tissue. The lesion site comprised translucent tissue in contrast to the opaque white appearance of intact healthy spinal cord. In animals which received complete transection or gap injuries, fibrous tissue was found filling the wound, physically connecting the rostral and caudal spinal cord stumps. A segment of spinal cord which included the wound site was easily removed as one continuous piece.

3.3.3 Histological Observations

Measurements of the size of each lesion were made from histological sections. For animals receiving hemisection lesions, the goal was to reproducibly cut through 50 percent of the spinal cord cross section. In the 8 animals with hemisection lesions, between 36 and 56 percent of the tissue was actually severed with an average of 45 percent. For animals receiving a complete transection lesion, the goal was to completely sever the spinal cord in every animal. Of the 11 animals receiving a complete transection lesion, histology confirmed that the spinal cord was completely severed in only 10 animals. In the one remaining animal, 20 percent of the spinal cord remained intact. For animals receiving a gap lesion, the spinal cord was completely transected, and a 6-mm segment of cord was removed, leaving a clear gap. Histological observation confirmed that the spinal cord was completely severed in all 6 of the animals in this group.

Examination of trichrome stained tissue revealed that fibrous scar tissue was found in the wound site of all animals. Scar tissue fibers were predominantly oriented in a direction transverse to the spinal cord axis. A representative lesion site from an animal which received a hemisection lesion with a CG dorsal barrier (Group IB) is shown in Figure 3.5 below. Fibrous scar tissue (S) is stained blue, and intact spinal cord is stained red.

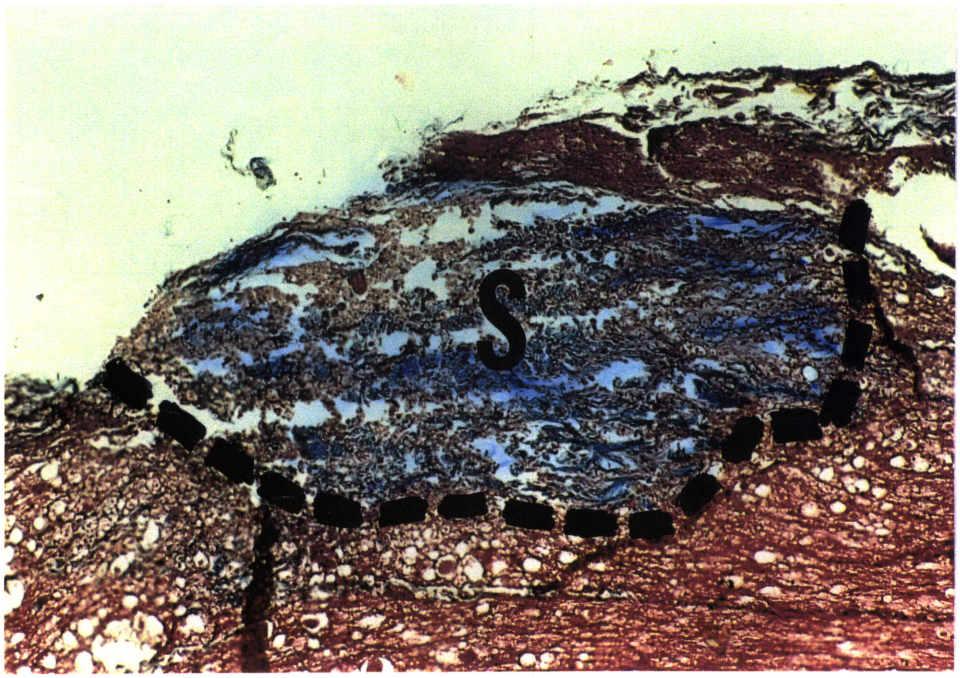

Figure 3.5. Fibrous scar filling a spinal cord wound.

As described in section 3.2.6, the tissue of each animal was given a qualitative score between 0 and 5 based on the amount of fibrous scar found in the wound site. The results of scoring for fibrous scar for each experimental group are summarized in Table 3.4 below. The score for each group is the average of all animals in that particular group.

Surgical Lesion	CG Dorsal Barrier	
	A. No	B. Yes
I. Hemi-section	2.5	1.0
II. Complete Transection	4.3	2.5
III. 6-mm Gap	4.0	3.5

Table 3.4. Scoring for Scar Tissue by Experimental Group

3.3.4 Device Implantation

As described in section 3.2.6, each lesion type (hemisection, complete transection, and gap) was evaluated for the feasibility of implanting various experimental devices. For reference, the diameter of the rat spinal cord is approximately 3 mm. Hemisection and complete transection procedures generate a very small cavity (less than 0.5 mm wide) between the two cut ends due to slight retraction of the cord after cutting. The implant devices which fit these cavities (ref. Figure 3.3) are also extremely small (3.0 mm x 0.5 mm). The surgeon found it very difficult to handle

the small implants which fit into hemisection and complete transection lesions. In the surgeon's opinion, the gap lesion was the most favorable for the implantation of a device. The large 6-mm gap allowed sufficient space for a much larger implant device (6.0 mm x 3.0 mm) which the surgeon could easily handle with forceps, insert, and position within the wound.

3.4 Discussion

3.4.1 Animal Survival and Bladder Function

When animals were grouped together by lesion type only (regardless of CG dorsal barrier), the group receiving hemisection lesions showed a post-operative survival rate of 63 percent, animals receiving complete transection lesions had a survival rate of 46 percent, and animals receiving 6-mm gap lesions had a survival rate of 50 percent. This data shows that neither of the three lesion types resulted in a survival rate substantially different from the overall survival rate of 52 percent.

Data for the number of days required to regain reflex bladder function show that animals in the hemisection group recovered bladder function in an average of 2.0 days, the complete transection group in 11.6 days, and the 6-mm gap lesion group in 13.7 days . The difference between hemisection and complete transection was statistically significant ($p=0.001$, student's "t" test), as was the difference between hemisection and gap lesions ($p=0.003$, student's "t" test). The difference between the complete transection and 6-mm gap groups was not statistically significant ($p=0.6$). These data show a trend of increasing time for bladder recovery with increasing severity of the lesion.

When animals are grouped together depending on the use of the CG dorsal barrier (regardless of lesion type), animals with a CG dorsal barrier had a slightly higher survival rate (58 percent) than animals without a CG dorsal barrier (46 percent). However, animals with a CG dorsal barrier recovered reflex bladder function slower (8.7 days) than animals without a CG dorsal barrier (8.0 days). These differences between groups were not statistically significant.

3.4.2 Lesion Reproducibility

Based on the histological findings, the gap lesion is the most reproducible. The spinal cord was completely severed in all animals of that group. With a 6-mm gap, it was easy to visually verify that the spinal cord was completely severed at the time of surgery. The complete transection lesion was less repeatable, as illustrated by the fact that the spinal cord was not completely severed in one animal of that group. The surgeon found that it was more difficult to visually verify that the spinal cord was completely cut when a gap was not created. The hemisection lesion was the least repeatable. As little as 36 percent or as much as 56 percent of the cord was severed in some animals. This amount of variation away from the desired 50 percent was deemed to be unacceptably large.

3.4.3 Device Implantation

The surgeon was not able to effectively implant devices into hemisection or complete transection lesions due to the small size of the implants (refer to section 3.3.4 and Figure 3.3). Since the overall goal of this project is to study the use of various devices in the spinal cord, this finding eliminates hemisection and complete transection lesions as options for this study.

The gap lesion most easily lends itself to the implantation of a device. The large size of the lesion allows for a larger device which is preferred by the surgeon for handling.

3.4.4 The CG Dorsal Barrier and Fibrous Scar Formation

Hemisection lesions showed the least amount of fibrous scar tissue formed at the wound site (score of 2.5 without the CG dorsal barrier and 1.0 with it in place). This is expected, since less damage is initially caused by a hemisection than by a complete transection or a gap. The scores for scar tissue for the complete transection (4.3 without CG dorsal barrier and 2.5 with it in place) were similar to the scores for the 6-mm gap group (4.0 without CG dorsal barrier and 3.5 with it in place).

Within each lesion group (hemisection, complete transection, and gap), animals with a CG dorsal barrier had lower average scores for fibrous scar (see Table 3.4). This confirms the results of previous studies in which synthetic membranes were used as barriers against the invasion of fibrous scar into spinal cord wounds[36,48,68,81]. Figure 3.6 on the following page shows a complete transection lesion site which was not covered with a CG dorsal barrier at 5 weeks post-operative. Figure 3.7 on the following page shows a complete transection which was covered with a CG dorsal barrier. The wound which was covered with a dorsal barrier contains less fibrous scar (stained intensely blue by Masson's trichrome).

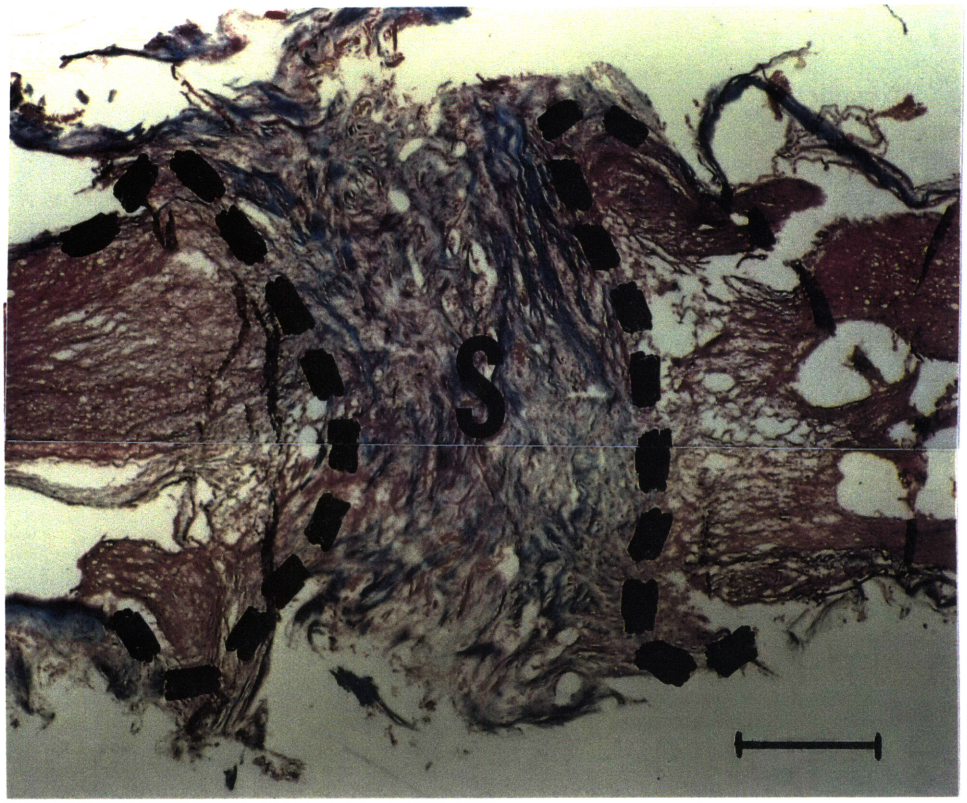

Figure 3.6. Tissue from an animal receiving a complete transection without CG dorsal barrier. Stained with Masson's trichrome. A large amount of fibrous scar (S) has formed in the wound site (outlined by dashes). Scale bar is 1.0 mm.

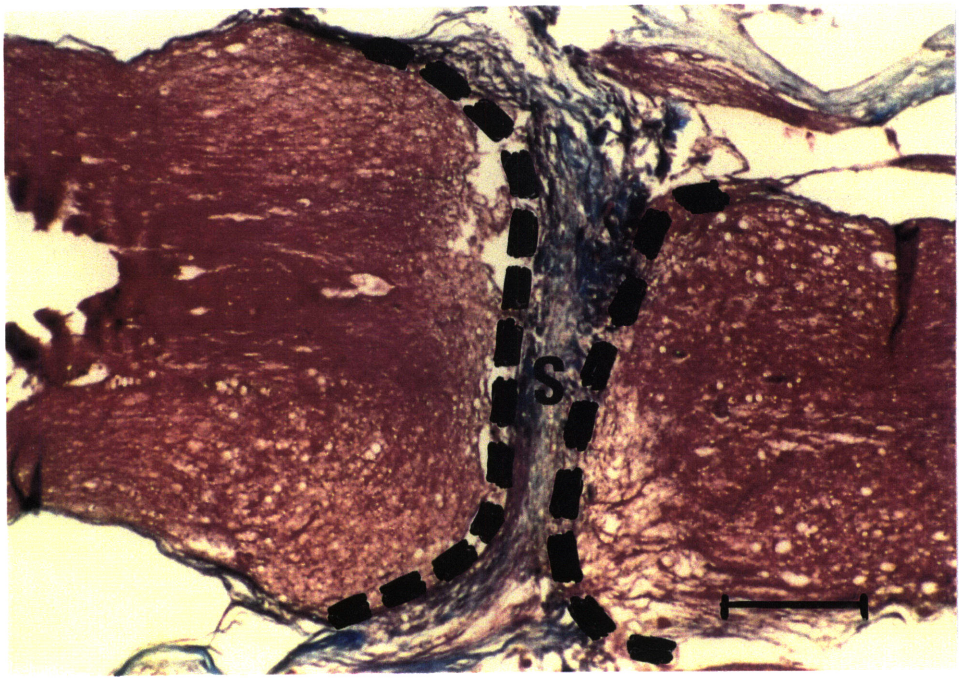

Figure 3.7. Tissue from an animal receiving a complete transection with a CG dorsal barrier. Stainedwith Masson's trichrome. Less fibrous scar (S) is found within the wound site (outlined by dashes). Scale bar is 1.0 mm.

3.5 Conclusions

Based on the results of this study, the 6-mm gap lesion was found to be the most suited to our purposes. The post-operative animal survival rate (50 percent) was acceptable, and all animals regained bladder function within a reasonable amount of time (average of 10.5 days). The size of this lesion was reproducible, and, during the surgical procedure, it was possible to visually verify that the spinal cord has been completely severed. It was also relatively simple to insert an experimental implant device into a 6-mm lesion cavity, which was not the case with hemisection and complete transection lesions.

Use of a CG dorsal barrier limited the invasion of fibrous scar tissue into spinal cord lesions. As discussed in section 3.1.4, reducing the presence of fibrous scar at the site of the wound has been associated in the literature with a positive healing response. However, the CG dorsal barrier was not able to eliminate invasion of fibrous scar.

In conclusion, a 6-mm spinal cord gap with a CG dorsal barrier can provide an animal model in which the effects of experimental implant devices can be tested.

CHAPTER 4: IMPLANTATION OF TUBULAR DEVICES INTO THE INJURED ADULT RAT SPINAL CORD

4.1 Introduction

In chapter 3, an animal model of spinal cord injury was established. This model consisted of a 6-mm gap in the thoracic spinal cord of the adult rat. The goal of the work presented in this chapter was to use this model to examine the effects of fully resorbable devices on spinal cord healing. These devices consisted of collagen tubes which either remained empty or were filled with collagen-glycosaminoglycan (collagen-GAG) matrix. The rationale for using a collagen tube and the collagen-GAG matrix is discussed in sections 4.1.1 and 4.1.2 below.

4.1.1 Use of Tubes to Repair Peripheral and Central Nervous System Injury

Peripheral Nervous System (PNS)

Tubes were first used to repair the injured peripheral nervous system (PNS) in the late 1800s when Glück used a tube derived from decalcified bone to connect the injured nerve stumps. Glück was not successful in restoring function to the denervated region, however, contemporary investigators have used tubes composed of numerous materials with varying degrees of success. Other tube materials from animal tissue sources have included arteries[16], veins[23], and preformed mesothelia[55]. Synthetic tubes have been composed of nylon/millipore[6], silicone[78], and polysulfone[1]. Synthetic tubes have the disadvantage that they are not resorbed by the body and must eventually be removed. Recent studies have investigated the possibility of using degradable tubes which would be eventually resorbed by the body. Degradable tubes have been formed from collagen[3,17,49], polyglactin[62], polyglycolic acid[77], and polylactic acid[2]. Tubes implanted at the site of peripheral nerve injury perform three important functions: 1) isolate the nerve injury site from invasion by non-nervous tissue originating from sources outside the injured nerve; 2) allow trophic factors produced by the injured nerve to accumulate; 3) they direct the regrowth of nerve tissue (including axons) toward the distal stump[56].

Central Nervous System (CNS)

The implantation of tubes into spinal cord lesions has been studied by investigators as early as 1957[14]. As discussed in the introduction, axons of the central nervous system show little capacity to spontaneously regenerate, and functional connections are not restored. Investigators have shown that a limited number of spinal cord axons regrow with the aid of tube implants, but a return of function has not been demonstrated. Tubes implanted in the spinal cord have been composed of many substances: nylon/millipore[6,14], PAN-PVC[81], and polycarbonate[63]. None of these tube materials are resorbable within the body. To date, the implantation of resorbable tubes into spinal cord lesions has not been studied.

We hypothesize that, in a similar fashion to peripheral nerves, entubulating the site of a spinal cord injury serves three purposes: 1) isolate the wound site from invading non-neural tissue; 2) contain trophic factors produced by the injured spinal cord stumps; and 3) orient the regrowth of spinal cord tissue to connect the injured stumps. Entubulating the site of spinal cord injury would also provide an isolated experimental system which consists of the injured spinal cord stumps and the gap between them.

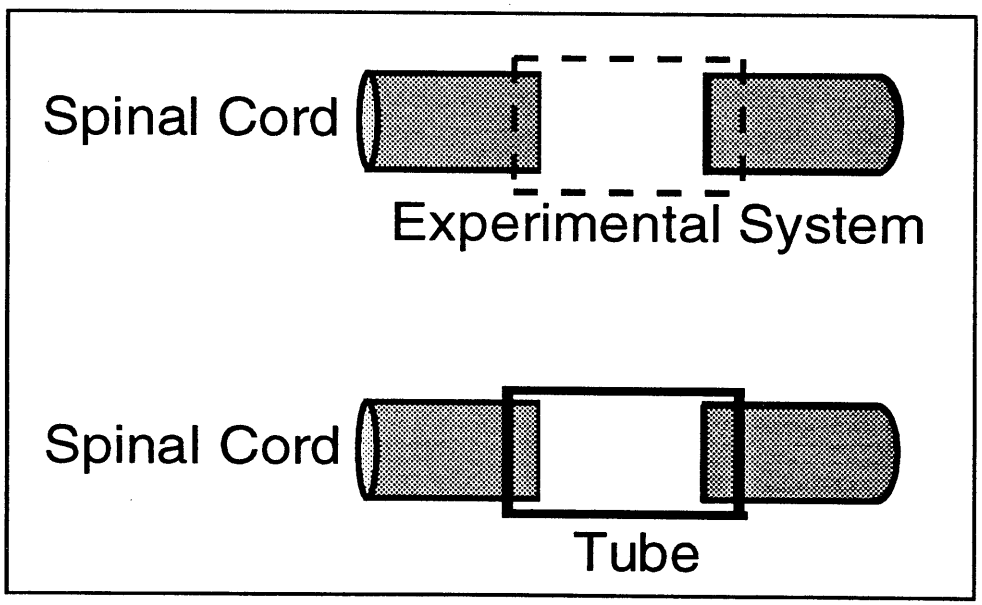

Figure 4.1. Isolation of spinal cord injury: Experimental system.

This closed system can be used to test the effects of exogenous influences which may be introduced into the tube. In this chapter, two collagen-GAG matrices of different pore structure were implanted within the tube.

4.1.2 Substrate Preferences of Regrowing Axons

One factor which may contribute to the inability of central nervous system axons to regrow over significant distances within a lesion may be the absence of an appropriate substrate capable of supporting the advancement of axon growth cones. Studies *in vitro* have shown that CNS axons require a specific environment for regrowth[11,47,60]. Other studies have demonstrated that the direction of axon outgrowth can be controlled *in vitro* by providing an aligned substrate material[44]. The regrowth of spinal cord axons along an aligned substrate has also been documented *in vivo* [45,81].

Previous work in this laboratory has shown that injured axons in the peripheral nervous system (PNS) are able to regenerate across a 15-mm gap in the rat sciatic nerve when the gap is bridged with a silicone tube containing a collagen-GAG matrix[88]. Axons did not regrow across the gap when the collagen-GAG matrix substrate was not present within the tube. In a more recent study, a 10-mm gap in the rat sciatic nerve was bridged with a silicone tube filled with collagen-GAG matrix with pore channels aligned along the axis of the nerve. The regenerative response was enhanced by the use of collagen-GAG substrate with aligned pore channels[18,19,53]. This study also established that PNS axon regrowth supported by collagen-GAG matrix depends on the pore structure of the matrix. Collagen-GAG matrix with small pores (5-10 μm average pore diameter) promotes more efficient regrowth of peripheral nerve axons then collagen-GAG matrix with large pores (60-300 μm average pore diameter)[19,20].

The success of tubes filled with collagen-GAG matrix in promoting the regrowth of PNS axons suggests that a similar implant device may be capable of promoting the regrowth of spinal cord axons. In this study, collagen tubes containing two collagen-GAG matrices of different pore size were implanted into spinal cord wounds. Large-pore matrix contains pores with an average

diameter of 95 μm and small-pore matrix contains pores 5 μm in diameter. One purpose of this study was to determine if collagen-GAG matrix has an effect on early healing response following spinal cord injury, and if these differences are detectable at the early time point of 30 days.

4.1.3 Fibrous Scarring in Spinal Cord Injury

One factor responsible for the lack of regeneration of axons in the mammalian spinal cord is the formation of dense fibrous scar tissue in the wound site[33,46,59,64]. The densely packed collagen fibers of scar tissue have been hypothesized to act as a mechanical barrier to elongating axons[46,79]. Also, scar tissue may not contain trophic factors which promote axon regrowth or may not provide vascularity necessary to support growing axons[28,30,72]. Axonal regeneration has been reported by investigators who have used various methods to modify the organization of fibrous scar within spinal cord wounds[14,59,79].

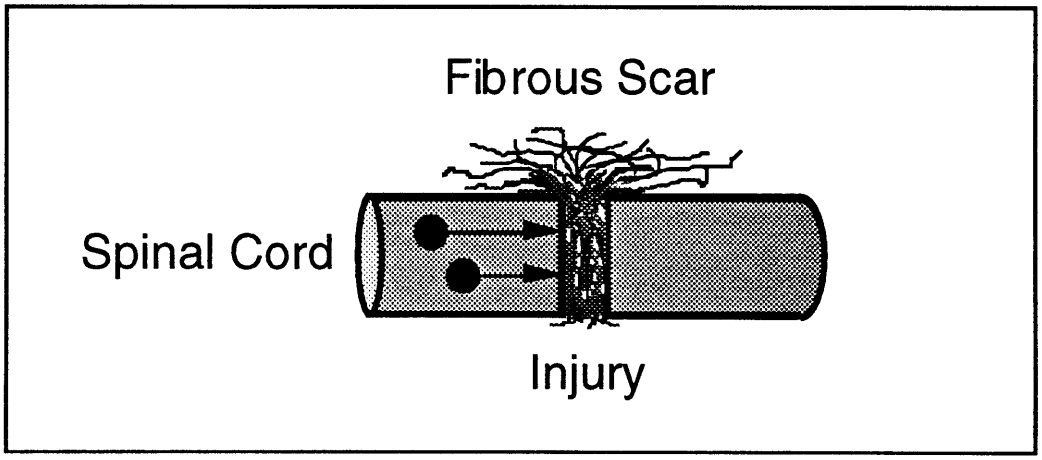

Figure 4.2. Fibrous scar at the site of spinal cord injury.

Sources of scar tissue in spinal cord wounds include injured muscle tissue, injured bone tissue, or the meninges (the connective tissue sheath which surrounds the spinal cord)[48,79]. In chapter 3, it was shown that the CG dorsal barrier was effective in reducing fibrous scar ingrowth from muscle tissue, however, scar was not completely eliminated. The major objective of the work presented in this chapter was to examine the hypothesis that a collagen tube implant further isolates the injured spinal cord from intrusion by fibrous scar beyond the protection provided by

the CG dorsal barrier. A reduction in fibrous scar in the wound site has been hypothesized to lead to increased regrowth of axons.

4.1.4 Glial Scarring in Spinal Cord Injury

The presence of an intact glial scar at the site of spinal cord injury has also been hypothesized to inhibit the regrowth of axons[31,39,60,65]. The process of glial scarring consists of the proliferation of astrocytes, which are support cells in the CNS, and hypertrophy of the astrocyte processes at the interface between intact neural tissue and damaged or necrotic tissue.

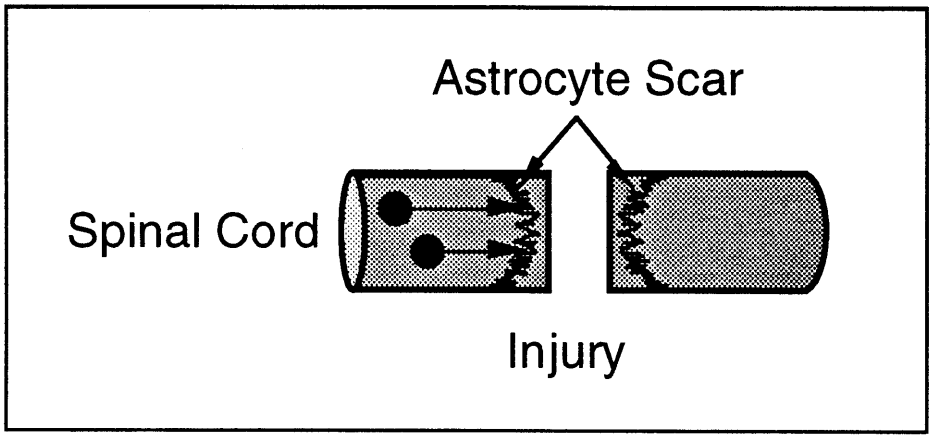

Figure 4.3. Astrocyte (glial) scar at the site of spinal cord injury.

The glial scar serves to encapsulate the intact spinal cord tissue[65,79]. The continuous glial scar which forms surrounding the injured spinal cord stump also prevents axons from regrowing out of the intact tissue[29,43]. Previous investigators have hypothesized that spinal cord axons will regrow if the glial scar does not encapsulate the intact spinal cord. Studies have shown that altering the formation of a glial scar leads to increased axon regeneration[39]. An additional purpose of the study described in this chapter was to test the hypothesis that tubular collagen-based implants are capable of inhibiting the formation of the glial scar.

4.1.5 Objectives of Work in this Chapter

To summarize, the goal of the work presented in this chapter was to compare the effects various collagen-based devices on early spinal cord healing. Implants consisted of collagen tubes either empty or filled with collagen-GAG matrix substrate of a well characterized pore structure. The results were evaluated based on three hypotheses: 1) tube implants prevent the ingrowth of fibrous scar; 2) tube implants inhibit the formation of the glial scar; and 3) tube implants support the regrowth of axons.

4.2 Materials and Methods

4.2.1 Animal Model

As described in the previous chapter, an animal model of spinal cord injury was established. The lesion consisted of a 6-mm gap created in the rat spinal cord at the level of thoracic 7-9. This lesion can be reproducibly created from one animal to the next and provides a cavity large enough for the implantation of a device. However, our experience suggested that if the length of the gap was reduced to 5 mm, a less invasive surgical procedure could be used and trauma to the animal could be reduced. For the experiments discussed in this chapter, a 5-mm gap lesion was used.

Also in the previous chapter, it was demonstrated that the CG dorsal barrier was effective in reducing the amount of fibrous scar tissue invading from injured muscle. For this reason, the CG dorsal barrier was incorporated into the animal model. For all animals in this study the wounds were covered with the CG dorsal barrier. All animals were allowed to survive for 30 days.

4.2.2 Experimental Groups

The goal of the work presented in this chapter is to examine the effects of two variables on the healing of the injured spinal cord: first, the presence of a collagen tube in the wound site, and second, the presence of collagen-GAG matrix substrate within the tube. In this study, two types

of collagen-GAG matrix were tested: "large-pore" (average pore diameter of approximately 95 μm) and "small-pore" (average pore diameter of approximately 5 μm diameter). The combination of these variables yielded four experimental groups:

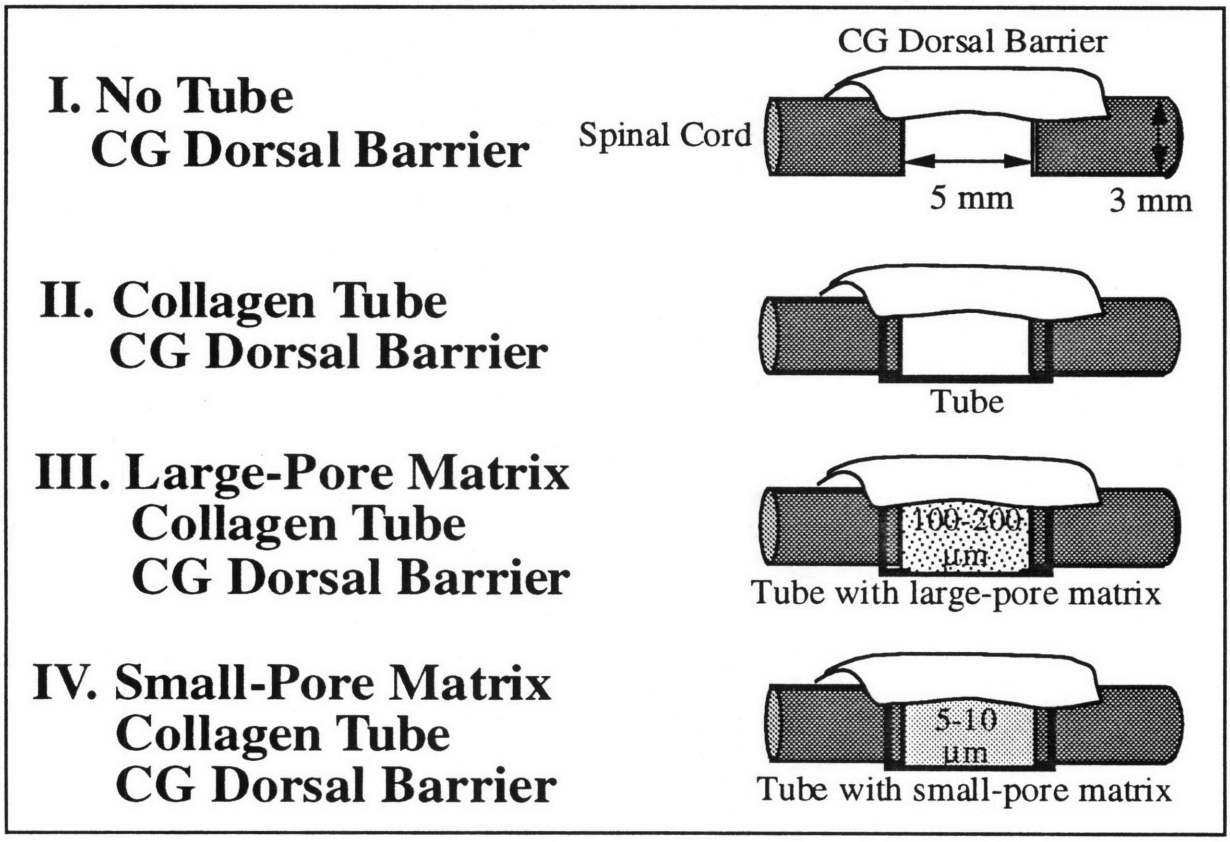

Figure 4.4. Experimental Groups.

The purpose of Group I is to study the intrinsic healing response of the spinal cord without a tube implanted into the lesion. The purpose of Group II is to study healing when the gap is bridged with an empty collagen tube. In Groups III and IV, the effect of a collagen-GAG matrix within the tube was studied. The comparison between Groups III and IV determines if the pore structure of the collagen-GAG matrix has an effect on the healing response.

4.2.3 Preparation of Implants

Referring to Figure 4.4, implants consisted of a maximum of three components: CG dorsal barrier, a collagen tube, and collagen-GAG matrix. Group I implants consisted of only the CG

dorsal barrier covering the wound. For Group II, a collagen tube was implanted in the wound, and the wound was covered with the CG dorsal barrier. Group III implants included three components: a collagen tube, which contained large-pore collagen-GAG matrix, and the CG dorsal barrier. Group IV implants consisted of a collagen tube, which contained small-pore collagen-GAG matrix, and the CG dorsal barrier. The individual components and the insertion of collagen-GAG matrix into collagen tubes are described below.

Sterile rectangles of CG dorsal barrier were prepared as described in section 3.2.2. Glass vials containing sterile CG dorsal barrier were provided to the surgeon at the time of the procedure. The CG dorsal barrier was used in all animals in this study.

Type I collagen tubes with 3.0 mm ID and 3.1 mm OD were provided in 10-cm lengths by Integra LifeSciences Corporation (Plainsboro, NJ). The 3.0-mm ID approximately matches the diameter of the mid-thoracic rat spinal cord allowing for insertion of the spinal cord stumps into the ends of the tube. These tubes are nominally non-porous but have been shown to allow the passage of very small molecules such as glucose (180 kDa)[50]. The tube walls contain very small pores (less than 38 Å in diameter) which are not permeable to larger proteins or cells. Tubes were sterilized by dehydrothermal (DHT) treatment at 105°C and a vacuum of 30 mm Hg for 24 hours before implant assembly discussed below.

Cylinders of collagen-GAG matrix 3.0 mm in diameter were prepared as described in section 2.2.1. Collagen-GAG matrices of two pore sizes were used in this study: large-pore matrix (95 μm average pore diameter) and small-pore matrix (5 μm average pore diameter). Both large and small-pore matrix contain pore channels which are aligned along the axis of the cylinder.

Preparation of implants was performed in a laminar flow hood (Relialab, Tenney Engineering Inc., Union NJ) using sterile gloves, gown, mask, and instruments. A detailed protocol for assembly of implants can be found in appendix A. Group I implants consisted of only the CG dorsal barrier which was described above. Empty tube implants for Group II (see Figure 4.4) were prepared by cutting an 8-mm segment of collagen tube using a scalpel. Segments of collagen tube, 8 mm in length, were also cut for implants for Group III and IV (see Figure 4.4).

However, these tubes are filled with collagen-GAG matrix; either large-pore for Group III or small-pore for Group IV. Using forceps, a 5-mm long cylinder of collagen-GAG matrix was gently inserted into the open end of an 8-mm segment of collagen tube (see figure 4.5).

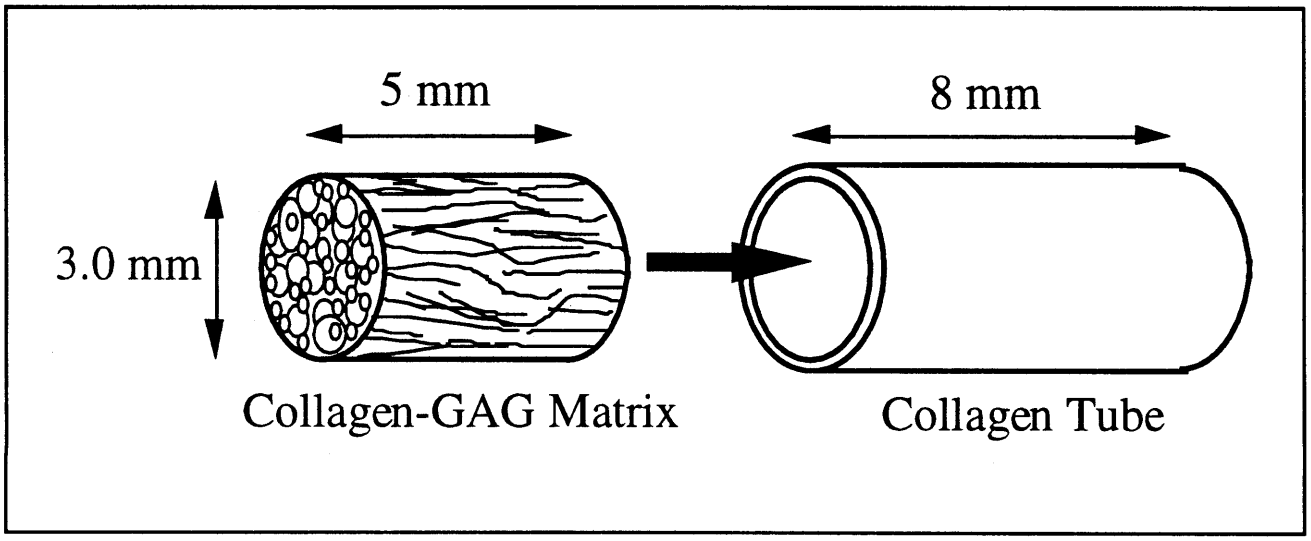

Figure 4.5. Assembly of tube implants which contain collagen-GAG matrix.

All implants were briefly immersed in sterile 100 percent ethanol followed by two rinses in sterile phosphate buffered saline (PBS, Sigma, St. Louis, MO). Implants were placed in sterile glass vials containing sterile PBS. Bottles were transported to surgery in sealed sterile bags (Sterile Sampling Bags, Fisher Scientific, Pittsburgh, PA).

4.2.4 Surgical Procedure, Device Implantation, and Post-operative Animal Care

The surgical procedure used in this experiment is similar to that described in section 3.2.3. The animals were adult female Sprague-Dawley rats weighing 250-350 grams (Taconic, Germantown, NY). Each animal was anesthetized by intraperitoneal injection with sodium pentobarbital (Nembutal solution, 50 mg/ml, Abbot Laboratories, North Chicago, IL) with a dosage of 45 mg per kilogram of animal body weight. For some animals an additional injection of 0.05 cc Nembutal was necessary for complete anesthesia. When completely unconscious, animals were gently restrained in a prone position on a flat operating board. Hair was shaved from the

back, and the skin was cleaned with Betadine disinfectant scrub (Redi Products, Prichard, WV). The thoracic region of the spine was elevated by placing a gauze pad under the animal.

Surgical procedures were performed in room 101 of the West Roxbury Veterans Administration Medical Center animal facility, West Roxbury, MA. A 2-inch long incision was made through the skin

above the thoracic spine. The underlying musculature was incised along the midline and pulled laterally using retractors fashioned from paper clips. Muscles attached to the spinous processes were removed, and the dorsal aspect of thoracic vertebrae 6-10 were identified. A laminectomy was performed removing the dorsal half of the spinal bones of thoracic 7, 8, and one half of 9. This procedure exposes about 10 mm of thoracic spinal cord.

A 5-mm gap was created by performing two complete transections at approximately thoracic 7 and 9. The segment of tissue between the two transections was removed creating a gap 5 mm in length. In animals of Group I (see Figure 4.4 for schematic) the 5-mm gap was created, and the wound bed was covered with a CG dorsal barrier. In animals of Group II, a 5-mm gap was produced, and the rostral and spinal cord stumps were delicately inserted into the open ends of an 8-mm long segment of collagen tube. Saline was injected to fill the tube, and care was taken to ensure that no air bubbles were present within the tube. With the tube in place, the CG dorsal barrier was placed dorsally covering the tube as well as both spinal cord stumps. In animals of Groups III and IV, a 5-mm gap was created, and a collagen tube containing either large-pore (Group III) or small-pore (Group IV) collagen-GAG matrix was placed between the spinal cord stumps. Each stump was inserted into the end of the tube abutting the matrix (see Figure 4.4). Again, the CG dorsal barrier was placed flat over the tube and spinal cord stumps. The opened muscle and skin were closed separately using 4-0 vicryl sutures (Johnson & Johnson, Sommerville, NJ) and wound clips. While unconscious, all rats were given a subcutaneous injection of 100 mg antibiotic (Cefazolin sodium, Abbot Laboratories, North Chicago, IL) diluted in 0.5 ml distilled water. Antibiotic administration was continued at a dosage of 50 mg per day for 10 days.

Following surgery, animals remained unconscious for 4 to 6 hours. During this time, the rats were placed on a heating pad to maintain adequately warm body temperature. When the animals regained consciousness, they were transferred to plastic cages with cellulose bedding material. Free access to food and water was provided for the duration of the study. Animals temporarily lost reflex bladder function, and bladders were voided manually twice daily until reflex function returned. To compensate for blood volume lost during surgery, 5 ml of lactated Ringer's solution was injected subcutaneously for the first two days following surgery.

4.2.5 Animal Sacrifice

All rats were sacrificed at 30 days after surgery and device implantation. The procedures described here are similar to those in section 3.2.4 with some slight differences. Each animal was anesthetized with sodium pentobarbital (Nembutal solution, 50 mg/ml, Abbot Laboratories, North Chicago, IL) with a dosage of 55 mg per kilogram of animal body weight. The animal was placed lying on its back in a rectangular pyrex dish with the forelimbs extended and secured using surgical tape. The chest was opened using heavy scissors exposing the heart. An 18 gauge needle was used to deliver the perfusate into the left ventricle. The right ventricle was punctured to allow for the outflow of body fluids. Reservoirs containing cold heparinized saline and cold 4 percent paraformaldehyde were elevated at a height 1 meter above the level of the animal. Cold heparinized saline was prepared by adding 20 units of heparin (Abbot Laboratories, North Chicago, IL) for every one ml of PBS. 4 percent paraformaldehyde was mixed fresh and cooled to 4°C (see appendix A for a detailed protocol). 200 ml of heparinized saline were perfused followed by 150 ml of 4 percent paraformaldehyde.

4.2.6 Tissue Retrieval and Processing

When each animal was thoroughly perfused, the skin and musculature above the spinal cord were reopened. The entire thoracic spinal cord (about 20 mm in length) including the lesion

site and implant were removed. The retrieved tissue was cut into 5 segments as schematically shown in figure 4.6 below.

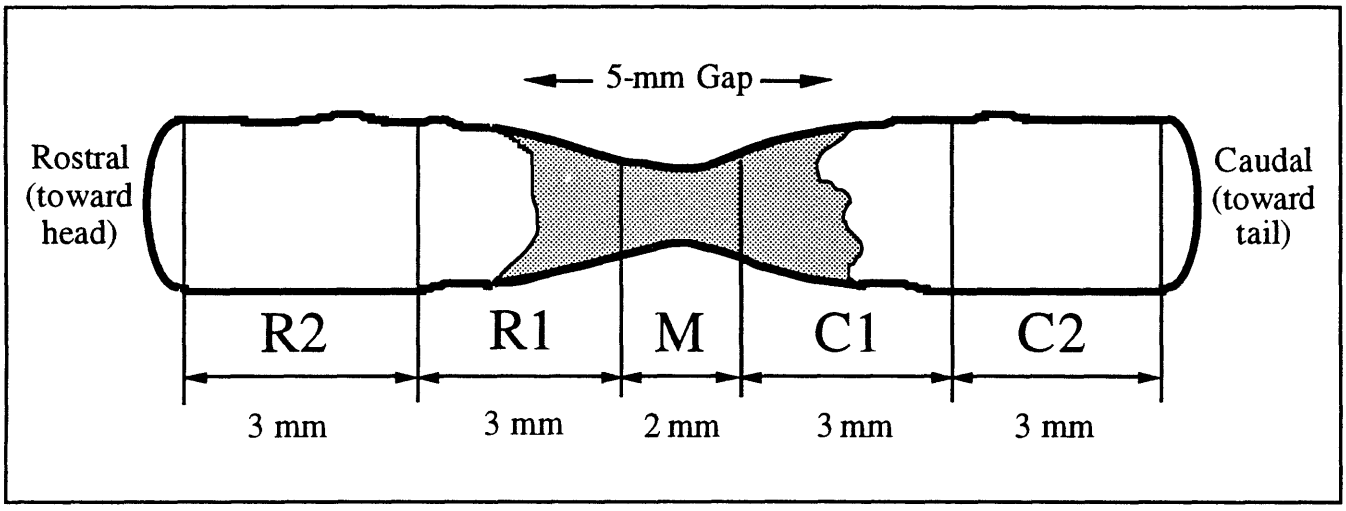

Figure 4.6. Allocation of retrieved spinal cord tissue.

A 2-mm segment of tissue from the middle of the gap, designated with the label M, was retrieved and set aside for histological analysis for myelinated axons (see section 4.2.7 below) . Tissue comprising the transition between the intact rostral spinal cord and new tissue which had formed within the gap was designated R1, and tissue comprising the transition between intact caudal spinal cord and tissue within the gap was designated C1. These segments of transition tissue were set aside for conventional histology and immunohistochemical staining as described in section 4.2.9. Segments of intact spinal cord tissue farthest away from the gap were cut and stored for future analysis. These segments were designated R2 and C2.

4.2.7 Tissue Segments from the Middle of the Gap (M)

The 2-mm segment of tissue from the middle of the gap was placed in Yannof's fixative for an additional 24 hours followed by 10 percent neutral buffered formalin for 24 hours. To label myelinated axons, the tissue was post-fixed in 1 percent osmium tetroxide (see appendix A for a detailed protocol). The tissue was then dehydrated through graded alcohols and embedded in Epon (PolyBed 812, Ploysciences Inc., Warrington, PA). A detailed protocol for Epon embedding can

be found in appendix A. Transverse sections were cut at 1 μm on an ultramicrotome and captured on glass microscope slides (Gold Seal Rite-On, Gold Seal Products, Highland Park, IL). Sections were stained with 1 percent toluidine blue solution (Toluidine Blue O, Fisher Biotech, Boston, MA) and coverslipped with Cytoseal (Stephens Scientific, Riverdale, NJ).

Initial examination of slides was performed with a light microscope (Optiphot, Nikon, Tokyo, Japan). Myelinated axons were identified by examination with 100X objective lens using immersion oil. The entire cross section of tissue was examined in an orderly fashion by using an eyepiece with a transparent grid. For each experimental animal all myelinted axons in the cross section were counted and recorded. The result was the number of myelinated axons which have regrown into the middle of the gap at 30 days.

4.2.8 Measurement of Axon Diameters

A quantitative measurement of the diameter of the myelinated axons at the middle of the gap was obtained via computerized image analysis of the histological images of section 4.2.7 above. A detailed protocol is located in appendix A. Graphic images (TIFF format) were obtained using a light microscope (Olympus Vanox-T, Olympus, Japan) equipped with a video camera (Hamamatsu CCD Video Camera, Hamamatsu, Japan) and video box (Hamamatsu CCD Camera Control, Hamamatsu, Japan). DIGIT software was used to capture images from the camera.

Computerized stereology software (NIH Image) was used to analyze digitized images. NIH Image is available on the internet by anonymous ftp from zippy.nimh.gov or on floppy disk from NTIS, 5285 Port Royal Road, Springfield, VA 22161, part no. PB 93-504868. For each myelinated axon in an image, the outer surface of the myelin sheath was traced using the mouse, completely circumscribing the axon. The NIH Image software contains an automated routine which identifies each axon and measures the length of the perimeter of the axon and the cross sectional area of the axon. A sample image before and after analysis is shown in figure 4.7 on the following page. Figure 4.7a shows a digitized image containing numerous myelinated axons. Figure 4.7b shows the same image after computerized analysis.

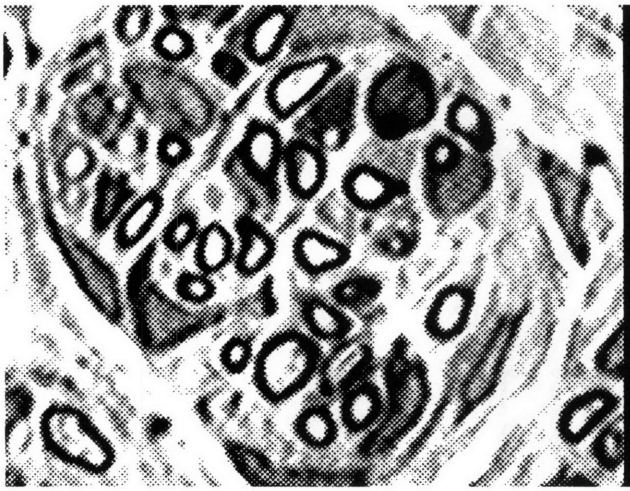

Figure 4.7a. Histological image of axons before analysis.

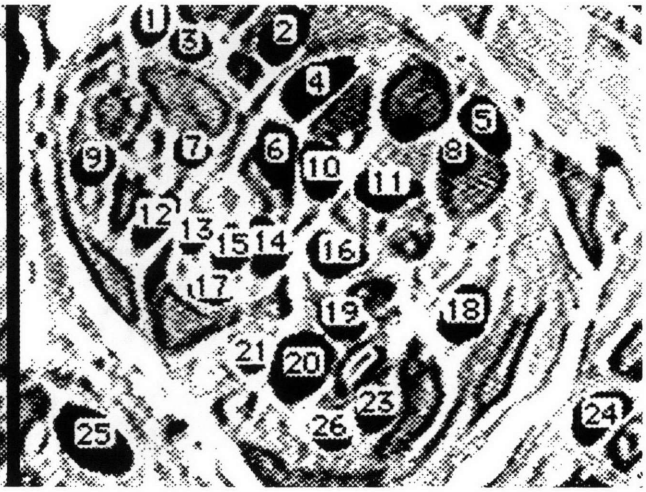

Figure 4.7b. Image with analyzed axons.

Since axons are not exactly circular in shape, it is not possible to directly measure a true diameter. The following equation defines an equivalent (hydraulic) diameter for each axon:

$$D_h = \frac{4 \cdot A_{axon}}{P_{axon}}$$

where D_h is the equivalent hydraulic diameter of the axon in units of μm, A_{axon} is the measured area of the axon in μm^2, and P_{axon} is the measured perimeter of the axon in μm.

4.2.9 Transition Tissue (R1 and C1)

Following retrieval, tissue segments comprising the transition between intact spinal cord tissue and new tissue within the gap (R1 and C1 from figure 4.6) were post-fixed in 4 percent paraformaldehyde for 2-4 hours. The tissue was transferred to a cryoprotective solution of 30 percent sucrose in phosphate buffer for an additional 18-24 hours. Individual tissue segments were frozen in isopentane (Aldrich Chemical Company Inc., Milwaukee, WI) maintained at -40°C using dry ice. A detailed protocol can be found in appendix A.

Frozen R1 and C1 segments of tissue were cut longitudinally on a cryostat (Jung Frigolut, Leica Instruments, Nusseloch, Germany) at 12-20 μm. Sections were captured on pre-treated glass microscope slides (Superfrost Plus, VWR Scientific, West Chester, PA). Slides were allowed to air-dry for 45 minutes before conventional or immunohistochemical staining.

Conventional Histology

Slides were rehydrated with two rinses of distilled water and stained with either hematoxylin and eosin (H&E) or Masson's trichrome. H&E staining was performed to asses general morphology and to identify cell types present within the tissue. staining with Masson's trichrome identifies the presence of collagenous tissue. Following staining, tissue sections were dehydrated through graded ethanol solutions and cleared with two rinses of xylenes. Slides were coverslipped with Permount (Fisher Scientific, Fair Lawn, NJ). Detailed histological protocols are located in appendix A.

Immunohistochemistry

Tissue sections adjacent to those used for conventional histology were stained as follows using immunohistochemical methods. Following air-drying, liquid rubber cement was used to create a well around each tissue section. The sections are rinsed three times in phosphate buffered saline (PBS) for 5 minutes each by applying PBS using a pipette. A blocking solution of 10 percent normal goat serum (Gibco Inc., Gaithersburg, MD) was applied for 20 minutes. The blocking solution was poured from the slides and excess serum was blotted from the section. The sections were then incubated overnight at 4°C with one of two primary antibodies: anti-glial fibrillary acidic protein (αGFAP, Incstar Corp., Stillwater, MN) diluted 1:6 or anti-68 kDa neurofilament (Oncogene Sciences, Uniondale, NY) diluted 1:400. The GFAP antibody is polyclonal (made in rabbit) and labels fibrous astrocytes of the glial scar, and the neurofilament antibody is monoclonal (made in mouse) and labels axons. Following incubation with primary antibody, the slides are rinsed three times for five minutes each in PBS. The sections are then incubated for 30 minutes in the appropriate biotinylated secondary antibody solution. Sections with GFAP primary antibody are incubated in biotinylated goat anti-rabbit IgG (Vector Laboratories, Burlingame, CA) diluted 1:400, and sections with neurofilament primary antibody are incubated in biotinylated goat anti-mouse IgG (Pierce, Rockford, IL) diluted 1:400.

Following incubation with the secondary antibody solution, the sections are rinsed three times for five minutes each in PBS. A solution containing avidin-biotin complex (Vectastain Elite

Kit components, Vector Laboratories, Burlingame, CA) is then applied to the sections for 30 minutes. The sections are again rinsed three times for five minutes each in PBS. The slides are then developed in a peroxidase substrate solution containing diaminobenzidine (DAB, Sigma, St. Louis, MO) and hydrogen peroxide. The slides are washed in tap water, dehydrated through graded ethanol, cleared with two rinses of xylenes, and coverslipped using Permount (Fisher Scientific, Fair Lawn, NJ). A detailed protocol for immunohistochemical staining is located in appendix A.

4.3 Results

4.3.1 General Observations

In this study, 24 of 43 operated animals survived to the end of the 30-day period of investigation. Animals lost function of their hindlimbs following surgery but maintained adequate mobility, grooming, and access to food and water by use of the forelimbs. Spinal reflexes remained functional and all animals exhibited a withdrawal reflex in response to cutaneous pinch of hindlimbs. Reflex bladder voiding function was temporarily lost as a result of spinal cord transection, and bladders were voided manually until automatic bladder function returned, usually within two weeks. Recovery of hindlimb motor function was not formally assessed, however no animals regained the ability to walk or bear weight with the hindlimbs.

4.3.2 Gross Morphology

Gross observation of the excised spinal cord tissue at 30 days revealed that reparative tissue had formed within the gap between spinal cord stumps in all animals. In animals not receiving a tube implant (Group I), tissue was found filling the neural canal contiguous with both rostral and caudal spinal cord stumps. Collagen tubes implanted in animals of Groups II, III, and IV were found intact and easily identifiable. The tubes had become integrated with the host spinal cord. Within implanted tubes, a cable of tissue approximately 1.5 mm in diameter was found connecting the rostral and caudal spinal cord stumps. Grossly, there was no difference in size and appearance

of the cables of tissue found within tubes which were empty (Group II) or filled with collagen-GAG matrix (Groups III and IV).

Figures 4.8 and 4.9 are photographs of spinal cord tissue which was retrieved at 30 days from an animal which received a collagen tube implant which contained small-pore collagen-GAG matrix (Group IV). In figure 4.8 the collagen tube is intact and identifiable in the wound site. In figure 4.9, the tube has been removed exposing the cable of reparative tissue.

Figure 4.8. Spinal cord tissue retrieved from an animal which received a collagen tube implant containing small-pore collagen-GAG matrix. The tube is shown intact integrated between the spinal cord stumps.

Figure 4.9. The same tissue shown in figure 4.8. The tube has been removed exposing the cable of reparative tissue within.

4.3.3 General Histological Observations

Examination of histological sections stained with Masson's trichrome revealed that at 30 days, the reparative tissue within the gap contained significant amounts of collagen (stained blue by trichrome). Staining with hematoxylin and eosin identified the dominant cell types as fibroblast-like cells and macrophages engulfing debris from necrotic tissue and myelin degradation. The absence of polymorphonuclear nuetrophils (PMNs), lymphocytes, and granulocytes confirmed that the implant devices did not elicit prolonged acute inflammatory reaction or foreign body response. At 30 days, the collagen tube remained intact, but the collagen-GAG matrix was no longer present within the wound site. This correlates well with previous studies of the peripheral nerve in which implanted collagen tubes were found intact, but the collagen-GAG matrix had been completely resorbed by 6 weeks post-implantation[49]. It is expected that the collagen tubes will eventually be resorbed, and other investigators have found that similar collagen tubes were completely degraded after 3.5 years post-implantation in the monkey median nerve[4].

Tissue surrounding implanted tubes was not found to adhere to the tube surface, and tubes were easily removed intact. Histologically, the tissue adjacent to the tube resembled synovium, being a definite layer of fibroblasts and macrophages. Tissue found within implanted tubes was composed of primarily of collagen, and contained fibroblasts, myelinating cells (Schwann cells or oligodendrocytes), and axons.

4.3.4 Fibrous Scar

Light microscopic examination of tissue sections stained with Masson's trichrome revealed that reparative tissue found within the 5-mm gap of all groups was composed predominantly of collagen. Tissue within the injury site of animals not receiving a tube implant (Group I) exhibited many characteristics of fibrous scar. The collagen fibers within this tissue were densely packed as identified by intensely blue staining by trichrome. Collagen fibers were observed to be highly organized and predominantly aligned in a direction perpendicular to the long axis of the spinal cord. This tissue was also less cellular than tissue found within implanted tubes.

Tissue found within implanted tubes (Groups II, III, and IV) was composed of collagen, but did not resemble fibrous scar. This tissue was composed of a loosely arranged scaffold of collagen containing numerous cells resembling fibroblasts and macrophages. This tissue was less densely organized than fibrous scar. The primary direction of orientation was along the long axis of the spinal cord.

Figure 4.10 on the following page illustrates the difference between tissue formed in the absence of a tube and tissue which formed within a tube implant. Both micrographs show tissue sections taken from the transition between rostral intact spinal cord (stained red by Masson's trichrome) and newly synthesized tissue within the gap (stained blue by Masson's trichrome). The tissue section at the top was retrieved from an animal which did not receive a tube implant (Group I). Collagen fibers within the wound site are densely packed and stain intensely blue. These fibers are aligned in a direction perpendicular to the long axis of the spinal cord. This tissue resembles fibrous scar. The tissue section at the bottom was retrieved from an animal which received an empty tube implant (Group II). The tube has been removed. The reparative tissue is more loosely organized and aligned in a direction parallel to the long axis of the spinal cord. The loose arrangement and parallel alignment of reparative tissue was consistent for all animals receiving tube implants either empty (Group I) or filled with collagen-GAG matrix (Groups III and IV).

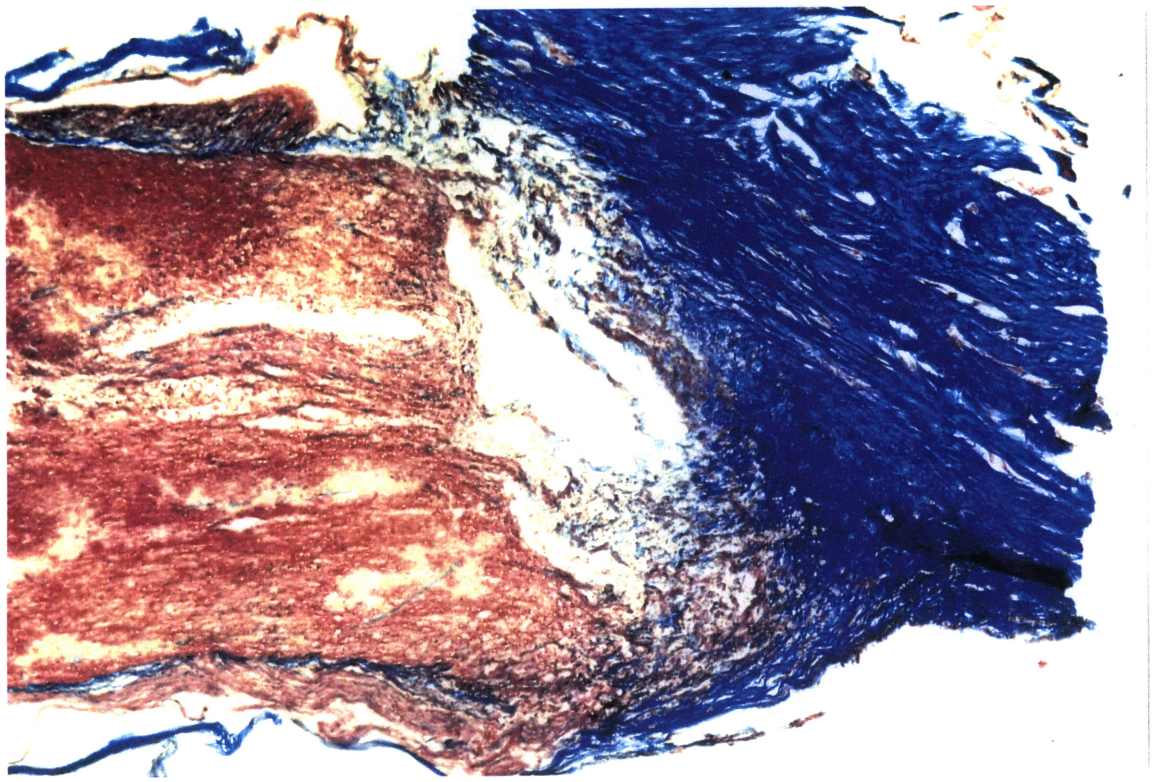

Figure 4.10a. Tissue retrieved from an animal not receiving a tube implant (Group I). Stained with Masson's trichrome. Dense fibrous scar within the wound stains intensely blue. Collagen fibers oriented predominantly transerse to the spinal cord axis.

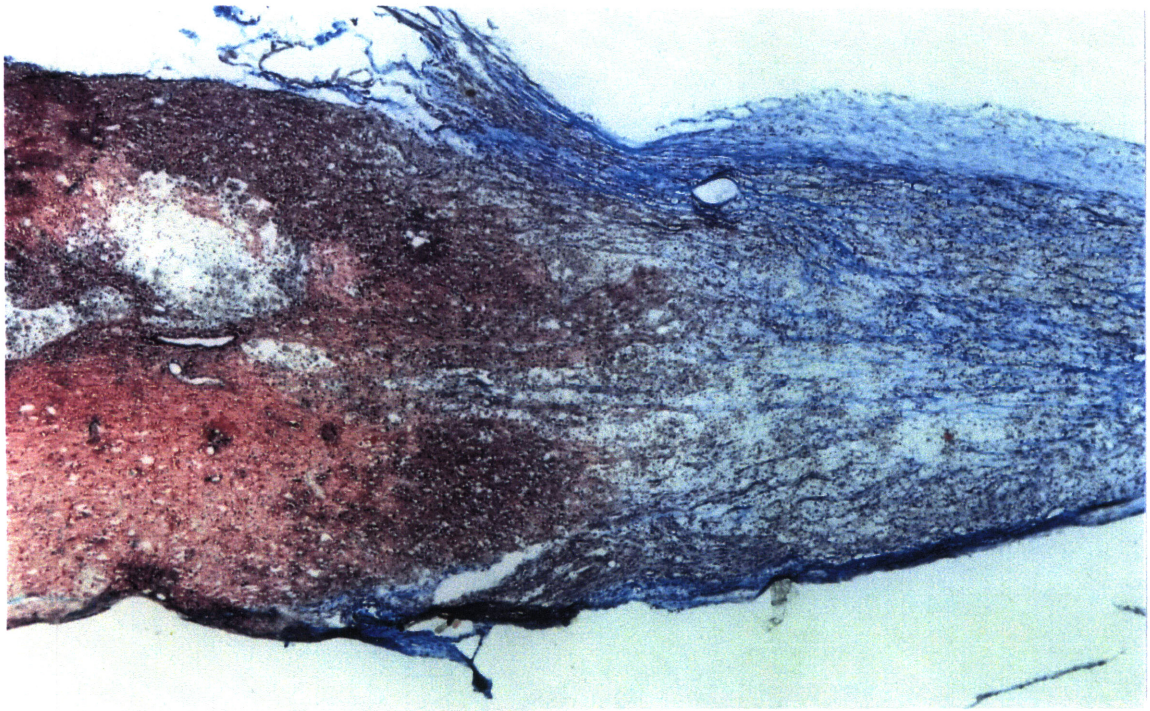

Figure 4.10b. Tissue which had regrown within an empty tube implant. Stained with Masson's trichrome. Collagenous tissue is loosely organized and stains lightly. Fibers are oriented predominantly parallel to the spinal cord axis.

4.3.5 Glial Scar

As described in section 4.2.9, tissue sections were stained with antibodies for GFAP which positively identify reactive astrocytes, a distinct component of the glial scar. Light microscopic examination of tissue sections stained with antibodies for GFAP was used to evaluate the pattern of glial scar formation.

The glial scar which formed at the wound site of animals which did not receive tube implants (Group I) was consistently found as a continuous barrier between intact spinal cord tissue and the fibrous scar within the gap. A distinct border of intensely staining GFAP-positive astrocytes was present in all Group I animals. Reactive astrocytes remained confined to intact spinal cord tissue and did not grow into the fibrous scar.

Astrocytes had migrated significant distances (greater than 1 mm) into the gap only in animals receiving tube implants (Groups II, III, and IV). The glial scar was not found to be the continuous border between intact and reparative tissue, but the border was interrupted by processes of astrocytes penetrating into the reparative tissue. The interrupted appearance of the glial scar was common to all animals which received tube implants either empty (Group I) or filled with collagen-GAG matrix (Groups III and IV).

Figure 4.11 on the following page illustrates the difference in glial scarring caused by the presence of a tube implant. Tissue sections are adjacent sections to those in figure 4.10 but have been stained with antibodies to GFAP. The tissue section at the top was retrieved from an animal which did not receive a tube implant (Group I). The fibrous scar within the gap is unstained and is barely visible (marked by dashed line). GFAP-positive astrocytes form a distinct border between intact spinal cord and fibrous scar tissue. The tissue section at the bottom was taken from an animal which was implanted with an empty collagen tube (Group II). Positively stained astrocytes (arrows) have migrated into the gap. The glial scar is not continuous and definitely does not form an intact barrier.

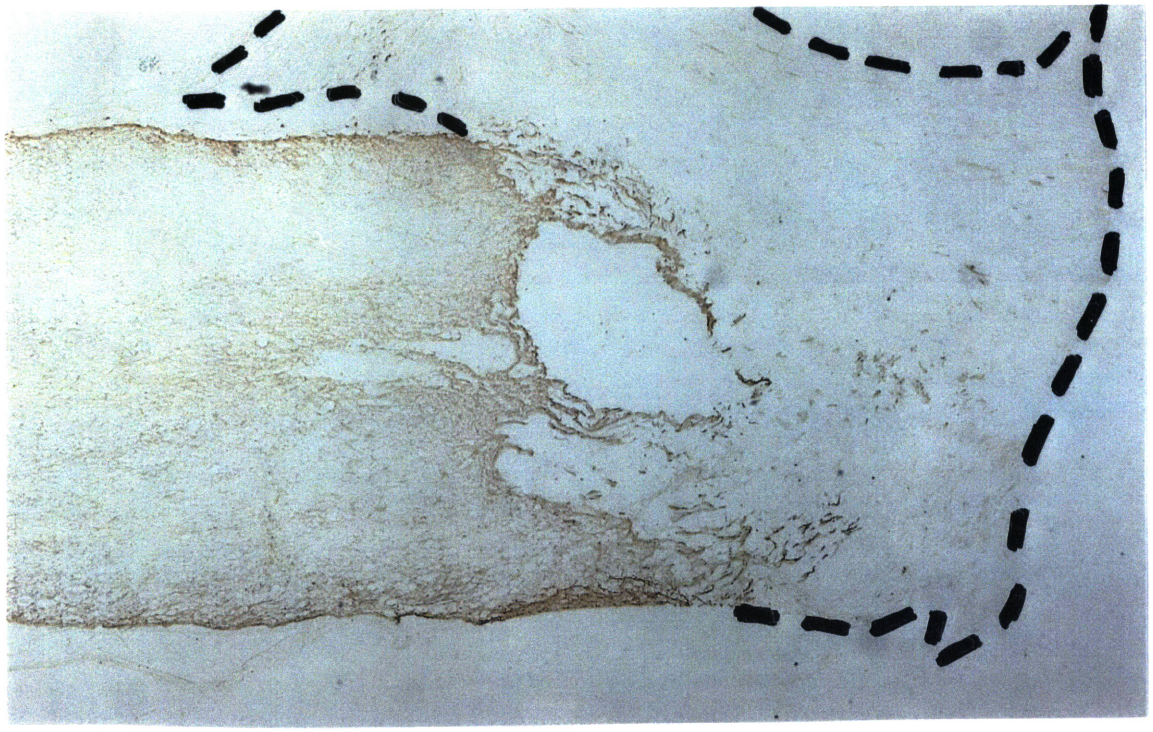

Figure 4.11a. Adjacent tissue section to that of figure 4.10a (No Tube - Group I). Stained with GFAP antibodies. Glial scar forms as a distinct border between intact spinal cord (positive staining) and scar tissue within the gap (unstained as outlined with dashed line). Astrocytes remain confined to intact spinal cord.

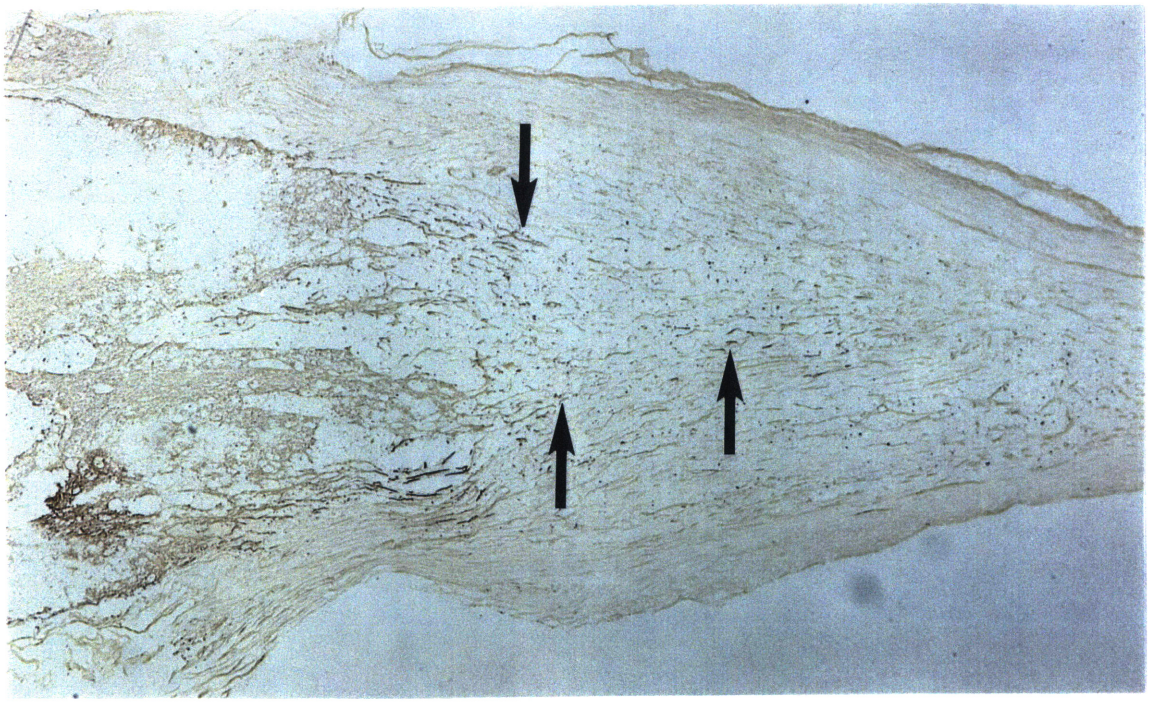

Figure 4.11b. Adjacent tissue section to that of figure 4.10b (Empty Tube - Group II). Stained with GFAP antibodies. Glial scar is disrupted by positively staining astroytes (arrows) extending into the tissue cable. Astrocytes have migrated into the tissue cable.

4.3.6 Myelinated Axons at the Middle of the Gap

Transverse sections of Epon embedded tissue from the midpoint of the gap revealed that the reparative tissue of all animals was well-vasularized, containing numerous blood vessels and vascular channels. This tissue also contained myelinated axons in 20 of 24 animals including animals of all experimental groups. Axons were typically organized into small bundles or fascicles closely associated with myelinating cells which appeared to be Schwann cells. Figure 4.12 below is a micrograph of mature myelinated axons (arrows) in a normal rat spinal cord. Myelin is stained darkly blue by toluidine blue. Figure 4.13 is a micrograph of tissue from an animal which received a collagen tube containing large-pore collagen-GAG matrix. Numerous myelinated axons have regrown at 30 days (arrows).

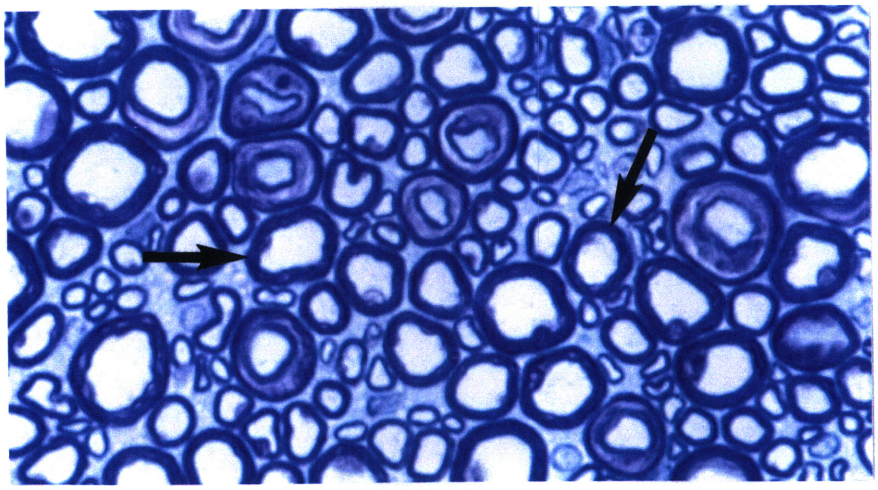

Figure 4.12. Mature myelinated axons (arrows) in a normal adult rat spinal cord.

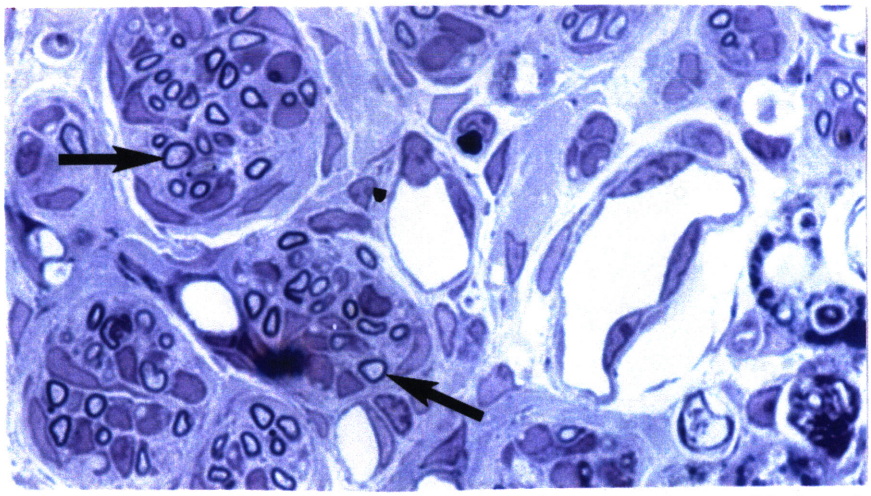

Figure 4.13. Myelinated axons (arrows) which have regrown at 30 days into a collagen tube which contained large-pore collagen-GAG matrix.

The chart in figure 4.14 shows the total number of axons counted at the middle of the gap for each of the four experimental groups. Each value is shown as the average for animals in each group with error bars expressing standard error of the mean (SEM). The number of animals in each group is also shown.

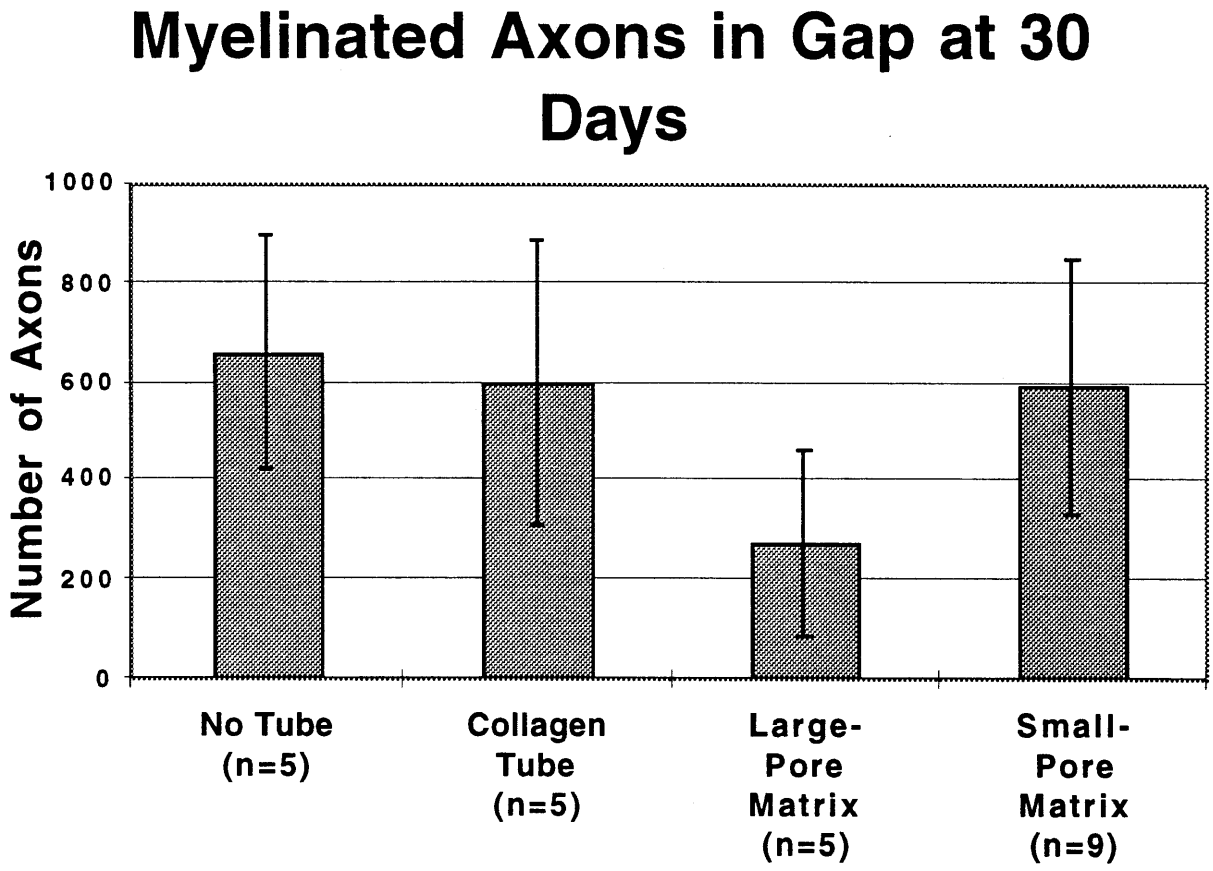

Figure 4.14. Results of axons counting for the four experimental groups.

Animals of Group I showed the largest number of myelinated axons at the center of the wound with 658 ± 238 (mean ± SEM, n=5) myelinated axons. The average number of axons for Group II was 594 ± 289 (n=5). Animals of Group III showed the smallest number of regrowing axons with 272 ± 186 (n=5), and Group IV animals showed 587 ± 258 (n=9) myelinated axons.

For each group, the individual data points were not normally distributed about the mean. This fact invalidates the use of a standard ANOVA or student's t-test for statistical comparisons among groups. The Mann-Whitney non-parametric test does not assume normal distribution and was applied to the data for statistical comparisons[70]. Using the Mann-Whitney test, theere were no statistical differences ($p>0.05$ for all comparisons) between groups for the number of myelinated axons found in the wound at 30 days.

As described in section 4.2.8, the diameters of axons found in the wound site were measured. Myelinated axons ranging between 1 and 9 μm were identified. The data was compiled as a histogram showing the size distribution of regenerated axons for each experimental group. Figures 4.15 through 4.18 on the following pages show the diameter distribution for myelinated axons in each of the four experimental groups. Axons 3-4 μm in diameter were most numerous with fewer small diameter (<3 μm) and large diameter (>4 μm) axons. The diameter distributions were qualitatively similar among groups.

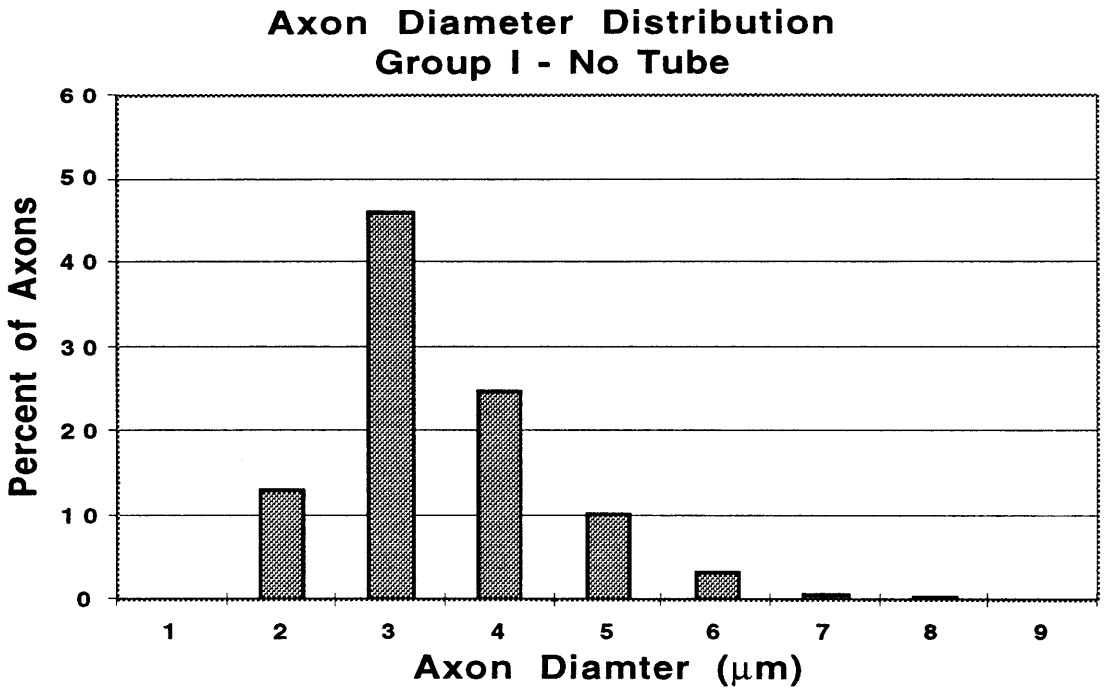

Figure 4.15. Histogram showing the axon diameter distribution for all animals of Group I (No Tube). Axon diameters divided into bins from 1 to 9 μm.

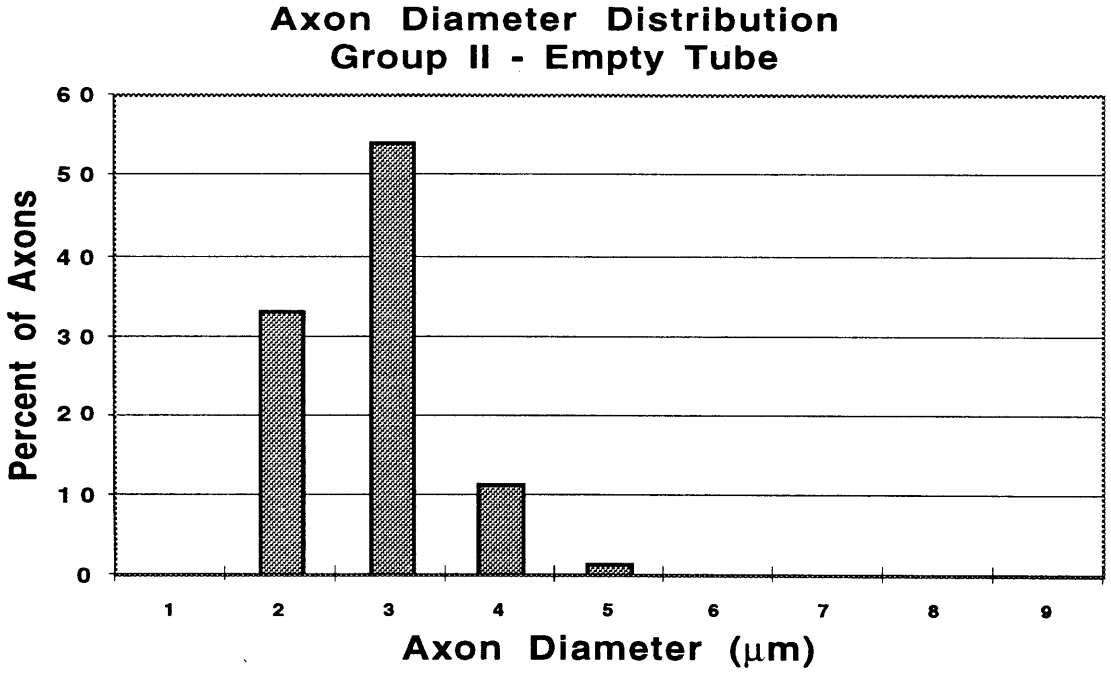

Figure 4.16. Histogram showing the axon diameter distribution for all animals of Group II (Empty Tube). Axon diameters divided into bins from 1 to 9 μm.

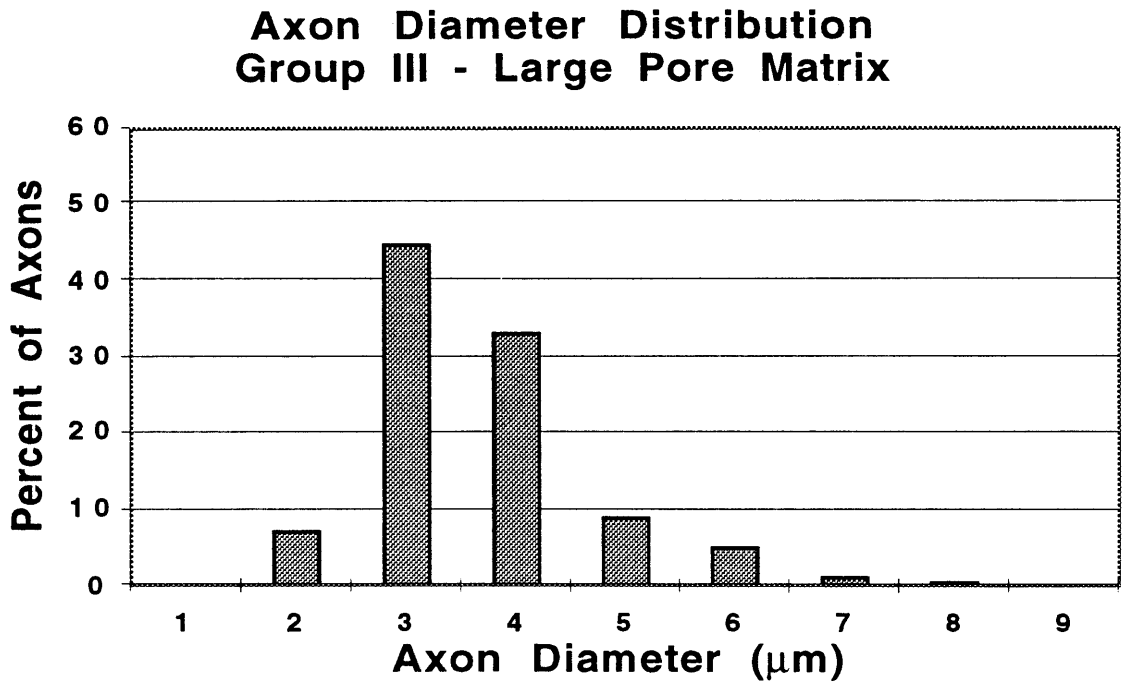

Figure 4.17. Histogram showing the axon diameter distribution for all animals of Group III (Large-Pore Matrix). Axon diameters divided into bins from 1 to 9 μm.

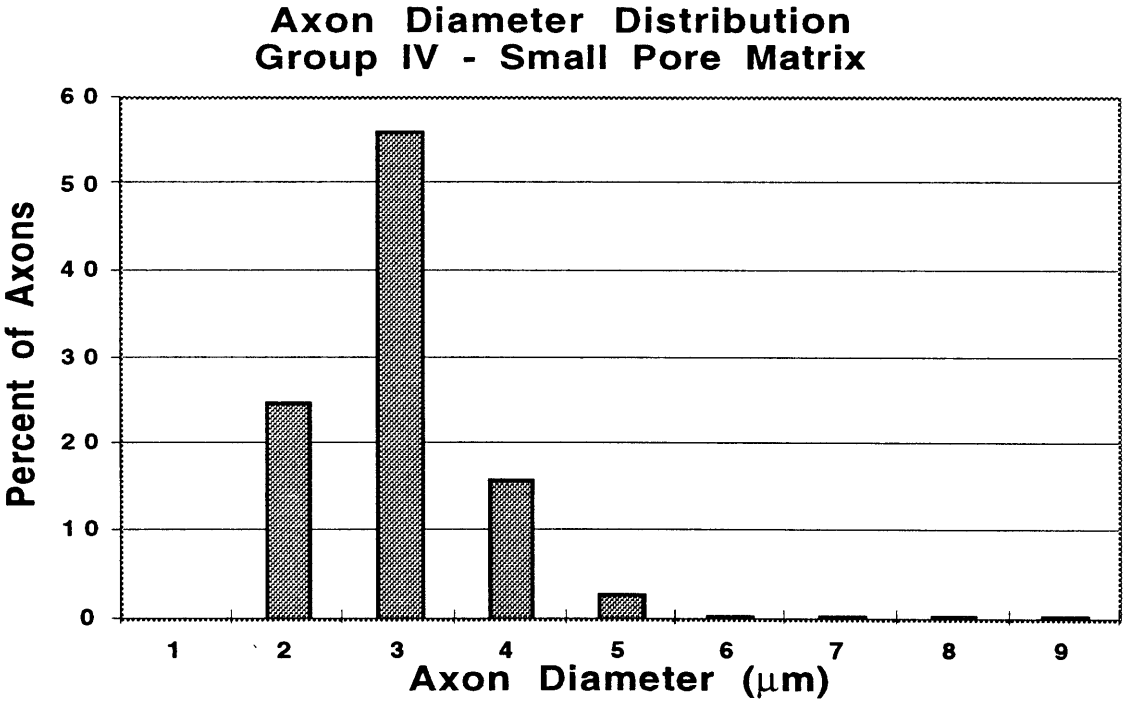

Figure 4.18. Histogram showing the axon diameter distribution for all animals of Group IV (Small-Pore Matrix). Axon diameters divided into bins from 1 to 9 μm.

4.4 Discussion

The goal of this study was to evaluate the effects of various collagen-based implant devices on spinal cord healing. The devices consisted of a collagen tube which was either empty or filled with large-pore or small-pore collagen-GAG matrix. The effects of the presence or absence of the collagen tube and the presence or absence of collagen-GAG matrix are discussed below. The differences in healing response among implant groups is discussed in terms of the endpoints of fibrous scar, glial scar, and the regrowth of axons.

4.4.1 Effects of Collagen Tube Implants on Spinal Cord Healing

General examination of excised tissue and histological observation revealed that collagen tubes did not elicit an untoward inflammatory response or a foreign body reaction. At 30 days, tubes had become integrated with the host spinal cord tissue, and tissue formed within the tube contiguous with the rostral and caudal spinal cord stumps. These findings are similar to previous observations from this laboratory in work with peripheral nerves[17-20,49,53,88].

As expressed in section 4.3.4, fibrous scar had formed in the wound site of animals when collagen tubes were absent (Group I). Fibrous scar was not present in the wound site of animals receiving collagen tube implants either empty (Group II) or filled with collagen-GAG matrix (Groups III and IV). We hypothesize that the collagen tube excluded the invasion of fibrous scar from external connective tissue sources. The tissue within the tube contained collagen but lacked the dense organization characteristic of fibrous scar. The alignment of collagenous tissue within implanted tubes suggest that the tubes provide guidance for the regrowth of tissue between the injured stumps. Although it was not formally addressed by this study, aligned collagen fibers within implanted tubes may provide for the directed regrowth of axons.

The presence of collagen tubes also altered the pattern of glial scar formation (see section 4.3.5). In the absence of implanted tubes (Group I), astrocytes remained confined to the intact spinal cord tissue and did not migrate into the wound site. The glial scar also formed a distinct

continuous border between intact spinal cord tissue and fibrous scar within the gap. When collagen tubes were implanted (Groups II, III, and IV) astrocytes were able to migrate significant distances (> 1 mm) into the gap. Also, the glial scar was visibly disrupted at the interface between intact spinal cord and reparative tissue. We hypothesize that the tube provides guidance for the regrowth of tissue from spinal cord sources within the gap. This tissue includes astrocytes and myelinating cells. Myelinating cells were identified at the middle of the gap in Epon embedded sections stained with toluidine blue. The growth of tissue of spinal cord origin into the wound site is encouraging.

Animals receiving tube implants did not show a significantly larger number of axons at the middle of the wound site at 30 days than animals without tube implants (see section 4.3.6). At the relatively early time point of 30 days, the scatter in the data is somewhat large. Changes caused by the implantation of a tube may not be evident at 30 days, and a longer interval of evaluation may be necessary.

Tube implants also provided an isolated experimental system for the study of spinal cord healing. At 30 days, both spinal cord stumps were found in place within the tube in all experimental animals. This experimental system introduces the possibility of testing the effects of other therapeutic elements which could be delivered within the tube.

4.4.2 Effects of Collagen-GAG Matrix on Spinal Cord Healing

The presence or absence of the collagen-GAG matrix within implanted tubes did not have as striking effect on the healing response as the presence or absence of the tube itself. The formation of fibrous scar within the wound was not noticeably different when collagen-GAG matrix of either pore size was present. Also, the pattern of glial scarring which formed in animals receiving implants containing collagen-GAG matrix was not different from animals with empty tubes. The pore geometry of the matrix did not effect fibrous or glial scar formation.

There were no statistically significant differences ($p>0.05$ for all comparisons) in the number of axons which had regrown into empty tubes (Group I) or those containing large-pore

matrix (Group III) or small-pore matrix (Group IV). It appears that at the early time point of 30 days, no conclusions can be reached about the effects of collagen-GAG matrix on the spinal cord healing response. Perhaps a longer evaluation period is necessary to detect differences between implant groups.

4.4.3 General Remarks

The overall goal of research in spinal cord healing and regeneration is to re-establish functional connection through a lesion site. The first step in this process is to encourage damaged axons to regrow through a lesion site. Our results demonstrate that a number of axons are able to regrow into the lesion. At 30 days, there were no statistically significant differences in the number of axons among groups. A longer period of observation may yield more information about the effects of implant devices on healing and axon regeneration.

Axons which have regrown into a spinal cord wound can originate in three possible sources. The regrowing axon may belong to a neuron cell body located in the brain or brainstem, in the spinal cord itself, or in the peripheral nerve roots. When evaluating the regeneration of spinal cord axons, it is important to identify the source of regrowing axons since axons from different sources correspond to the return of different types of function. Future studies will determine the origin of the regrowing axons.

4.5 Conclusions

In this experiment, the healing response within the closed environment within implanted tubes was characterized. An experimental system for the study of spinal cord injury has been established. We have also shown that with the implantation of collagen-based devices, we are capable of controlling aspects of the healing response which may affect successful regeneration. The presence of collagen tubes reduces the ingrowth of fibrous scar which has been shown to inhibit successful regeneration. Also, the tube provided guidance for the regrowth of tissue from neural sources into the wound site. The experimental system also provides an opportunity for

future research in which various therapeutic elements (pharmaceutical agents, growth factors, cultured cells, etc.) may be delivered to the injury site and tested.

The presence of myelinated axons within the wound site is encouraging. The regeneration of axons is the first step toward the recovery of function. We have also established an experimental system that will allow for the testing and identification of other factors which may encourage a more robust regrowth of axons. Future work in this lab will also be focused on guiding these axons toward their original endpoints.

Fully resorbable collagen-based devices show promise in facilitating regenerative changes following profound injury in the central nervous system.

APPENDIX A1: COLLAGEN SLURRY PROTOCOL

PROCEDURE:

1. Defrost wet (Integra) tendon collagen. 30 min. - 1 hr.

2. Also, cool blenders for 30 min to 4°C.

3. Fill one blender with 600 ml of 0.05M acetic acid

4. Weigh 13.69g of wet tendon collagen. The collagen is in pre-packaged bags, but still needs to be weighed.

5. Pull the collagen into small bits using forceps and drop collagen in blender.

6. Blend for 90 min. on high.

7. Add 120 ml of chondroitin 6-sulfate solution over 15 min using the peristaltic pump. (0.32g C-6-S in 120 ml 0.05M acetic acid.)

8. After the addition, blend the mixture for an additional 90 min. on high.

9. Pour out slurry and refrigerate.

10. If using immediately, de-gas slurry with a vacuum flask in the hood. It is now ready to pour into the freeze-drying tray.

APPENDIX A2: PREPARATION OF COLLAGEN-GAG MATRIX

PROCEDURE:

1. Connect the freezing bath hose to the "liquid" port on the liquid nitrogen tank. Open the valve on the tank by turning counter-clockwise. Press the switch turning the freezing bath power on. The liquid nitrogen should start flowing immediately. Set the desired temperature on the controller dial. The temperatures marked may not be accurate, you may need to make adjustments. The freezing bath should cool in about 30 minutes, depending on the desired temperature.

2. Turn on the Vitrtis freezedryer. Power: ON, Freeze: ON, Heat: ON, Condenser: ON,. Set the temperature (SV) to -20° C. Turn on the ventilation fan located behind the freezedryer. Place the implant tray in the freezedryer to cool. It will take about 30 minutes to cool down.

3. Prepare each implant for freezing as follows. Cut 10 cm of PVC Tygon jacket tubing (1/4" ID, 3/8" OD). Cut 15 cm of silicone tubing (5/32" ID, 7/32" OD, Cole Parmer #06411-65). Clamp one end of the silicone tube with a non-hanging clamp. Thread the unclamped end into the section of PVC jacket tubing until the PVC abuts the clamp. Open the clamp slightly. Remove the slurry from the refrigerator (if the slurry has been sitting for more than one week re-blending may be necessary). Using a syringe without a needle, carefully draw slurry without air bubbles. Inject slurry into the free end of the silicone tube until the slurry completely fills the tube. Inspect the tube for air bubbles in the slurry. Close the clamp securely and remove the syringe. Push the free end of the silicone tube into a hanging clamp until the PVC tubing abuts the clamp. Close this clamp securely. The implant is now ready to be frozen.

4. Check the temperature of the freezing bath. Check the size of the gear on the lowering motor. Hang the implant from the lowering track. Align the implant so that it will not stick to the freezing coils or the sides of the bath. Turn on the lowing motor and wait for the implant and clamps to become completely submersed in the coolant (20 minutes - 2 hours for different speeds). Wait 30 minutes for complete freezing. While the implant is lowering prepare labels for the individual specimen sections.

5. Before removing the implant from the bath, retrieve the cold tray from the freeze dryer. Remove the implant from the bath. Remove the clamps. Cut away the excess silicone tubing outside of the PVC keeping track of which end of the tube had entered the bath first . Cut the PVC and silicone into 2.5 cm sections. Label each section accordingly (1-4 with section 1 entering the bath first). Place these sections quickly onto the cold tray.

6. Place the tray in the freeze dryer and close the door securely. Check the condenser temperature to make sure it is below -40° C. Make sure the chamber release button if OFF. Turn the vacuum ON. **Make sure the front door seals**. Once the vacuum is below 200 mtorr (about 30 minutes) change the temperature setting to 0° C. Leave both the freeze and heat buttons ON. Leave at 0° C overnight.

7. The next day change the temperature setting to 20° C and turn OFF the freeze button (leave the heat button ON). While the temperature is rising (about 20 minutes), prepare individual foil packets for implants labeled with specimen number, date, and sterile condition. When the temperature reaches 20° C turn the heat, vacuum, and condenser

buttons OFF. Turn the chamber release button to ON. When the vacuum is fully released, remove the implants into the foil packets leaving the top edge wide open.

8. Place the foil packets containing the implants in the DHT oven at 105° C overnight with the vacuum on. In the morning, release the vacuum and carefully close the tops of the packets trying to maintain the sterile condition. Place the packets in the desiccating boxes for storage.

APPENDIX A3: IMPLANT ASSEMBLY

Sterilized Equipment:
Forceps (2 pair)
Small scissors
3 small specimen vials
Scalpel holder
Teflon pad enclosed in packet
Ruler
2 small glass culture dishes for PBS and EtOH

Other Equipment (pre-sterilized - just open and drop into or near sterile field):
#10 scalpel blade
Sterile collagen tubes
Sterile matrix
Sterile collagen membranes
3 sterile disposable transfer pipettes
Sterile 100% EtOH
Sterile PBS
Whirl-Pak

PROCEDURE:

Day before implant preparation (at least 3 hours before):

1. Enclose instruments in autoclave bag and seal with autoclave tape.
2. Enclose teflon pad in wrap and seal with autoclave tape.
3. Place both in autclave upright leaning against walls.
4. Replace Plug and fill autoclave with water. Turn timer to 45 mintues on FAST exhaust setting.
5. Allow instruments to cool before removing.

Day of implant preparation:

1. Turn on the sterile hood blower at least 1 hour before working.
2. Spray entire bench surface with 70% EtOH and wipe with Kimwipe.
3. Open EtOH and PBS bottles and Whirl-Pak.
4. Open packet containing teflon pad to create sterile field.
5. Drop equipment into sterile field.
6. Put on sterile gloves
7. Using forceps gently push matrix segments into collagen tubes.
8. Dropwise flow sterile 70% EtOH through matrix within tube for 1 mintue.
9. Dropwise flow sterile PBS for 1 mintue.
10. Place implant and one piece of collagen membrane in vial filled with PBS and close lid.
11. Place vials in Whirl-E-Packs and close

APPENDIX A4: PREPARATION OF CG DORSAL BARRIER

PROCEDURE:

1. Pour degassed collagen-GAG slurry into an aluminum weigh boat to depth of about 3/8" (3.5 ml per square cm of drying pan area).

2. Place in the Fisher vacuum oven at room temperature and 25-30 mm Hg vacuum until no more bubbles form (about 30 minutes).

3. Remove from oven and place under the laminar flow bench or sterile hood at room temperature for 3 to 4 days until dry.

4. Prepare foil packets large enough to hold three implantable pieces of collagen-GAG membrane. Remove the membrane from the weigh boat using jeweler's forceps. The membrane should be removed in one piece.

5. Measure the thickness of the membrane using micrometer in a number of locations and record the result. The thickness should be within the range 0.004 and 0.006 inches.

6. Cut the membrane into rectangular pieces 8 mm by 12 mm. Place three of these pieces in each foil packet leaving the end wide open.

7. Place the packets into the Fisher oven at 105 degrees Celsius and 25-30 mm Hg vacuum for 24 hours.

8. The next day remove the packets, seal the opening by folding twice and place in the desiccating box for storage.

APPENDIX A5: ANIMAL SACRIFICE BY CARDIAC PERFUSION

EQUIPMENT:

IV bottle with 2-hole plug and breather tube
IV tubing (2 sets)
3-way stopcock
Pyrex dish
1 liter IV bag of PBS
18 gage needle
dissection instruments
specimen jars
Nembutal solution
tuberculin syringes/needles

SOULUTIONS:

Heparinized Saline (20 units/ml)

1 liter IV bag of PBS
2 ml of heparin sodium (10,000 units/ml)

Measure heparin by drawing into tuberculin syringe and inject into IV bag. Mix and keep cold (4°C) until use.

Yannof's Fixative

Stock A: 1.67g Sodium Phosphate (monobasic, anhydrous)
8.95g Sodium Phosphate (dibasic, anhydrous)
960 ml distilled water
40 ml 25 percent glutaraldehyde

Stock B: 4.0g Sodium Phosphate (monobasic, anhydrous)
8.95g Sodium Phosphate (dibasic, anhydrous)
900 ml distilled water
100 ml 38-40 percent formaldehyde

Mix equal parts of stock A and B. Keep refrigerated (4°C) until use.

4 % Paraformaldehyde (100 ml, pH 7.4)

4.0g paraformaldehyde powder
50 ml distilled water
1N Sodium Hydroxide Solution
50 ml 0.2 M phosphate buffer

Add 4.0g paraformaldehyde to 50 ml distilled water; heat to 60°C. Add a few drops of sodium hydroxide until the solution clears slightly. Cool to room temperature. Add 50 ml of 0.2 M phosphate buffer. Filter and pH to 7.4. Mix fresh for each group of animals and keep cold (4°C) until use.

SOULUTIONS (CONTINUED):

0.2 M Phosphate Buffer (500 ml, pH 7.4)

500 ml distilled water
3.0g Sodium Phosphate (monobasic, anhydrous)
11.0g Sodium Phosphate (dibasic, anhydrous)

Mix constituents and pH to 7.4.

PROCEDURE: (note the procedure is the same for perfusion with Yannof's or 4 % paraformaldehyde)

1. Prepare necessary solutions and cool to 4°C.

2. Inject animal IP with pentobarbital with dosage of 55 mg per kg of animal body weight.

3. Hang IV bottle of cold perfusate and IV bag of cold saline 1 m above the level of the animal using harness or IV stand. Connect the IV tubing with 3-way stopcock connected to perfusate, saline, and 18 gage needle.

4. Place unconscious animal lying on its back in the pyrex dish with arms constrained slightly extended using tape.

5. Using heavy dissecting scissors, open the chest, exposing the heart. Partially open the stopcock to allow some saline through the needle. Insert the needle into the left ventricle of the heart without puncturing the opposite side of the heart. Open the flow of saline and cut the right atrium to allow for outflow of body fluids. Allow 200 ml of heparinized saline to flow.

6. Change the stopcock to allow for the flow of perfusate (either Yannof's fixative or 4 % paraformaldehyde). Allow 150 ml of perfusate to flow.

APPENDIX A6: PARAFFIN EMBEDDING PROTOCOL

EQUIPMENT:

Hot plate
square metal baking pan
2 wide-mouth bottles for paraffin
thermometer (range 0-100°C)
long forceps
Tissue-tek cartridges
paraffin molds
Blue-ice block
Papaplast+

PROCEDURE:

1. Fill the square metal baking pan with water and place on hot plate (setting of around 4 on our hot plates). Also nearly fill two wide-mouth bottles with paraffin chips and place them in the water on the hot plate.

2. While the paraffin is melting dehydrate the tissue pieces through graded alcohols as designated below. Also thoroughly clear with two xylene rinses.

3. Once the paraffin has reached 58°C and the tissue is dehydrated and cleared, place each tissue piece into a Tissue-tek cassette for handling. Be careful not to heat the paraffin above 60°C. Infiltrate the tissue within the cassettes for 30 minutes each in two baths of paraffin.

4. When the tissue has been infiltrated, remove it from the cassette and place into a paraffin mold with melted paraffin. Position the tissue in the desired orientation and immerse the "chuck" half of the cassette into the paraffin above the tissue. Place the paraffin mold on the ice block to solidify the paraffin. Using a pencil, label the sample on the surface of the "chuck" half of the cassette.

1.	70% EtOH	5 minutes	Room Temp
2.	70% EtOH	5 minutes	Room Temp
3.	80% EtOH	5 minutes	Room Temp
4.	95% EtOH	5 minutes	Room Temp
5.	95% EtOH	5 minutes	Room Temp
6.	100% EtOH	5 minutes	Room Temp
7.	100% EtOH	5 minutes	Room Temp
8.	100% EtOH	5 minutes	Room Temp
9.	Xylenes	5-10 minutes	Room Temp
10.	Xylenes	5-10 minutes	Room Temp
11.	Paraffin	30-45 minutes	58°C
12.	Paraffin	30-45 minutes	58°C

APPENDIX A7: EPON EMBEDDING PROTOCOL

SOLUTIONS:

Cacodylate Buffer (pH 7.4)

Stock A: 0.2 M sodium cacodylate (mw 214)
4.28g sodium cacodylate in 100 ml of distilled water

Stock B: 0.2 M HCl (mw 36.46)
1.7 ml HCl in 100 ml of distilled water

Mix 25 ml of stock A + 1.4 ml of stock B (for pH 7.4) +73.6 ml of distilled water.

2 % Cacodylate Buffered Glutaraldehyde

8 ml of 25% glutaraldehyde
92 ml cacodylate buffer

0.2 M Cacodylate Buffered Sucrose Solution

6.846g sucrose (mw 342.3)
100 ml cacodylate buffer

1% Osmium Tetroxide

2 ml 4% osmium tetroxide solution
6 ml distilled water

PROCEDURE:

1. Soak tissue pieces in 2% cacodylate buffered glutaraldehyde overnight at 4°C.

2. Soak tissue pieces in 0.2 M cacodylate buffered sucrose overnight at 4°C.

3. Rinse tissue one time in cacodylate buffer for 10 minutes at 4°C.

4. Fix in 1% osmium tetroxide for 1.5 - 2.0 hours at room temperature (in the hood).

5. Dehydrate tissue through graded alcohol:

30% EtOH	5 minutes
50% EtOH	5 minutes
70% EtOH	5 minutes
80% EtOH	5 minutes
90% EtOH	5 minutes
95% EtOH	5 minutes
100% EtOH	5 minutes
100% EtOH	5 minutes
100% EtOH	5 minutes

6. Clear in acetone with 2 rinses for 5 minutes each.

7. Infiltrate in 1:1 acetone/Epon* mixture overnight at room temperature.

8. Infiltrate in 1:3 acetone/Epon* mixture overnight at room temperature.

9. Infiltrate in 100% Epon* overnight at room temperature.

10. Embed with 100% Epon with hardener using flexible molds. A small piece of paper containing identification for each specimen can be solidified into the Epon block.

11. Let cure for 24 hours in the oven at 60°C. Some samples may take longer to harden.

*During infiltration, the Epon mixture should not contain hardener.

APPENDIX A8: TISSUE FREEZING

EQUIPMENT:

Low temperature thermometer (-100°C to 0°C)
Ring stand with clamp
Small metal vessel (~50 ml volume)
Larger metal bowl (~500 ml volume)
Isopentane
Dry Ice
Forceps
Tissue-tek OCT embedding compound
Strips of filter paper

PROCEDURE:

1. Place enough dry ice pieces in the bottom of the 500 ml bowl to cover the bottom.

2. Place the 50 ml vessel in the center of the dry ice in the bowl.

3. Clamp the thermometer in the ring stand so that the tip is placed within the 50 ml vessel.

4. Fill the 50 ml vessel with isopentane. Adjust the amount of dry ice in the bowl until the temperature equilibrates to -40°C. The dry ice will need to be replenished to maintain the temperature.

5. Label a strip of filter paper corresponding to a tissue segment. Place a drop of OCT compound on the end of the paper, and place the tissue on the drop of OCT in the correct orientation.

6. Immerse the tissue in the isopentane by dipping the end of the paper strip into the isopentane for about 10 seconds (larger tissue pieces will take longer). Immediately place the frozen tissue into the freezer at -80°C.

APPENDIX A9: HEMATOXYLIN AND EOSIN STAINING

SOLUTIONS:

Harris Hematoxylin Solution
(Sigma Co,)

.25% Acid Alcohol Solution

HCl, conc.	2.5 ml
70% EtOH	1000.0 ml

Ammonia Water Solution

ammonium hydroxide	5-6 drops
Distilled water	200.0 ml

Eosin Y Solution, Aqueous
(Sigma Co., Cat No. HT110-2-16)

STAINING PROCEDURE:

1. Deparaffinize and hydrate to distilled water.

xylene	2 minutes	2X
100% EtOH	1 minute	2X
95% EtOH	1 minute	
80% EtOH	1 minute	
70% EtOH	1 minute	
tap water	10 minutes	

2. Stain with Harris Hematoxylin for 2-3 minutes.
3. Rinse with distilled water.
4. Differentiate with acid alcohol solution for 1-2 dips.
5. Rinse with distilled water for 5- 10 seconds.
6. Dip in ammonium hydroxide solution 5-60 seconds
7. Rinse with distilled water for 2 minutes.
8. Dip in eosin for 3 seconds.

9. Dehydrate and clear .

70% EtOH	1 minute	
80% EtOH	1 minute	
95% EtOH	1 minute	
100% EtOH	1 minute	2X
xylene	2 minutes	2X

10. Mount with Permount or Histoclad.

APPENDIX A10: MASSON'S TRICHROME STAINING

(Manual of Histological Staining: Methods of the Armed Forces Institute of Pathology, III Ed, 1968, pp.94-95)

SOLUTIONS:

Bouin's Solution

(Sigma Co.)

Weigert's Iron Hematoxylin Solution

Solution A:

Hematoxylin crystal	1.0 gm
Alcohol, 95%	100.0 ml

Solution B:

Ferric Chloride, 29% aqueous	4.0 ml
distilled water	95.0 ml
HCl, conc	1.0 ml

Mix equal part of solution A and solution B.

Biebrich Scarlet-Acid Fuchsin Solution

Biebrich scarlet, aqueous, 1%	90.0 ml
Acid fuchsin, aqueous, 1%	10.0 ml
Glacial acetic acid	1.0 ml

Phosphomolybdic-Phosphotungstic Acid Solution

Phosphomolybdic acid	5.0 gm
Phosphotungstic acid	5.0 gm
Distilled water	200.0 ml

Aniline Blue Solution

Aniline blue	2.5 gm
Glacial acetic acid	2.0 ml
Distilled water	100.0 ml

1% Glacial Acetic Acid Solution

Glacial acetic acid	1.0 ml
Distilled water	100.0 ml

STAINING PROCEDURE:

1. Deparaffinize and hydrate to distilled water.

xylene	2 minutes	2X
100% EtOH	1 minute	2X

95% EtOH	1 minute	
80% EtOH	1 minute	
70% EtOH	1 minute	
tap water	10 minutes	

2. Mordant in Bouin's solution for 1 hour at 56°C, or overnight at room temperature, if formalin fixed.
3. Cool and wash in running water until yellow color disappears.
4. Rinse in distilled water.
5. Weigert's iron hematoxylin solution for 10 minutes. Wash in running water 10 minutes.
6. Rinse in distilled water.
7. Biebrich scarlet-acid fuchsin solution for 2 minutes. Save solution.
8. Rinse in distilled water.
9. Phosphomolybdic-phosphotungtic acid for 10 to 15 minutes before aniline blue solution. Discard solution.
10. Aniline blue solution for 5 minutes. Save solution.
11. Rinse in distilled water.
12. Glacial acetic solution for 3 to 5 minutes. Discard solution.
13. Dehydrate and clear .

70% EtOH	1 minute	
80% EtOH	1 minute	
95% EtOH	1 minute	
100% EtOH	1 minute	2X
xylene	2 minutes	2X

14. Mount with Permount or Histoclad.

APPENDIX A11: TOLUIDINE BLUE STAINING

SOLUTIONS:

Toluidine Blue Solution

Toluidine Blue Powder	1 gm
Sodium Borate Powder	1 gm
Distilled Water	100 ml

Solution should be filtered and stored in a stopped bottle.

STAINING PROCEDURE:

1. Heat slide on hot plate to 60 - 80°C.

2. Stain with Toluidine Blue Solution for 30 - 60 seconds. Thicker sections will take less time.

3. Wipe away excess stain and allow to dry on hot plate for 2 - 3 minutes.

4. Mount with Permount or Histoclad.

APPENDIX A12: IMMUNOHISTOCHEMICAL STAINING

SOLUTIONS:

0.2 M Phosphate Buffer (500 ml, pH 7.4)

500 ml distilled water
3.0g Sodium Phosphate (monobasic, anhydrous)
11.0g Sodium Phosphate (dibasic, anhydrous)

Mix constituents and pH to 7.4.

Primary Antibody Dilutant

	10 ml	5 ml	2.5 ml
PBS	9.488 ml	4.744 ml	2.372 ml
10% Triton X-100	0.300 ml	0.150 ml	0.075 ml
Goat Serum*	0.200 ml	0.100 ml	0.050 ml

(*species is chosen based on the species of the secondary antibody)

Secondary Antibody Dilutant

	10 ml	5 ml	2.5 ml
PBS	9.500 ml	4.750 ml	2.375 ml
Normal Goat Serum	0.150 ml	0.075 ml	0.0375 ml
10% Triton X-100	0.300 ml	0.150 ml	0.075 ml

10% Normal Goat Serum (First Block)

	10 ml	5 ml	2.5 ml
PBS	8.700 ml	4.350 ml	2.175 ml
Goat Serum	1.000 ml	0.500 ml	0.250 ml
10% Triton X-100	0.300 ml	0.150 ml	0.075 ml

DAB Substrate Solution

Tris (room temp)	25 ml
Diaminobenzidine (Sigma)	12.5 mg
Just before use add:	
Hydrogen Peroxide (30%)	8.3 µl

Phosphate Buffered Saline (PBS)

Distilled Water	1000 ml
Sodium Phosphate (monobasic, anhydrous)	3.0 g
Sodium Phosphate (dibasic, anhydrous)	11.0 g
Sodium Chloride	8.5 g
pH to 7.4	

SOLUTIONS (CONTINUED):

Avidin-Biotin Complex (ABC) Solution

PBS	4.85 ml
10% Triton X-100	0.075 ml
Solution A (Vector Kit)	0.025 ml
Shaken then add:	
Solution B (Vector Kit)	0.025 ml

Mix approximately 30 minutes before use

Tris Buffer

Distilled water	1000 ml
Trizma Base	6.0 g

STAINING PROCEDURES (for frozen cut sections):

1. Air dry slides 30 minutes to one hour. Make wells around tissue sections while the slides are drying using a syringe.

2. PBS rinse three times for 5 minutes each. Keep slides in a humidified chamber (we use a slide box with wet paper towels in the bottom.

3. Incubate in 10% Normal Goat Serum for 20 minutes.

4. Apply the primary antibody (whichever antibody is appropriate) diluted to desired concentration with primary antibody dilutant. Incubate overnight in a coldroom at 4°C.

5. PBS rinse three times for 5 minutes each.

6. Apply the appropriate secondary antibody diluted with secondary antibody dilutant. Incubate for 30 minutes at room temp.

7. PBS rinse three times for 5 minutes each.

8. Apply avidin-biotin complex (ABC) solution for 30-45 minutes. Be sure to mix the ABC solution 30 minutes in advance.

9. PBS rinse three times for 5 minutes each.

10. Develop tissue sections in freshly mixed DAB substrate solution for 30-60 seconds.

11. Immediate PBS rinse three times for 5 minutes each.

12. Dehydrate through graded alcohols:

70% EtOH	5 minute	
80% EtOH	5 minute	
95% EtOH	5 minute	
100% EtOH	5 minute	2X
xylene	5 minutes	2X

13. Coverslip with Permount.

APPENDIX A13: IMAGE CAPTURE AND ANALYSIS

COMPUTER SETUP:

1. Go to the apple menu under 'Control Panels' select 'MODE32'. Make sure that MODE32 is enabled.

2. Go to the apple menu, under 'Control Panels' select 'Memory'. 32 Bit Addressing should be on.

3. Go to the apple menu, under 'Control Panels' select 'Monitors'. Set colors to millions.

4. Restart the computer if any changes were made.

MICROSCOPE SETUP:

1. Turn the microscope on (green button on the right side).

2. Select the white button (max) for light level (on right side of the scope, there are 3 choices)

3. Locate the two knobs on the top portion of the microscope , one on the left and one on the right. Pull both knobs out to the TV position.

VIDEO BOX SETUP:

1. Turn the video box on. Watch the video level on the box at all times to make sure the 'Normal' indicator light is on. If the 'Over' light is on, there is too much light and it can damage the computer screen. If the 'Over' light comes on, adjust the light level of the microscope accordingly.

IMAGE CAPTURING:

1. Open the 'Tsunami' drive. Open the 'Applications' folder. Open the July version of DIGIT.

2. Find the tissue on the microscope at the appropriate magnification.

3. Select 'Grab Live Video' from the 'View" menu.

4. Select 'Full Size' and then 'Grab Frames'.

5. Select images which contain a sufficient number of myelinated axons (or pores) for analysis.

6. For each image captured, remember to 'Save' the file. Each time 'Close' the document and select a 'New' document.

IMAGE ANALYSIS:

1. Open NIH Image.

2. Open the captured image graphic file and save immediately using the NIH format.

3. Go to the 'Analyze' menu and select 'Set Scale'. Select micrometers as the unit of measure. Use the following table to fill in the 'Known Distance' and the 'Pixels' entries. (This table is calibrated for the microscope at the Brigham). When the scale is set, a diamond appears next to the file name on the top bar of the window.

Magnification	Known Distance	Pixels
4	4.15	1
10	1.66	1
20	0.83	1
40	0.415	1
100	0.166	1

4. Use 'Smooth' and/or 'Sharpen' from the 'Enhance' menu to improve the quality of the image if needed. If you do not like the effect of these, choose 'Undo' from the 'Edit' menu before proceeding.

5. From the 'Enhance' menu, choose 'Arithmetic Subtract'. Subtract 3.

6. From the 'Options' menu, select 'Density Slice'. By dragging the border of the red color on the color scale with the mouse, threshold al the way to black so that no red is showing in the image.

7. Select the ink dropper from the toolbar. Select the red color from the small portion of red remaining in the color scale. Once red has been selected, select the pencil from the toolbar.

8. Circle the axons (or pores) with the pencil along the OUTSIDE perimeter of the myelin sheath.

9. When all axons have been circled, go to the 'Analyze' menu and select the 'Options'. Chose 'Area', 'Perimeter/Length', and 'Headings'.

10. Use 'Save As' to save the image as an edited file. The image must be saved at this point to retain the meaningful information.

11. In the 'Analyze' menu, choose 'Analyze Particles'. Enter the following:
    Minimum particle size: 5 pixels
    Maximum particle size: 30000 pixels
    Label
    Outline
    Include Interior Holes
    Reset

12. Print the analyzed image if desired.

13. Choose 'Show Results' from the 'Analyze' menu. Copy the results and paste into Excel for analysis.

14. Close the image. <u>Do not save the changes to your edited file!</u>

REFERENCES

1. Aebischer, P., Guenard, V., and Brace, S., "Peripheral Nerve Regeneration Through Semipermeable Guidance Channels: Effect of the Molecular Weight Cut-off," *Journal of Neuroscience*, **9** 3590-3595, 1989.

2. Aldini, N.N., Perego, G., Cella, G.D., Maltarello, M.C., Fini, M., Rocca, M., and Giardino, R., "Effectiveness of a Bioabsorbable Conduit in the Repair of Peripheral Nerves," *Biomaterials*, **17** 959-962, 1996.

3. Archibald, S.J., Krarup, C., Shefner, J., Li, S-T., and Madison, R.D., "A collagen-based Nerve Guide Conduit for Peripheral Nerve Repair: An Electrophysiological Study of Nerve Regeneration in Rodents and Nonhuman Primates," *Journal of Comparative Neurology*, **306** 685-696, 1991.

4. Archibald, S.J., Shefner, J., Krarup, C., and Madison, R.D., "Monkey Median Nerve Repaired by Nerve Graft or Collagen Nerve Guide Tube," *Journal of Neuroscience*, **15(5)** 4109-4123, 1995.

5. Barr, M.L. and Kiernan, J.A., *The Human Nervous System: An Anatomical Viewpoint*, J.B. Lippincott Company, Philadelphia, PA, 1993.

6. Bassett, C.A.L., Campbell, J.B., and Husby, J., "Peripheral Nerve and Spinal Cord Regeneration: Factors Leading to Success of a Tubulation Technique Employing Millipore," *Experimental Neurology*, **1** 386-406, 1959.

7. Bignami, A., Chi, N.H., and Dahl, D., "The Astroglial Response to Stabbing. Immunofluorescence Studies with Antibodies to Astrocyte-specific Protein (GFA) in Mammalian and Submammalian Vertebrates," *Neuropathol. Appl. Neurobiol.*, **2** 99-110, 1976.

8. Blight, A.R. and Decrescito, V., "Morphometric Analysis of Experimental Spinal Cord Injury in the Cat: The Relation of Injury Intensity to Survival of Myelinated Axons," *Neuroscience*, **19** 321-341, 1986.

9. Borges, L.F., "Spinal Cord Regeneration: A Review of the First International Symposium on Spinal Cord Reconstruction," *Neurosurgery*, **7** 71-74, 1980.

10. Bregman, Kunkel-Bagden, E., Schnell, L., Dai, H.N., Gao, D., and Schwab, M.E., "Recovery from Spinal Cord Injury Mediated by Antibodies to Neurite Growth Inhibitors," *Nature*, **378** 498-501, 1995.

11. Bunge, M.B., Johnson, M.I., Ard, M.D., and Kleitman, N., "Factors Influencing the Growth of Regenerating Nerve Fibers in Culture," in *Progress in Brain Research*, edited by F.J. Seil, E. Herbert, and B.M. Carlson, Elsevier Press, Amsterdam, 1987.

12. Burke, J.F., Yannas, I.V., Quinby, W.C., Bondoc, C.C., and Jung, W.K., "Successful Use of a Physiologically Acceptable Artificial Skin in the Treatment of Extensive Burn Injury," *Annals of Surgery*, **194** 413-428, 1981.

13. Cajal, S. Ramon y, *Degeneration and Regeneration of the Nervous System*, trans by R.M. May, Oxford University Press, London, 1928.

14. Campbell, J.B., Bassett, C.A.L., Husby, J., and Nobak, R., "Regeneration of Adult Mammalian Spinal Cord," *Science*, **126** 929, 1957.

15. Carson, C.E., *Spinal Cord Society Newsletter*, August 1986, and personal communication, 1993.

16. Catatelpe, O., Ozcan, O.E., Demirhan, B., Ruacan, S., and Erbengi, A., "Arterial Bridging for Repair of Peripheral Nerve Gap: A Comparative Study," *Acta Neurochir (Wien)*, **121** 181-186, 1993.

17. Chamberlain, L.J., "Long Term Functional and Morphological Evaluation of Peripheral Nerves Regenerated Through Degradable Collagen Implants," Master of Science Thesis, Massachusetts Institute of Technology, 1996.

18. Chang, A.S., "Electrophysiological Recovery of Peripheral Nerves Regenerated by Biodegradable Polymer Matrix," Master of Science Thesis, Massachusetts Institute of Technology, 1988.

19. Chang, A., Yannas, I.V., Perutz, S., Loree, H.M., Sethi, R.R., Krarup, C., Norregaard, T.V., Zervas, N.T., and Silver, J., "Electrophysiological Study of Recovery of Peripheral Nerves Regenerated by a Collagen-Glycosaminoglycan Copolymer Matrix," in *Progress in Biomedical Polymers*, edited by C.G. Gebelein and R.L. Dunn, Plenum Press, New York, NY, 1990.

20. Chang, A.S., "Peripheral Nerve Regeneration," in *Neuroscience Year* (supplement 2 to the *Encyclopedia of Neuroscience*, edited by B. Smith and G. Adelman, Birkhauser, Boston, MA, 1992.

21. Chen, E.H.-Y., "The Effect of Porosity and Crosslinking of a Collagen Based Artificial Skin on Wound Healing"; Master of Science Thesis. Massachusetts Institute of Technology, 1982.

22. Cheng, H., Cao, Y., and Olson, L., "Spinal Cord Repair in Adult Paraplegic Rats: Partial Restoration of Hind Limb Function," *Science*, **273** 510-513, 1996.

23. Chiu, D.T.W., Janecka, I., Krizek, T.J., Wolff, M., and Lovelace, R.E., "Autogenous Vein Graft as a Conduit for Nerve Regeneration," *Surgery*, **91(2)** 226-232, 1982.

24. Clemente, C.D. and Windle, W.F., "Regneration of Severed Nerve Fibers in the Spinal Cord of the Adult Cat," *Journal of Comparative Neurology*, **101** 691-731, 1954.

25. Dagalakis, N., Flink, J., Stasikelis, P., Burke, J.F., and Yannas, I.V., "Design of an Artificial Skin. III. Control of Pore Structure," *Journal of Biomedical Materials Research*, **14** 511-528, 1980.

26. David, S. and Aguayo, A.J., "Axon Elongation into Peripheral Nervous System 'Bridges' After Central Nervous System Injury in Adult Rats," *Science*, **214** 931-933, 1981.

27. De La Torre, J.C., Hill, P.K., Gonzalez-Carvajal, M., and Parker, J.C. Jr., "Evaluation of Transected Spinal Cord Regeneration in the Rat," *Experimental Neurology*, **84** 188-206, 1984.

28. De La Torre, J.C. and Goldsmith, H.S., "Coerulospinal Fiber Regeneration in Transected Feline Spinal Cord," **35** 413-417, 1994.

29. Feringa, E.R., Kowalski, T.F., and Vahlsing, H.L., "Basal Lamina at the Site of Spinal Cord Injury in Normal, Immunotolerant, and Immunosuppressed Rats," *Neuroscience Letters*, **54** 225-230, 1985.

30. Gelderd, J.B., "Evaluation of Blood Vessel and Neurite Growth into a Collagen Matrix Placed Within a Surgically Created Gap in Rat Spinal Cord," **511** 80-92, 1990.

31. Guth, L., "Regeneration in the Mammalian Peripheral Nervous System," *Physiol. Rev.*, **36** 441-478, 1956.

32. Guth, L., "History of Central Nervous System Regeneration Research," *Experimental Neurology*, **48** 3-15, 1975.

33. Guth, L., Barrett, C.P., Donati, E.J., Anderson, F.D., Smith, M.V., and Lifson, M., "Essentiality of a Specific Cellular Terrain for Growth of Axons into a Spinal Cord Lesion," *Experimental Neurology* , **88** 1-12, 1985.

34. Heimbach, D., Luterman, A., Burke, J., Cram, A., Herndon, D., Hunt, J., Jordan, M., McManus, W., Solem, L., Warden, G., and Zawacki, B., "Artificial Dermis for Major Burns," *Annals of Surgery*, **208** 313-320, 1988.

35. Heimer, L., *The Human Brain and Spinal Cord: Functional Neuroanatomy and Disection Guide*, Springer-Verlag Inc., New York, NY, 1995.

36. Houle, J.D. and Reier, P.J., "Transplantation of Fetal Spinal Cord Tissue into the Chronically Injured Adult Rat Spinal Cord," *Journal of Comparative Neurology*, **269** 535-547, 1988.

37. Houle, J.D. and Johnson, J.E., "Nerve Growth Factor (NGF)-treated Nitrocellulose Enhances and Directs the Regeneration of Adult Rat Dorsal Root Axons Through Intraspinal Neural Tissue Transplants," *Neuroscience Letters*, **103** 17-23, 1989.

38. Houle, J.D., "Demonstration of the Potential for Chronically Injured Neurons to Regenerate Axons into Intraspinal Peripheral Nerve Grafts," *Experimental Neurology*, **113** 1-9, 1991.

39. Houle, J., "The Structural Integrity of Glial Scar Tissue Associated with a Chronic Spinal Cord Lesion Can Be Altered by Transplanted Fetal Spinal Cord Tissue," *Journal of Neuroscience Research*, **31** 120-130, 1992.

40. Howley, S., American Paralyis Association, personal communication, 1993.

41. Irving, H., "The Effect of Freeze-Drying Temperature on Pore Size in Collagen-GAG Artificial Skin"; Bachelor of Science Thesis. Massachusetts Institute of Technology, 1986.

42. Kao, C.C., Shimizu, Y., Perkins, L.C., and Freeman, L.W., "Experimental Use of Cultured Cerebellar Cortical Tissue to Inhibit the Collagenous Scar Following Spinal Cord Transection," *Journal of Neurosurgery*, **33** 127-139, 1970.

43. Kao, C.C., Chang, L.W., and Bloodworth, J.M.B. Jr., "Axonal Regeneration Across Transected Mammalian Spinal Cords: An Electron Microscopic Study of Delayed Microsurgical Nerve Grafting," *Experimental Neurology*, **54** 591-615, 1977.

44. Khan, T., Sayers, S., Gaik, G., and Dauzvardis, M., "Culture of Rat Fetal Spinal Cord Explants on Carbon Filaments," *Neuroscience Letters*, **118** 172-176, 1990.

45. Khan, T., Dauzvardis, M., and Sayers, S., "Carbon Filament Implants Promote Axonal Growth Across the Transected Rat Spinal Cord," *Brain Research*, **541** 139-145, 1991.

46. Kiernan, J.A., "Hypotheses Conserned with Axonal Regeneration in the Mammalian Nervous System," *Biological Review*, **54** 155-197, 1979.

47. Kleitman, N., Wood, P., Johnson, M.I., and Bunge, R.P., "Schwann Cell Surfaces but Not Extracellular Matrix Organized by Schwann Cells support Neurite Outgrowth from Embryonic Rat Retina," *Journal of Neuroscience*, **8** 653-663, 1988.

48. Krikorian, J.G., Guth, L., and Donati, E.J., "Origin of the Connective Tissue Scar in the Transected Rat Spinal Cord," *Exp. Neurol.*, **72** 698, 1981.

49. Landstrom, A., "Nerve Regeneration Induced by Collagen-GAG Matrix in Collagen Tubes," Master of Science Thesis, Massachusetts Institute of Technology, 1994.

50. Li, S-T., Archibald, S.J., Krarup, C., and Madison, R., "Semipermeable Collagen Nerve Conduits for Peripheral Nerve Regeneration," *Polymeric Materials Science Engineering*, **62** 575-582, 1990.

51. Liuzzi, F.J., and Lasek, R.J., "Astrocytes Block Axonal Regeneration in Mammals by Activating the Physiological Stop Pathway," *Science*, **237** 642-645, 1987.

52. Loree, H., "A Freeze-Drying Process for Fabrication of Polymeric Bridges for Peripheral Nerve Regeneration"; Master of Science Thesis. Massachusetts Institute of Technology, 1988.

53. Loree, H.M., Yannas, I.V., Mikic, B., Chang, A.S., and Perutz, S.M., "A Freeze-drying Process for Fabrication of Polymeric Bridges for Peripheral Nerve Regeneration," from *Proceddings of the Fifteenth Annual Northeast Bioengineering Conference*, Boston, MA, 1989.

54. Louie, L.K., "Effect of a Porous Collagen-Glycosaminoglycan Copolymer on Early Tendon Healing in a Novel Animal Model"; Doctor of Philosophy Thesis. Massachusetts Institute of Technology, 1997.

55. Lundborg, G., Dahlin, L.B., Danielsen, N., Gelberman, R.H., Longo, F.M., Powell, H.C., and Varon, S., "Nerve Regeneration in Silicone Chambers: Influence of Gap Length and Distal Stump Components," *Experimental Neurology*, **76** 361-375, 1982.

56. Madison, R.D., Archibald, S.J., and Krarup, C., "Peripheral Nerve Injury," in *Wound Healing: Biochemical and Clinical Aspects*, Edited by Cohen, I.K, Diegelman, R.F., and Lindblad, W.J. W.B. Saunders Company, Philadelphia, 1992.

57. Marchand, R. and Woerly, S., "Transected Spinal Cords Grafted with *In Situ* Self-Assembled Collagen Matrices," *Neuroscience*, **36** 45-60, 1990.

58. Marchand, R., Woerly, S., Bertrand, L., and Valdes, N., "Evalutaion of Two Cross-linked Collagen Gels Implanted in the Transected Spinal Cord," *Brain Research Bulletin*, **30** 415-422, 1993.

59. Matthews, M.A., St. Onge, M.F., Faciane, C.L., and Gelderd, J.B., "Spinal Cord Transection: a Quantitative Analysis of Elements of the Connective Tissue Matrix Formed within the Site of Lesion Following Administration of Piromen, Cytoxan or Trypsin," *Neuropathology and Applied Neurobiology*, **5** 161-180, 1979.

60. McKeon, R.J., Schreiber, R.C., Rudge, J.S., and Silver, J., "Reduction of Neurite Outgrowth in a Model of Glial Scarring Following CNS Injury is Correlated with the Expression of Inhibitory Molecules on Reactive Astrocytes," *Journal of Neuroscience*, **11** 3398-3411, 1991.

61. Midha, R., Fehlings, M.G., Tator, C.H., Saint-Cyr, J.A., and Guha, A., "Assessment of Spinal Cord Injury by Counting Corticospinal and Rubrospinal Neurons," *Brain Research*, **410** 299-308, 1987.

62. Molander, H., Olsson, Y., Engkvist, O., Bowald, S., and Eriksson, I., "Regeneration of Peripheral Nerve Through a Polyglactin Tube," *Muscle and Nerve*, **5** 54-57, 1982.

63. Montgomery, C.T., Tenaglia, E.A., and Robson, J.A., "Axonal Growth into Tubes Implanted within Lesions in the Spinal Cords of Adult Rats," *Experimental Neurology*, **137** 277-290, 1996.

64. Puchala, E. and Windle, W.F., "The possibility of Structural and Functional Restitution after Spinal Cord Injury: A Review," *Experimental Neurology*, **55** 1-42, 1977.

65. Reier, P.J., Stensaas, L.J., and Guth, L., "The Astrocyte Scar As an Impediment to Regeneration in the Central Nervous System," in *Spinal Cord Reconstruction*, edited by C.C. Kao, R.P. Bunge, and P.J. Reier, Raven Press, New York, NY, 1983.

66. Reier, P.J., Bregman, B.S., and Wujek, J.R., "Intraspinal Transplantation of Embryonic Spinal Cord Tissue in Neonatal and Adult Rats," *Journal of Comparative Neurology*, **247**, 275-296, 1986.

67. Richardson, P.M., McGuiness, U.M., and Aguayo, A.J., "Axons from CNS Neurones Regenerate into PNS Grafts," *Nature*, **284** 264-265, 1980.

68. Schnell, L., and Schwab, M.E., "Sprouting and Regeneration of Lesioned Corticospinal Tract Fibres in the Adult Rat Spinal Cord," *European Journal of Neuroscience*, **5** 1156-1171, 1993.

69. Schwab, M.E., "Myelin-associated Inhibitors of Neurite Growth and Regeneration in the CNS," *Experimental Neurology*, **109** 2-5, 1990.

70. Snedecor, G.W. and Cochran, W.G., *Statistical Methods*, Iowa State University Press, Ames, IA, 1989.

71. Stern, R., McPherson, M., and Longaker, M.T., "Histological Study of Artificial Skin Used in the Treatment of Full-Thickness Thermal Injury," *Journal of Burn Care and Rehabilitation*, **11(1)** 7-13, 1990.

72. Stokes, B.T. and Reier, P.J., "Oxygen Transport in Intraspinal Fetal Grafts: Graft-Host Relations," *Experimental Neurology*, **111** 312-323, 1991.

73. Stokes, B.T. and Reier, P.J., "Fetal Grafts Alter Chronic Behavioral Outcome after Contusion Damage to the Adult Rat Spinal Cord," *Experimental Neurology*, **116** 1-12, 1992.

74. Stone, K.R., Rodkey, W.R., Webber, R.J., McKinney, L., and Steadman, J.R., "Future Directions: Collagen-Based Prostheses for Meniscal Regeneration," *Clinical Orthopaedic and Related Research*, **252** 129-135, 1990.

75. Theriault, E., and Tator, C.H., "Persistence of Rubrospinal Projections Following Spinal Cord Injury in the Rat," *Journal of Comparative Neurology*, **342** 249-258, 1994.

76. Thompson, F.J., Reier, P.J., Lucas, C.C., and Parmer, R., "Altered Patterns of Reflex Excitability Subsequent to Contusion Injury of the Rat Spinal Cord," *Journal of Neurophysiology*, **68** 1473-1486, 1992.

77. Tountas, C.P., Bergman, R.A., Lewis, T.W., Stone, H.E., Pyrek, J.D., and Mendenhall, H.V., "A Comparison of Peripheral Nerve Repair Using an Absorbable Tubulization Device and Conventional Suture in Primates," *Journal of Applied Biomaterials*, **4** 261-268, 1993.

78. Willliams, L.R., Longo, F.M., Powell, H.C., Lundborg, G., and Varon, S., "Spatial-temporal progress of Peripheral Nerve Regeneration within a Silicone Chamber: Parameters for a Bioassay," *Journal of Comparative Neurology*, **218** 460-470, 1983.

79. Windle, W.F. and Chambers, W.W., "Regeneration in the Spinal Cord of the Cat and Dog," *Journal of Comparative Neurology*, **93** 241-257, 1950.

80. Wrathall, J.R., Rigamonti, D.D., Braford, M.R., and Kao, C.C., "Reconstruction of the Contused Cat Spinal Cord by the Delayed Nerve Graft Technique and Cultured Peripheral Non-neuronal Cells," *Acta Neuropathologica*, **57** 59-69, 1982.

81. Xu, X.M., Guenard, V., Kleitman, N., and Bunge, M.B., "Axonal Regeneration into Schwann Cell-Seeded Guidance Channels Grafted into Transected Adult Rat Spinal Cord," *Journal of Comparative Neurology*, **351** 145-160, 1995.

82. Yannas, I.V. and Tobolsky, A.V., "Crosslinking of Gelatin by Dehydration," *Nature*, **215** 509-510, 1967.

83. Yannas, I.V., "Collagen and Gelatin in the Solid State," *Journal of Macromolecular Science*, **C7** 49-104, 1972.

84. Yannas, I.V. and Burke, J.F., "Design of an Artificial Skin. I. Basic Design Principles," *Journal of Biomedical Materials Research*, **14** 65-81, 1980.

85. Yannas, I.V., Burke, J.F., Gordon, P.L., Huang, C., and Rubenstein, R.H., "Design of an Artificial Skin. II. Control of Chemical Composition," *Journal of Biomedical Materials Research*, **14** 107-131, 1980.

86. Yannas, I.V., "Use of Artificial Skin in Wound Management", Chapter 15 in *The Surgical Wound*, Edited by P. Dineen, Lea and Febiger, Philadelphia, 1981.

87. Yannas, I.V., Burke, J.F., Orgill, D.P., and Skrabut, E.M., "Wound Tissue Can Utilize a Polymeric Template to Synthesize a Functional Extension of Skin", *Science*, **215** 174-176, 1982.

88. Yannas, I.V., Orgill, D.P., Silver, J., Norregaard, T.V., Zervas, N.T., and Schoene, W.C., "Regeneration of Sciatic Nerve Across 15-mm Gap by Use of a Polymeric Template," in *Advances in Biomedical Polymers.*, Edited by C.G. Gebelein. Plenum Publishing Corp., New York, 1987.

89. Yannas, I.V., Lee, E., Orgill, D.P., Skrabut, E.M., and Murphy, G.F., "Synthesis and Characterization of a Model Extracellular Matrix That Induces Partial Regeneration of Adult Mammalian Skin,", *Proc. Natl. Acad. Sci. USA*, **86** 933-937, 1989.